Atmospheric Effects
on
High Energy Cosmic Rays

by

Peter Robert Ashwell
P.R.A. Lyons, B.Sc. (Hons), University of Tasmania

submitted in fulfilment
of the requirements for the degree of
Doctor of Philosophy

UNIVERSITY OF TASMANIA
HOBART
August, 1981

To my parents

CONTENTS

CHAPTER 5. EXPLAINING THE ANOMALOUS COEFFICIENTS

PREFACE

This thesis contains no material which has been submitted or accepted for award of any other degree or diploma in any university.

To the best of my knowledge and belief, the thesis contains no material previously published or written by another person, except where due acknowledgement is made in the text.

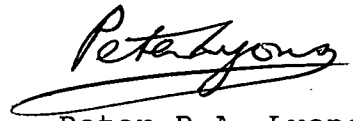

Peter R.A. Lyons

SUMMARY

The atmospheric effects on the muon intensity have been observed using muon telescopes at Poatina, Cambridge and Hobart, Tasmania. The detectors consist of a variety of Geiger counter telescopes located at ~ 357 hg cm^{-2} underground, ~ 47 hg cm^{-2} underground and at sea level, respectively. Least-squares regression analysis has been used to calculate the various pressure, height and temperature coefficients for the three sites. It is found that for the underground detectors, the apparent atmospheric effects tend to differ strongly from those expected. In particular, the total barometer coefficient at Poatina for the years 1972-76 is (-0.047 ± 0.002) % mb^{-1} (Humble et al., 1979). Using a generally-accepted model for the production and interaction of secondary particles in the atmosphere, extensive calculations predict a barometer coefficient of only ~ 0.003 % mb^{-1}. The partial pressure, height and temperature coefficients also differ greatly from their theoretical values.

A detailed review is presented of the theory and assumptions behind the least-squares method. It is shown analytically that if the regressor variables are intercorrelated and measured with error, their expectation values may be severely biased from their true values. It is found that the inflated Poatina total barometer coefficient is almost entirely due to a negative

correlation between air pressure and stratospheric temperature. The latter variable is thus shown to be the only significant influence on the intensity of muons deep underground. A comparison between the observed and predicted total temperature coefficients implies a temperature measurement error of ~ 2.2 K. This error is partly instrumental and partly due to the slow sampling rate of temperature provided by radiosondes. In all, these data problems are probably entirely responsible for the anomalous coefficients at Poatina.

A test parameter, based on the least-squares model, is shown to predict successfully the observed divergence between the observed and theoretical coefficients, as the muon threshold energy is increased. An extensive series of regressions has been carried out in order to determine the optimal set of atmospheric variables for correcting the Poatina intensity for atmospheric effects. However, the percentage of variation removed is still only ~ 40 %, because of the data intercorrelations and errors previously mentioned.

Using the temperature dependence of the Poatina muon intensity, the four-day mean temperature of the stratosphere has been reconstructed. The resulting correlation with radiosonde measurements is ~ 0.5. However, a variety of detectors with greater sensitive area would be required for the determination of the atmosphere's temperature profile from muon observations to be practicable.

ACKNOWLEDGEMENTS

I sincerely thank my supervisors, Dr A.G. Fenton and Dr K.B. Fenton, for their guidance, constructive criticisms and support during the course of this work, particularly under difficult conditions during the final few months.

It is also a pleasure to thank Dr R.M. Jacklyn and Dr J.E. Humble for their interest in the project and the many helpful discussions which followed. I am grateful to Mrs B.M. Jensen and Miss J.J. Whelan for their cheerful help in the preparation of data.

I am indebted to Mr M. Mason for his technical support and to Professor R.D. Terrel, of the Econometrics Department, The Australian National University and Mr K.B. Dunn for their stimulating discussions regarding the statistics used in the work.

Finally, my thanks go to Mr K. Smith for his photographic assistance and to Mrs R. Drury for patiently typing this thesis.

CHAPTER 1

INTRODUCTION TO ATMOSPHERIC EFFECTS ON COSMIC RAYS

1.1 History of Observations

It has long been known that the passage of cosmic radiation through the atmosphere is strongly influenced by changes in meteorological conditions. In particular, the count-rates of ground-based cosmic ray detectors are usually much more affected by meteorological variations than by variations of primary origin. The latter appear as relatively minor perturbations embedded in the massive atmospheric modulations. This is particularly so in the case of the muon component, because of the higher average energy of primary radiation detected by a muon telescope. Energetic primary particles are, in turn, less affected by Forbush decreases, particularly for observations at high latitudes.

As an example, a 1% change in sea level barometric pressure causes a 7% change in the neutron count-rate, while a 1 K change in mean atmospheric temperature results in a 0.3% change in the sea level muon count-rate. Over the last thirty years the identification of such meteorological effects has improved greatly.

The chief reason for most investigations of atmospheric effects has been to determine the appropriate corrections so that variations of atmospheric origin may be excluded. In addition, the results of theoretical

calculations of these effects may be compared with those actually observed. Thus a test is provided for the validity of assumptions concerning the particle interactions in the proton-meson cascade down through the atmosphere (see, for example, Cini Castagnoli and Dodero (1967)).

For muons up to medium energy ($\lesssim$ 10 GeV), the subject of meteorological corrections has been well-covered by many workers. These include Duperier (1949), Simpson et al. (1953), Dorman (1957), Fenton, Jacklyn and Taylor (1961), Bercovitch (1965), Torsti and Valtonen (1976), and many others. In general, a self-consistent model has emerged with results in good agreement with those expected.

During the last decade, there has been a rapid growth in the study of muon variations of higher energies. One motivation for this work has been the search for variations in sidereal time. At high energies ($\gtrsim$ 100 GeV) the influence of the solar wind on the primary radiation is sufficiently small to allow sidereal anisotropies to be distinguished. The presence of these effects has been confirmed by Fenton and Fenton (1975,76), Gombosi et al. (1975), Nagashima (1975), Bergeson et al. (1979) and Cutler (1980).

However, the emergence of these results has been accompanied by inferred atmospheric coefficients which differ from those expected, especially at high cut-off energies. Sagisaka et al. (1979) have detailed the barometer coefficients observed at various underground stations. These results are shown in Figure 1.1, to which has been added the recent results from Poatina, Tasmania.

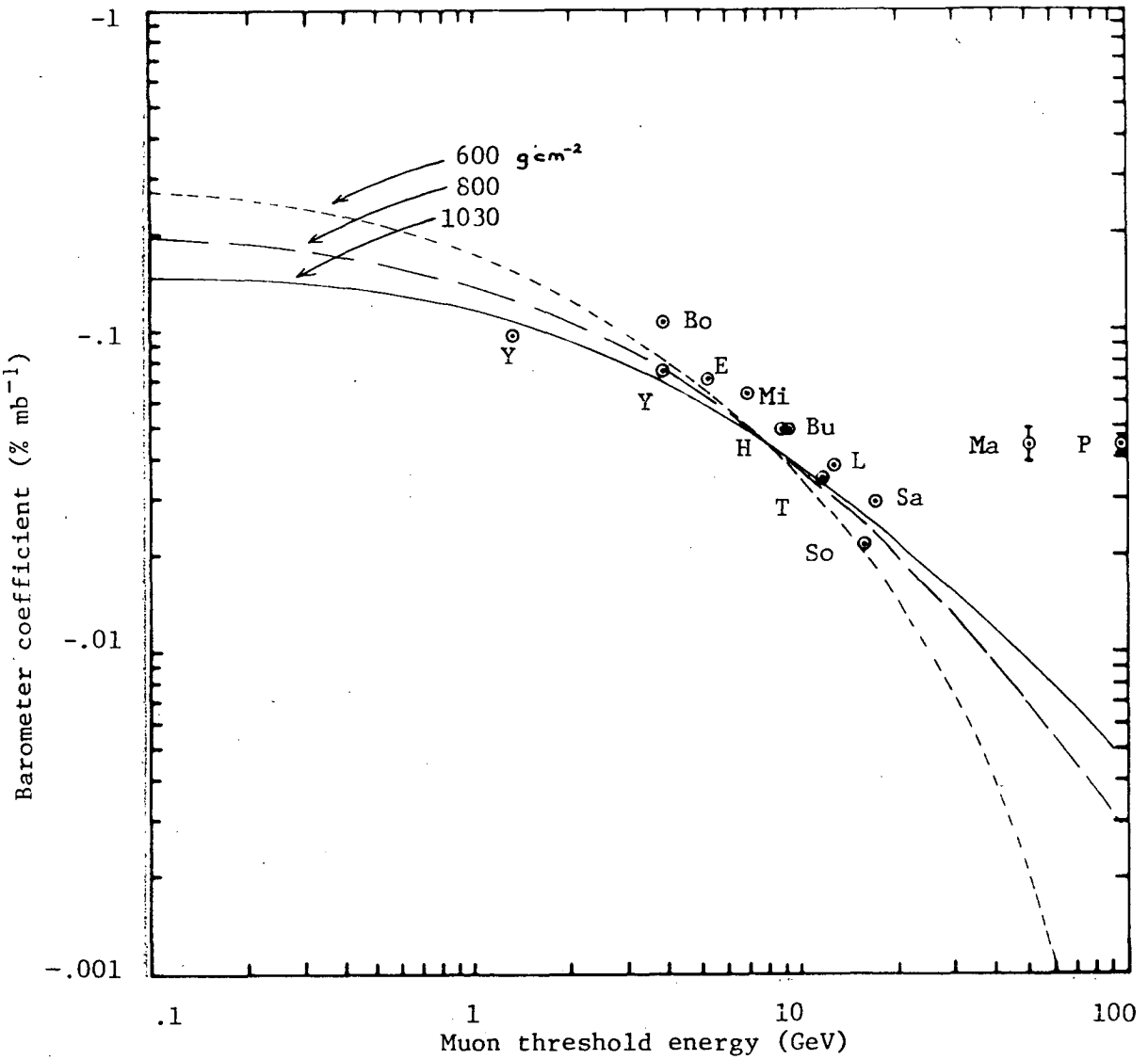

	Station	Atm. depth (g cm^{-2})
Bo	Bolivia	520
Bu	Budapest	980
E	Embudo	750
H	Hobart (Cambridge)	1000
L	London	sea level
Mi	Misato	940
Sa	Sakashita	980
So	Soccoro	850
Ta	Takeyama	sea level
Y	Yakutsk	1020
Ma	Matsushiro	—
P	Poatina	1000

Figure 1.1. Underground barometer coefficients (from Sagisaka et al., 1979).

The solid and dotted curves give the expected pressure coefficient as a function of muon threshold energy and the atmospheric depth of observation. These curves were calculated by Sagisaka et al. using the theory of Dorman (1957) and Maeda (1960). The latitude dependence is very small, as the barometer coefficient is almost invariant with respect to geomagnetic cut-off rigidity. For example, a change in rigidity of 10 GV causes only about a 4% change in the coefficient for a vertical muon telescope at sea level.

From the results in Figure 1.1 it is seen that the empirical coefficients are systematically slightly larger than expected. This trend has continued with the results of underground observations at Poatina and Cambridge. The search for a reason for this phenomenon is the main subject of this thesis.

1.2 The Mechanism of Atmospheric Effects on the Muon Intensity

As a basis for later chapters, it is desirable to briefly review the production mechanism of the secondary component of cosmic radiation and the influence of the atmosphere on it. Figure 1.2 shows the typical nucleon-meson cascase which produces the muon.

On entering the atmosphere from interplanetary space, a primary particle (of which 80-90% are protons) will most likely collide with an oxygen or nitrogen nucleus. Such interactions produce secondary particles such as pions, kaons or more nucleons. At low primary energies, the

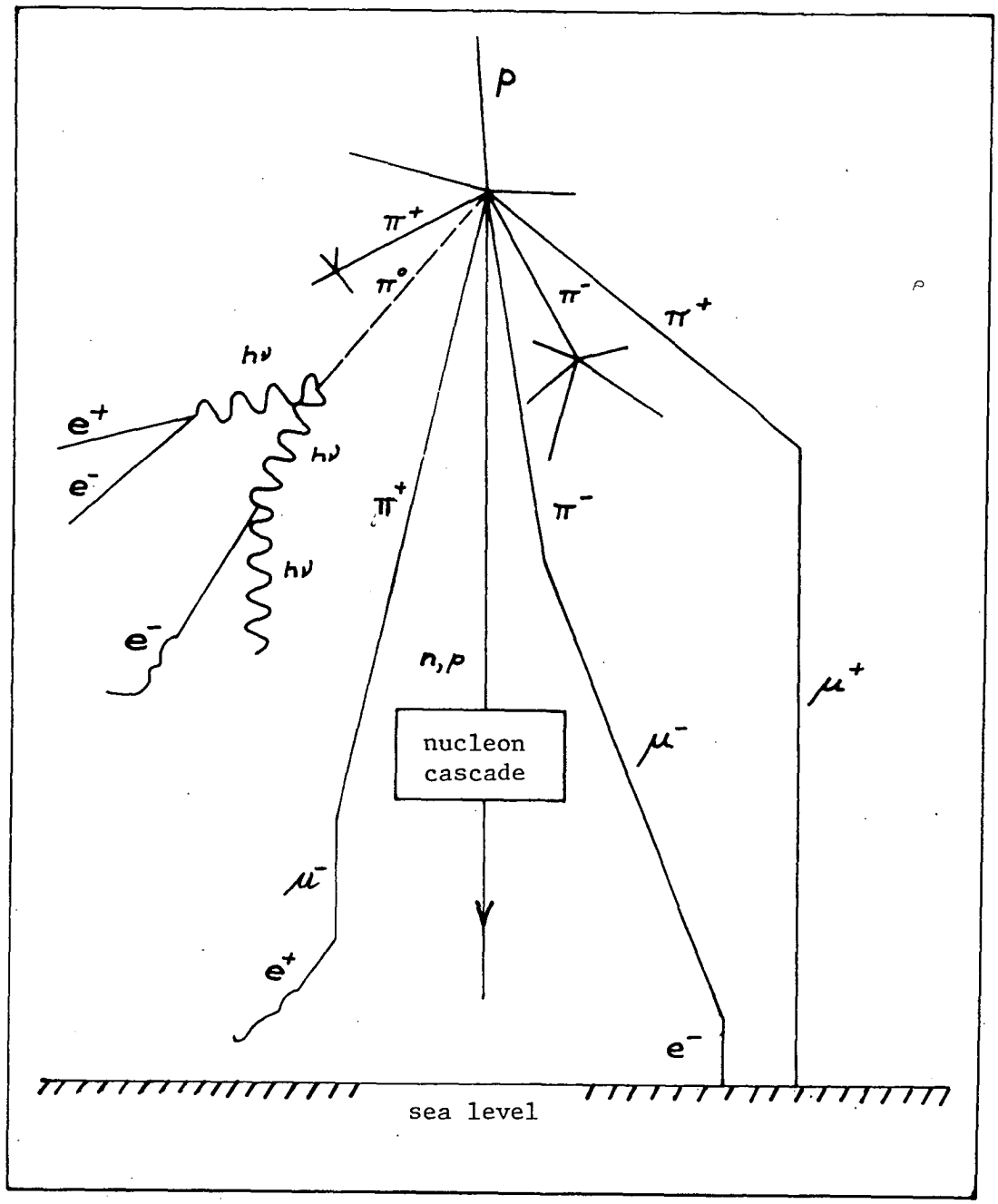

Figure 1.2. Secondary particle production in the atmosphere. The horizontal scale is greatly exaggerated.

relative proportion of kaons to pions is very small, but this figure increases somewhat for high energy primaries ($\gtrsim 10^{12}$ eV).

Most nucleons produced in the initial collision suffer further interactions, so producing more secondaries. However, the majority of charged pions and kaons decay spontaneously to produce muons of the same charge, on a one-to-one basis. The charged pion is a short-lived particle having a rest mass of $(273.27 \pm 0.12)m_e$, where m_e is the electron mass, and a mean proper lifetime of $(2.55 \pm 0.03) \times 10^{-8}$ s. The charged kaon is heavier, at $\sim 965\ m_e$, but shorter-lived at $\sim 1.23 \times 10^{-8}$ s. The most common decay processes for the two particles are

$$\pi^{\pm} \rightarrow \mu^{\pm} + \nu$$

$$K^{\pm} \rightarrow \mu^{\pm} + \nu$$

The charged muon has a rest mass of $(206.86 \pm 0.12)m_e$ and a relatively-long mean proper lifetime of $(2.20 \pm 0.01) \times 10^{-6}$ s. It decays according to the process

$$\mu^{\pm} \rightarrow e^{\pm} + 2\nu \ .$$

As the muon travels downwards through the atmosphere it loses energy, chiefly through ionization, at a rate of ~ 2 MeV cm^2 g^{-1}. The average flight energy of muons detected at sea is about 3 GeV and the Lorentz-dilated lifetime of such a muon is about equal to its time of flight from its production to sea level. The maximum rate of muon production is found to occur at an atmospheric

depth of ~ 100 g cm^{-2}. This is close to the absorption length of protons in air, ~ 120 g cm^{-2}. This distribution is shown in Figure 1.3 (from Rossi, 1952).

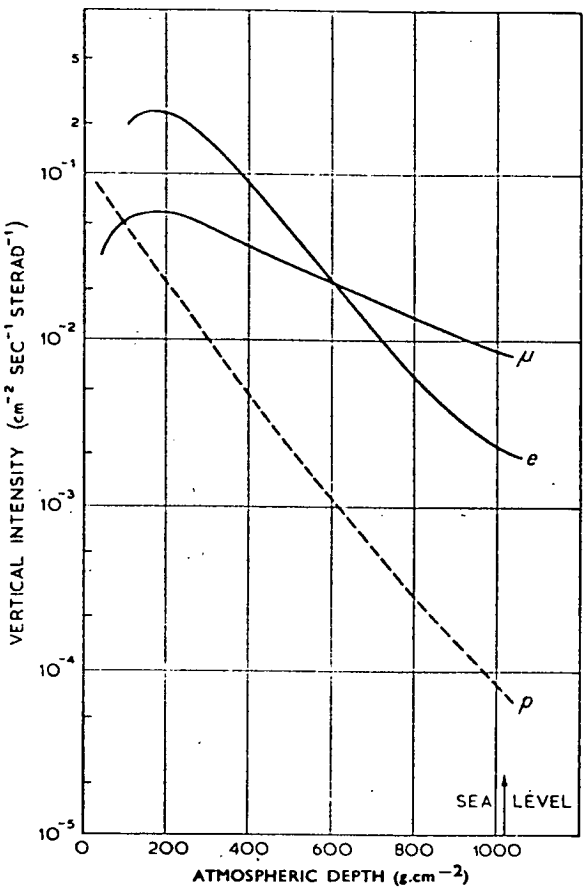

Figure 1.3. The variation of particle intensity with atmospheric depth.

Early investigations by Mysskowsky and Tuwim in 1928 revealed a negative correlation between the intensity of the hard component of muons and surface air pressure. This is the mass absorption effect which predominates at low energies. The empirical pressure correction coefficient, b_{IP}, is determined by the least squares process using the regression equation

$$\Delta I/\bar{I} = b_{IP} \Delta P \qquad (1.1)$$

where $\Delta I/\bar{I}$ represents the fractional change in muon intensity from some long-term mean, and ΔP is the corresponding change in pressure.

However, any increase in the production height H of the muons will increase their chance of decaying before reaching ground level. Therefore, a corresponding decrease in I is to be expected. At the same time, an increase in the temperature T around the pion production level causes a decrease in air density. This will increase the chance of pion decay per unit length, and result in an increase in I.

Thus Duperier (1944,49) and others found that a greater proportion of the variation in I could be explained using the four-fold regression equation

$$\Delta I/\bar{I} = b_{IP.HT}\Delta P + b_{IH.PT}\Delta H + b_{IT.PH}\Delta T \qquad (1.2)$$

where the three coefficients are, respectively, the "partial" pressure, height and temperature coefficients.

The Duperior method of (1.2) has been widely used owing to its simplicity and freedom from possible errors which might result from using purely theoretical correction methods. Provided the intensity is reasonably correlated with each of the chosen variates, the method is sound for predictive purposes. This is due to the fact that for any given sample set (P,H,T,I), the least squares coefficients can be shown to account for more variation in I than any other method of estimation using the same variates (Seber, 1977, Chapter 3).

In the following chapters, the underlying theory and shortcomings of the least-squares method will be examined in detail. It will be shown that the often-used dual aim of prediction and inference of an underlying physical mechanism may be unsound, particularly for muon observations at great depths underground.

CHAPTER 2

MATHEMATICAL NOTATION AND CONCEPTS OF LINEAR ALGEBRA

Most of the calculations in this thesis concern the analysis of, say, n observations made on p variables simultaneously. The constant n is typically the number of days in a month and p is perhaps 3 or 4. The best way to describe such large arrays of numbers is through a standardized system of matrix-vector notation which readily lends itself to any size problem. The following points are central to later chapters:

(i) Vectors are represented by underlined lower case letters, as in $\underline{x}$, and denote columns unless otherwise stated.

(ii) Matrices are represented by capital letters, as in X and consist of, say, n rows by p columns, where the j^{th} column of X is denoted $\underline{x}_j$. A matrix may be partitioned column-wise, as in $[X_1|X_2]$. The square brackets signify grouping where confusion might otherwise result.

(iii) A diagonal matrix D (say) is often denoted $D = \text{diag}(d_{11}, d_{22}, \ldots, d_{nn})$ where the $(i,j)^{th}$ element is $\delta_{ij} d_{ij}$ - viz. off-diagonal elements are zero. The identity matrix I is a special case where the $d_{jj} = 1$.

(iv) The inverse of a matrix M (say) is M^{-1} and is defined by $M^{-1}M = MM^{-1} = I$. M is therefore necessarily square.

The transpose of any matrix X is X^T, obtained from X by interchanging the $(i,j)^{th}$ element with the $(j,i)^{th}$, for all i and j.

Two columns $\underline{x}_j$ and $\underline{x}_k$ of X are orthogonal if the inner product $\underline{x}_j \cdot \underline{x}_k = \underline{x}_j^T \underline{x}_k = 0$. In the second form, the vectors are regarded as $(1\times n)$ and $(n\times 1)$ matrices respectively.

(v) In linear regression analysis the matrix product $A = X^T X$ is frequently encountered. It is by definition *symmetric* since $a_{kj} = a_{jk}$.

(vi) The eigensystem of a square matrix. If A is some $p\times p$ square matrix, the eigenvalues λ_j $(j=1,\ldots,p)$ are the roots of the polynomial equation

$$\det(A - \lambda I) = 0$$

and the eigenvectors $\underline{v}_j$ of A are defined by the matrix equation

$$A\,\underline{v}_j = \lambda_j\,\underline{v}_j$$

The (column) eigenvectors are mutually orthogonal and may be assembled to form the matrix

$$V = [\underline{v}_1 | \underline{v}_2 | \ldots | \underline{v}_p]$$

(vii) The trace of a $p\times p$ matrix A is defined by

$$\mathrm{tr}(A) = \sum_{j=1}^{p} a_{jj}$$

If A is symmetric with eigenvalues λ_j (j=1,...,p) where the λ_j are all non-negative, the following relations hold:

$$\mathrm{tr}(A) = \sum_{j=1}^{p} \lambda_j$$

and

$$\mathrm{tr}(A^{\ell}) = \sum_{j=1}^{p} \lambda_j^{\ell} \Rightarrow \mathrm{tr}(A^{-1}) = \sum_{j=1}^{p} \lambda_j^{-1}$$

Furthermore, if A is diagonal, the elements *are* the eigenvalues of A. If λ_j are at least non-negative, A is said to be positive semidefinite, and is positive definite if $\lambda_j > 0$ for all j.

(viii) If $A = X^T X$ we define the *singular values* of X by

$$\mu_j \equiv |(\lambda_j)^{\frac{1}{2}}| \quad (j=1,\ldots,p)$$

(ix) If $\underline{x}$ is a vector with n elements, the length or Euclidean norm of $\underline{x}$ is given by

$$\|\underline{x}\| = \underline{x}.\underline{x} = \underline{x}^T\underline{x} = (x_1^2 + x_2^2 + \ldots + x_n^2)^{\frac{1}{2}}$$

(x) The supremum (sup) and infremum (inf) are, respectively, the lowest upper bound and greatest lower bound of a set.

(xi) A limit in probability is denoted "plim".

CHAPTER 3

PREDICTED METEOROLOGICAL EFFECTS ON THE MUON INTENSITY UNDERGROUND

3.1 Approximate Methods

The Barometer Coefficient

The simplest calculation of this effect uses the intensity vs depth curve for muons. It is assumed that an increase in air pressure is equivalent to shifting the muon detector to an appropriately greater underground depth. Therefore this method does not take into account the contribution of muon decay to the pressure coefficient, which is expected to play a small part at depths where the muon threshold energy is less than about 10 GeV.

Barret et al. (1952) have collated the depth-intensity measurements of many workers; the results are shown in Figure 3.1. The relation between the integral intensity and thickness of matter h takes the form

$$I_\mu = I_{\mu o}\, h^{-n} \tag{3.1}$$

where the exponent n varies from about 2.0, near the surface, to 2.2 for great underground depths. Differentiation of (3.1) with respect to h yields, for the mass absorption coefficient,

$$\beta_p = \frac{1}{I_\mu}\,\frac{dI_\mu}{dh} \quad (g\ cm^{-2})^{-1}$$

$$= \frac{1}{I_\mu}\,\frac{dI_\mu}{dh}\cdot\frac{dh}{dP} \quad mb^{-1}$$

$$= -\frac{n}{h}\,\frac{dh}{dP}\ mb^{-1}$$

where h is now thought of as the mass of air above the detector.

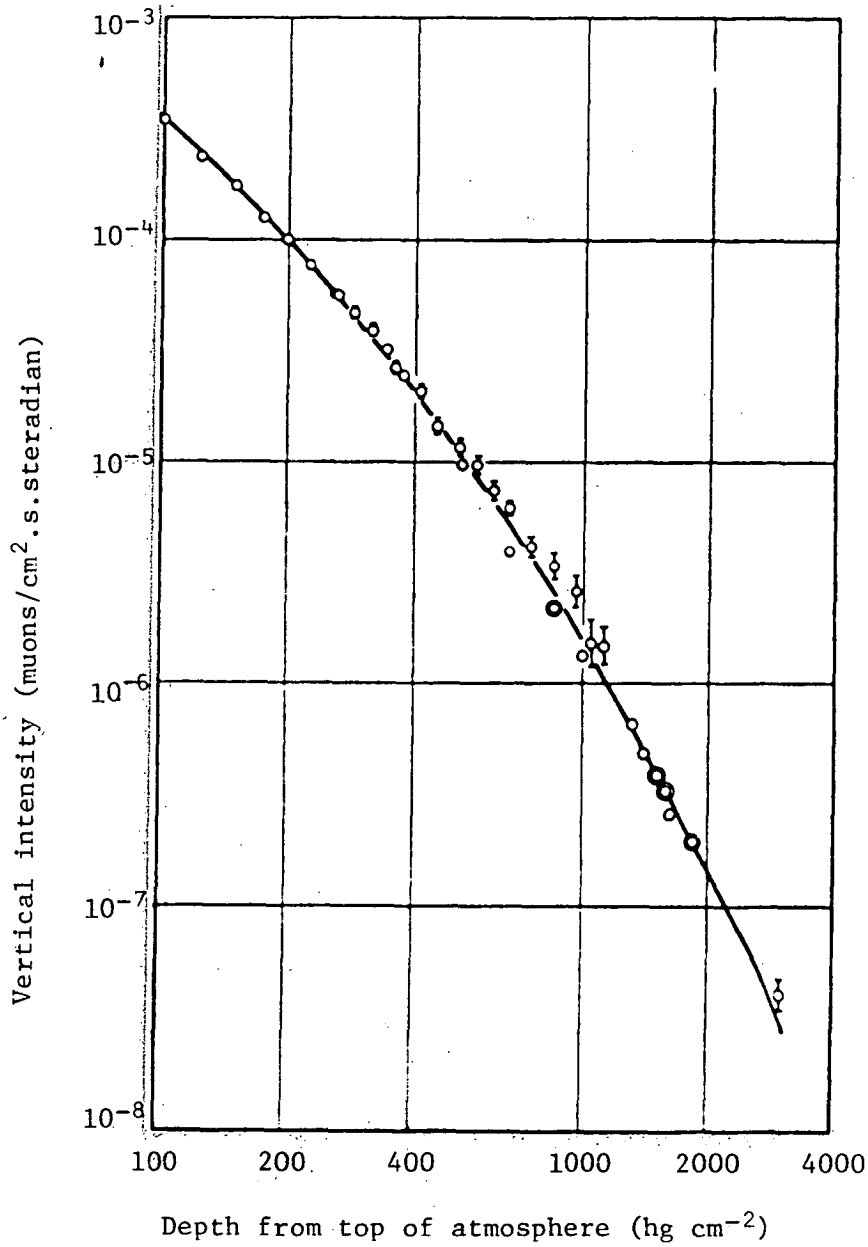

Figure 3.1. The variation of muon intensity with depth underground (Barret et al., 1952).

For non-zero zenith angles θ we have, provided n does not change,

$$\begin{aligned} \beta_p(\theta) &= -\frac{n}{h\sec\theta} \cdot \frac{dh\sec\theta}{dP} \\ &= -\frac{n}{h}\frac{dh}{dP} \\ &= -1.02\left(\frac{n}{h}\right) \end{aligned} \tag{3.2}$$

since

$$P[\text{mb}] = 0.981\ h\ [\text{g cm}^{-2}].$$

Therefore, the pressure coefficient is practically independent of zenith angle, as noted by Dutt and Thambyahpillai (1965). However, it will be shown later that at large depths, the coefficient tends to vary as $\cos\theta$, causing, for example, a semicubical telescope to see a smaller effective pressure coefficient.

The analysis of data from Cambridge and Poatina, Tasmania, is the subject of Chapters 4 and 5. Using the values $(h,n) = (3.7 \times 10^3, 2)$ for Cambridge and $(3.47 \times 10^4, 2.2)$ for Poatina, we obtain the following absorption coefficients for vertically incident particles:

Cambridge: $\beta_{abs} \cong -0.055\ \%\ \text{mb}^{-1}$

Poatina: $\beta_{abs} \cong -0.0065\ \%\ \text{mb}^{-1}$

Trefall (1955) has shown that up to medium depths underground, a small additional component, due to muon decay, is present in the barometer coefficient. This arises from the fact that the survival probability of a muon will decrease if its energy loss by ionization increases over

its flight-path. An increase in air pressure will cause such a loss of energy. For Cambridge (threshold energy 10 GeV) the muon decay component amounts to $\sim -0.01\ \%\ mb^{-1}$, resulting in a total barometer coefficient of ~ -0.06 to $-0.07\ \%\ mb^{-1}$. At Poatina (threshold energy 100 GeV) the muon decay effect is negligible.

The typical day-to-day pressure range observed at the two centres is $\sim 12 - 15$ mb. Therefore the barometer effect is expected to be large at Cambridge but insignificant for deep detectors, such as at Poatina.

The Height Coefficient

An increase in the average height of muon production will increase the probability of muon decay before reaching the level of observation, leading to a drop in intensity.

The rest lifetime of a muon follows the negative exponential distribution

$$f(t) = (1/\tau_\mu)\exp(-t/\tau_\mu)$$

where τ_μ is the mean proper lifetime, $\sim 2.2 \times 10^{-6}$ seconds. The geometric distance travelled by a muon in time t is then $z_\mu = \bar{\gamma}\,\tau_\mu\,c$, where $\bar{\gamma}$ is the "average" Lorentz factor over t and c is the speed of light. The survival probability of a muon created at height $H = z$ is then

$$\Pr(\text{no decay}) = \exp(-z/z_\mu)$$

and so the intensity of muons detected is

$$I_\mu = I_{\mu o}\exp(-z/z_\mu)\ . \qquad (3.3)$$

Differentiation of (3.3) yields for the height coefficient

$$\beta_H = \frac{1}{I_\mu} \frac{dI_\mu}{dz} = - \frac{1}{\bar{\gamma}\, \tau_\mu c} \quad . \tag{3.4}$$

To evaluate (3.4), $\bar{\gamma}$ must be estimated. The average muon loses about 2 GeV of energy through ionization during its flight from production to the ground, so to a first approximation a lower limit for $\bar{\gamma}$ is

$$\bar{\gamma} \simeq 1 + \frac{\Delta E + 2 \text{ [GeV]}}{m_\mu c^2 \text{ [GeV]}} \tag{3.5}$$

where ΔE is the muon threshold energy. Insertion of the appropriate values yields the following height coefficients:

Cambridge: $\beta_H \cong - 1.3 \text{ \% km}^{-1}$

Poatina: $\beta_H \cong - 0.15 \text{ \% km}^{-1}$

The typical diurnal fluctuation in H_{100} is ~ 0.3 km while the seasonal range is ~ 0.5 km. Thus the muon decay effect would appear to be small but significant for Cambridge but negligible for Poatina.

The Temperature Coefficient

As with the height coefficient, we assume that the temperature effect is characterized by temperature variations at the "mean" level of pion-muon production.

Barret et al. (1952), Pine et al. (1959) and others have shown that the probability that a pion with energy E_π, travelling vertically, will decay before interacting is

$$P_r(\text{decay}) \simeq \frac{B_\pi}{B_\pi + E_\pi} \tag{3.6}$$

where B_π is about 110 GeV and is proportional to temperature, T. Thus $B_\pi = k_1 T$, say, where k_1 is some constant. The muon intensity is proportional to the number of pion decays and may be written

$$I_\mu = I_{\mu o} \cdot \frac{k_1 T}{k_1 T + E_\pi} \quad . \tag{3.7}$$

Differentiation of (3.7) gives for the temperature coefficient

$$\beta_T = \frac{1}{I_\mu} \frac{dI_\mu}{dT} = \frac{E_\pi}{B_\pi + E_\pi} \cdot \frac{1}{T} \quad . \tag{3.8}$$

The typical threshold energies at muon production for Cambridge and Poatina are 12 and 102 GeV respectively. Since T ≃ 217 K (ICAO Standard Atmosphere) we have, for the temperature coefficients,

Cambridge: $\beta_T \cong 0.045 \ \% \ K^{-1}$

Poatina: $\beta_T \cong 0.22 \ \% \ K^{-1}$

It is shown in the next section that the temperature coefficient tends asymptotically towards $1/T \simeq 0.46 \ \% \ K^{-1}$ as $\Delta E \to \infty$. Whereas at great underground depths the mass absorption and muon decay effects become negligible, the effect of temperature on muon production is appreciable. The day-to-day range of temperature in the 100 - 200 mb region is about 5 degrees, which produces a sizeable influence on the muon intensity at Poatina.

3.2 The Integral Method for Calculating Atmospheric Effects on the Muon Intensity

3.2.1 Introduction

The expressions for atmospheric effects on muons have been developed by several authors, in particular Dorman (1957) and Maeda (1960). For this reason, the complete derivations will not be repeated here. Instead a simplified summary is presented, with calculations of the pressure and temperature effects for the Cambridge and Poatina detectors.

Fundamental assumptions are:

(i) The primary radiation consists of protons incident isotropically on the top of the atmosphere.

(ii) Secondary particles preserve the direction of travel of the parent proton. For muons with total energy $E_\mu \gtrsim 1$ GeV, the maximum angle between the pion and muon directions is $< 2°$. In turn, the angular deflection through scattering of muons at ~ 100 g cm^{-2} and energy 2 GeV is $< 10°$. At higher energies the deflection drops rapidly, so that over all energies, $\sim 98\%$ of muons be within a cone 4° wide, centered on the original proton direction (Bolli, 1971).

(iii) A negligible fraction of the muons detected at sea level and underground is derived through the decay of kaons rather than pions. This assumption breaks down at higher energies ($\gtrsim 30$ GeV). Corrections will be considered later.

Consider a primary proton incident at zenith angle θ on the top of the atmosphere. Let L_p denote the proton absorption length in air, 120 g cm^{-2} (Hook & Turver, 1974) and let γ denote the exponent of the primary proton spectrum (not to be confused with the Lorentz factor mentioned earlier). The differential proton spectrum varies as $E_p^{-\gamma}$ where $\gamma \approx 2.65$ over the range 10-10^4 GeV (Wolfendale, 1963) and is attenuated as $\exp(-h_1/L_p\, x)$ where h_1 is the atmospheric depth of the proton collision and $x = \cos\theta$. The differential pion production spectrum is therefore

$$f_\pi(E_\pi, h_1, x) = I_0\, E_p^{-\gamma} \exp(-h_1/L_p x) \qquad (3.9)$$

where I_o is a constant.

The pion of absorption length $L_\pi \simeq 120$ g cm^{-2} decays at depth h_2 to a muon. Both pions and muons lose energy through ionization at a rate $a \simeq 2$ MeV cm^{2}g^{-1} as they traverse the air, but the total energy lost by a pion is negligible owing to its very short decay length.

A pion of energy E_π produces a muon of energy $E_\mu = \alpha E_\pi$ where the mean value of α is 0.787 (see Appendix 2).

For a muon telescope with parallel-plane geometry, such as a cubical telescope, the minimum pion energy at generation corresponding to an absorber threshold ΔE is

$$E_{min} = [\Delta E + a(h_0 - h_2)]/\alpha x \qquad (3.10)$$

where h_0 is the atmospheric depth of the level of detection.

The directional intensity of muons, integrated over energy, is

$$I_\mu(h_0,\Delta E,x) = \int_{E_{min}}^{\infty} dE \int_0^{h_0} dh_2 \int_0^{h_2} dh_1 . F(E,h_1,h_2,h_0,x) \tag{3.11}$$

where $F(E,h_1,h_2,h_0,x) =$

$$\frac{m_\pi c}{\tau_\pi} \cdot \frac{f_\pi(E,h_1,x)}{\rho(h_2)Ex} \cdot \exp\left[-\frac{h_2 - h_1}{L_\pi x}\right] \cdot \exp\left[-\frac{m_\pi c}{\tau_\pi Ex} \int_{h_1}^{h_2} \frac{dh}{\rho(h)}\right] \cdot \exp\left[-\frac{m_\mu c}{\tau_\mu} \int_{h_2}^{h_0} \frac{dh}{\rho(h)} \cdot \frac{1}{\alpha Ex - a(h - h_2)}\right] \tag{3.12}$$

To proceed, assume that air obeys the perfect gas equation so that

$PV = \frac{m}{M} R'T$ where P = pressure, V = volume
m = mass of air, M = mean molecular weight of air = 28.97×10^{-3},
$R' = 8.314\ J\,mol^{-1}\,K^{-1}$ and
T = absolute temperature (K)

Thus

$$\rho = \frac{M}{R'} \cdot \left(\frac{P}{T}\right) .$$

But $P[Nm^{-2}] = 9.81\ h\ [kg\ m^{-2}]$ and so

$$\rho[kg\ m^{-3}] = \frac{h[kg\ m^{-2}]}{29.25T}$$

or

$$\rho[g\ cm^{-3}] = \frac{h[g\ cm^{-2}]}{RT} \tag{3.13}$$

where $R = 2.925 \times 10^3$ cm K^{-1}.

To simplify (3.12), we may assume that the atmosphere is isothermal at temperature T. This is acceptable for underground telescopes. Define

$$\left.\begin{aligned} b_{\pi,\mu} &= q_{\pi,\mu}\, T \\ \text{where} \qquad q_{\pi,\mu} &= \frac{m_{\pi,\mu} cR}{\tau_{\pi,\mu}} \end{aligned}\right\} \tag{3.14}$$

Then (3.12) becomes

$$F(E,h_1,h_2,h_0,x) = \frac{b_\pi}{h_2 x} \cdot I_0 E^{-\gamma-1} \cdot \exp\left[-\frac{h_1}{L_p x} - \frac{h_2-h_1}{L_\pi x}\right] \cdot \exp\left[-\int_{h_1}^{h_2} \frac{dh}{h} \cdot \frac{b_\pi}{Ex}\right] \cdot \exp\left[-\int_{h_2}^{h_0} \frac{dh}{h} \cdot \frac{b_\mu}{\alpha Ex - a(h-h_2)}\right] \ldots \tag{3.15}$$

Expression (3.15) is substituted into (3.11) and the various atmospheric effects are derived by taking partial derivatives of (3.11) with respect to the different atmospheric parameters.

3.2.2 The Barometer Effect

Differentiation of (3.11) with respect to h_0 gives

$$\delta I_\mu(h_0,\Delta E,x) = -\delta E_{min}\int_0^{h_0} dh_2 \int_0^{h_2} dh_1 \cdot F(E_{min},h_1,h_2,h_0,x)$$

$$+ \delta h_0 \int_{E_{min}}^{\infty} dE \left\{ - \frac{m_\mu c}{\tau_\mu \rho(h_0)} \int_0^{h_0} dh_2 \int_0^{h_2} dh_1 \cdot \frac{F(E,h_1,h_2,h_0,x)}{\alpha E x - a(h_0 - h_1)} \right.$$

$$\left. + \int_0^{h_0} dh_1 . F(E,h_1,h_2,h_0,x) \right\} \qquad (3.16)$$

From (3.10),

$$\delta E_{min} = \frac{a}{\alpha x} \cdot \delta h_0 \qquad (3.17)$$

which is substituted in (3.16). The right hand side of (3.16) is broken down as follows: the first term is the simple air mass absorption effect, while the second consists of two parts. The first of these expresses the contribution of muon decay to the barometer effect and the second results from variation in the number of pions being created. For detectors near sea level, or underground, the last part is negligible.

Choice of units

At this point, a certain choice of units will simplify further algebra considerably. As in Dorman (1957), we note that $a \simeq 2$ MeV cm^2 g^{-1} over a wide energy range. At very high energies, α rises, but the ionization loss term $a(h_0 - h_2)$ is negligible compared with the total energy of the muon. Thus, choosing 1000 g cm^{-2} as the unit of depth and 2 GeV as the unit of energy, $a = 1$. Finally, since both Cambridge and Poatina are near sea level, $h_0 = 1$.

The mass absorption term

(i) Integration over h_1

Define

$$\left.\begin{aligned} \eta &= h_1/h_2 \\ \psi_1 &= h_2/\lambda x \\ \psi_2 &= b_\pi/Ex \quad \text{where } 1/\lambda = 1/L_\pi - 1/L_p \end{aligned}\right\} \tag{3.18}$$

Then it may be shown that

$$\int_0^{h_2} dh_1 . F(E_{min}, h_1, h_2, h_0, x) = h_2 \int_0^1 d\eta . F(E_{min}, h_1, h_2, 1, x)$$

$$= \frac{I_0 E^{-\gamma} b_\pi}{x} . \exp(-h_2/L_\pi x) . h_2^{b_\mu/\alpha Ex} \int_0^1 \exp(\eta\psi_1)\, \eta^{\psi_2} d\eta \tag{3.19}$$

where $E = E_{min}$ and muon ionization losses in the atmosphere have been ignored.

To a first approximation, $L_\pi = L_p = L$ (say) $= 0.12$ (using our special units). Therefore $\psi_1 = 0$ and (3.19) becomes

$$\int_0^{h_2} dh_1 . F = \frac{I_0 E^{-\gamma} \exp(-h_2/Lx)\, h_2^{b_\mu/\alpha Ex}}{1 + (Ex/b_\pi)} \tag{3.20}$$

(ii) Integration over h_2

$$\int_0^{h_0} dh_2 \int_0^{h_2} dh_2 . F = \int_0^1 dh_2 \int_0^{h_2} dh_1 . F$$

$$= \frac{I_0 E^{-\gamma}}{1 + Ex/b_\pi} \int_0^1 \exp(-h_2/Lx)\, h_2^{b_\mu/\alpha Ex}\, dh_2 =$$

$$= \frac{I_0 E^{-\gamma}}{1 + Ex/b_\pi} (Lx)^{1+b_\mu/\alpha Ex} \int_0^{1/Lx} \exp(-t)\, t^{b_\mu/\alpha Ex}\, dt \quad \text{where } t = h_2/Lx$$

$$= \frac{I_0 E^{-\gamma}}{1 + Ex/b_\pi} (Lx)^{y} . \int_0^{1/Lx} \exp(-t)\, t^{y-1}\, dt \quad \text{where } y = 1 + b_\mu/\alpha Ex \quad . \tag{3.21}$$

Since $1/Lx >> 1$, the integral in (3.21) approximates the "gamma function" which is defined by

$$\Gamma(y) \equiv \int_0^{\infty} \exp(-t)\, t^{y-1}\, dt$$

$$\equiv \Gamma(y+1)/y \quad \text{where } \Gamma(1) \equiv 1.$$

Thus

$$\int_0^{1/Lx} dt \exp(-t)\, t^{y-1} \simeq (Lx)^{1+b_\mu/Ex} . \Gamma(1+b_\mu/\alpha Ex) \quad . \tag{3.22}$$

Evaluation of $b_\mu/\alpha Ex$ using (3.14) and the appropriate numbers yields $\sim 5 \times 10^{-11}$ and 5×10^{-12} for Cambridge and Poatina respectively, values which are negligible. Then

$$\int_0^1 dh_2 \int_0^{h_2} dh_1 . F \simeq \frac{I_0\, E^{-\gamma}}{1 + Ex/b_\pi} . Lx \tag{3.23}$$

Therefore from (3.16), (3.17) and (3.23), the final expression for the mass absorption term (which forms the numerator in the mass absorption *coefficient*) is

$$\delta I_\mu(1, \Delta E, x)_{abs} = - \delta E_{min} \int_0^1 dh_2 \int_0^{h_2} dh_1 . F = \frac{I_0 L E_{min}^{-\gamma}}{\alpha(1 + E_{min} x/b_\pi)} \cdot \delta h_0 \tag{3.24}$$

(iv) Integration over E

This final integration is required to derive an expression for

$$I_\mu(h_0 = 1, \Delta E, x) \cdot \delta h_0$$

which forms the denominator in the final formulae for the mass absorption and muon decay components of the barometer coefficient.

From (3.11) and (3.23)

$$I_\mu(1, \Delta E, x) = \int_{E_{min}}^{\infty} dE \int_0^1 dh_2 \int_0^{h_2} dh_1 . F$$

$$= I_0 L x \int_{E_{min}}^{\infty} \frac{E^{-\gamma}}{1 + Ex/b_\pi} dE \qquad (3.25)$$

At high energies, $\gamma \to 3$. From Gradshteyn and Rhyzik (1965, Equation 2.118-3) comes the standard integral

$$\int \frac{dx}{x^3(a + bx)} = \frac{-1}{2ax^3} + \frac{b}{a^2 x} - \frac{b^2}{a^3} \ln\left(\frac{a + bx}{x}\right) \qquad (3.26)$$

We use the fact that at higher energies,

$$E_{min} \simeq \frac{\Delta E}{\alpha x} . \qquad (3.27)$$

Applying (3.26) to (3.25) yields

$$I_\mu(1, \Delta E, x) = \frac{I_0 L b_\pi x^3}{3} \left(\frac{\alpha}{\Delta E}\right)^3 \qquad (3.28)$$

Finally, from (3.24), (3.27) and (3.28) the mass absorption coefficient is

$$\beta_{abs}(1,\Delta E,x) = \frac{1}{\delta h_0} \cdot \frac{\delta I_\mu(1,\Delta E,x)_{abs}}{I_\mu(1,\Delta E,x)} = \frac{-3x}{b_\pi \alpha + \Delta E}$$

From (3.14), $b_\pi \alpha$ is negligible, leaving

$$\beta_{abs}(1,\Delta E,x) = \frac{-3x}{\Delta E} \quad (1000\ g\ cm^{-2})^{-1}$$

$$\equiv \frac{-0.6x}{\Delta E[GeV]} \quad \% \quad (g\ cm^{-2})^{-1}$$

$$\simeq \frac{-0.6x}{\Delta E[GeV]} \quad \% \quad mb^{-1} \qquad (3.29)$$

The muon decay term

We consider the first part of the second term in (3.16). Since $a(h_0 - h_2) << \alpha E x$ we may again ignore ionization losses and the expression becomes

$$\delta I_\mu(h_0 = 1,\Delta E,x)_{decay} = \frac{-\delta h_0\, m_\mu\, c}{\tau_\mu \rho(h_0)\,\alpha x} \int_{E_{min}}^{\infty} \frac{dE}{E} \int_0^1 dh_2 \int_0^{h_2} dh_1 \cdot F$$

$$= \frac{-\ h_0\, m_\mu\, c\, I_0 L}{\alpha\ \tau_\mu\ \rho(h_0)} \int_{E_{min}}^{\infty} \frac{E^{-(\gamma+1)}}{1 + Ex/b_\pi} \cdot dE \qquad (3.30)$$

Again, $\gamma \simeq 3$. The expression may then be simplified using another standard integral (Gradshteyn and Rhyzik, Equation 2.117-4):

$$\int \frac{dx}{x^4(a+bx)} = \frac{-1}{3ax^3} + \frac{b}{2a^2x^2} - \frac{b^2}{a^3x} + \frac{b^3}{a^4} \ln\left(\frac{a+bx}{x}\right) \qquad (3.31)$$

Using (3.30) and (3.31) where the lower limit of the integral is again $E_{min} \simeq \Delta E/\alpha x$, the decay term simplifies to give

$$\delta I_\mu(1,\Delta E,x)_{decay} = \frac{-\delta h_0 m_\mu c I_0 L}{\tau_\mu \rho(h_0)} \cdot \frac{x^2}{4} \cdot \frac{b_\pi}{\Delta E} \left(\frac{\alpha}{\Delta E}\right)^3 \qquad (3.32)$$

Then from (3.12), (3.14), (3.28) and (3.32), the muon decay coefficient is

$$\beta_{decay}(1,\Delta E,x) = \frac{1}{\delta h_0'} \cdot \frac{\delta I_\mu(1,\Delta E,x)_{decay}}{I_\mu(1,\Delta E,x)}$$

$$= \frac{-3}{4\Delta E} \cdot \frac{m_\mu c}{\tau_\mu \rho(h_0)}$$

$$= -\frac{3}{4} \cdot \frac{m_\mu c\, RT}{\Delta E\, \tau_\mu} \qquad (1000 \text{ g cm}^{-2})^{-1}$$

$$\equiv -\frac{0.102}{\Delta E[\text{geV}]} \qquad \% \ (\text{g cm}^{-2})^{-1}$$

$$\simeq -\frac{0.1}{\Delta E[\text{GeV}]} \qquad \% \ \text{mb}^{-1} \qquad (3.33)$$

The complete barometer coefficient for an underground detector with threshold energy $\Delta E \gtrsim 10$ GeV is then

$$\beta_p(1,\Delta E,x) \simeq -\frac{(0.6x + 0.1)}{\Delta E} \ \% \ \text{mb}^{-1} \qquad (3.34)$$

From (3.34) it is seen that, for vertically incident particles, the mass absorption effect is six times as large as the muon decay effect.

Estimated Barometer Coefficients from Cambridge and Poatina

To obtain the barometer coefficient seen by an actual telescope having a finite viewing cone, it is necessary to integrate the *directional* (x-dependent) coefficient $\beta(1,\Delta E,x)$ over the radiation sensitivity function of the telescope. This function is denoted

$$RS(x) = GS(x)x^n$$

where GS(x) is the geometrical sensitivity function of the instrument and x^n represents the angular distribution of muon intensity. The best-fit value of n is ~ 2.2 for θ up to $\sim 70°$ (Parsons, 1959) - viz. x down to 0.342.

Calculations of $RS(\theta)$ for various telescope geometries and tilt angles have been carried out by Parsons (1959), Lindgren (1965) and others. Figure 3.2 shows the $RS(\theta)$ and $GS(\theta)$ dependence over a vertical semicubical telescope (Parsons). It is seen that the $RS(\theta)$ curve reaches a maximum at about 23°.

Reverting to the RS(x) formalism, the aperture-integrated pressure coefficient seen by an underground telescope is then

$$\beta_p(1,\Delta E) = \frac{\int_0^1 \beta_p(1,\Delta E,x).RS(x)\,dx}{\int_0^1 RS(x)\,dx} \qquad (3.35)$$

For Cambridge and Poatina, substitution of the appropriate muon threshold energies in (3.34) yields - 0.07

and -0.007 % mb^{-1} respectively, for vertically incident muons. These values agree quite well with those predicted by the simpler method in Section 3.1. However, as already pointed out, the dependence on x in (3.34) is not valid for small values of ΔE (such as at Cambridge). The latter formula is only approximate for small depths underground where muon energy losses due to ionization cannot be regarded as negligible, and γ is somewhat less than 3.

Thus the integrated barometer coefficient for Cambridge, for virtually any telescope geometry and angle of tilt, will be

$$\beta_p(1, \Delta E = 10 \text{ GeV})_{\text{Camb.}} \cong -0.07 \text{ \% } mb^{-1} \qquad (3.36a)$$

To obtain the integrated pressure coefficient for Poatina, a cubic spline was fitted to RS(x) and (3.35) evaluated numerically with (3.34) substituted in. The result obtained was

$$\beta_p(1, \Delta E = 100 \text{ GeV})_{\text{Poa.}} \cong -0.003 \text{ \% } mb^{-1} \qquad (3.36b)$$

[N.B. More significant figures are meaningless in view of the approximation $\gamma = 3$ used to obtain 3.34.]

3.2.3 The Temperature Effect

Case 1: Small Depths Underground

As for the barometer coefficient, for underground telescopes it is acceptable to assume an isothermal atmosphere of temperature $T \simeq 217$ K. However, in the interests of

accuracy, the muon energy loss term - $(h-h_2)$ in equation 3.15 will not be dropped in these calculations. As will be seen later, the temperature coefficient varies with atmospheric depth and omission of the energy loss term distorts the shape of the curve for low to medium cut-off energies.

Differentiation of (3.11) with respect to T gives

$$\delta I_\mu(1,\Delta E,x) = \int_{E_{min}}^{\infty} dE \int_0^1 dh_2 \int_0^{h_2} dh_1 . F(E,h_1,h_2,1,x)$$

$$\cdot \left\{ \frac{\delta T}{T} - \frac{b_\pi}{Ex} \int_{h_1}^{h_2} \frac{dh}{h} \frac{\delta T}{T} - b_\mu \int_{h_2}^{1} \frac{dh}{T.h} \frac{\delta T}{\alpha Ex - (h-h_2)} \right\} \qquad (3.37)$$

where, again, $a = h_0 = 1$. The first two terms in the brackets in (3.37) represent the positive temperature effect which is caused by competition between pion decay and interaction. The third term represents the negative temperature effect which is due to the effect of atmospheric expansion on the probability of muon decay.

(i) Integration over h_1

Consider the first term in brackets in (3.37); we have

$$\int_0^{h_2} dh_1 . F . \frac{\delta T}{T}$$

$$= \frac{\delta T}{T} \cdot \frac{I_0 b_\pi E^{-(\gamma+1)}}{x} \cdot \exp(-h_2/L_\pi x) \cdot \exp\left[- \int_{h_2}^{1} \frac{dh}{h} \cdot \frac{b_\mu}{\alpha E x - h + h_2} \right]$$

$$\cdot \int_0^1 \exp(\eta\psi_1)\, \eta^{\psi_2} d\eta$$

$$= \frac{\delta T}{T} \cdot \frac{I_0 b_\pi E^{-(\gamma+1)}}{x} \cdot \exp(-h_2/Lx) \cdot \exp\left[- \int_{h_2}^{1} \frac{dh}{h} \cdot \frac{b_\mu}{\alpha E x - h + h_2} \right]$$

$$\cdot \left(\frac{1}{1 + b_\pi/Ex} \right) \qquad (3.38)$$

where again we let $L_P = L_\pi = L$ so that ψ_1 vanishes. The argument in the second exponential in (3.38) may be simplified using the following method:

Let $t = E_{min}/E = (1 - h_2 + \Delta E)/\alpha E x$

$$\therefore \quad \alpha E x = (1 - h_2 + \Delta E)/t$$

Thus $$- \int_{h_2}^{1} \frac{dh}{h} \cdot \frac{b_\mu}{\alpha E x - h + h_2}$$

$$= b_\mu t \int_{h_2}^{1} \frac{dh}{th^2 - kh} \quad \text{where} \quad k = h_0 - h_2(1 - t) + \Delta E \ .$$

Using the standard integral

$$\int \frac{dh}{R} = \frac{1}{\sqrt{-\Delta}} \ln \frac{b + 2ch - \sqrt{-\Delta}}{b + 2ch + \sqrt{-\Delta}}$$

where $R = a + bh + ch^2$ and $\Delta = 4ac - b^2 < 0$ (Gradshteyn and Rhyzik, equation 2.172) the expression

$$\frac{b_\mu t}{h_0 - h_2(1-t) + \Delta E} \cdot \ln\left[h_2\left(1 - t \cdot \frac{1-h_2}{1-h_2+\Delta E}\right)\right]$$

$$= \nu t \quad \text{where} \quad \nu = \frac{b_\mu}{h_0 - h_2(1-t) + \Delta E} \ln\left[h_2\left(1 - t \cdot \frac{1-h_2}{1-h_2+\Delta E}\right)\right]$$

(3.39)

Thus (3.38) simplifies to

$$\int_0^{h_2} dh_1 . F . \frac{\delta T}{T} = \frac{\delta T}{T} \frac{I_0 b_\pi E^{-(\gamma+1)}}{x} . \exp(-h_2/Lx) . \frac{\exp(\nu t)}{1 + \frac{b_\pi}{E_x}}$$

$$= \frac{\frac{\delta T}{T} . I_0 E^{-\gamma} \exp(-h_2/Lx) \exp(\nu t)}{1 + \frac{E_x}{b_\pi}} \qquad (3.40)$$

Integrating the second term in brackets in (3.37), we have

$$\int_0^{h_2} dh_1 . F \left[- \frac{b_\pi}{Ex} \frac{\delta T}{T} \int_{h_1}^{h_2} \frac{dh}{h} \right]$$

$$= \frac{\delta T}{T} \frac{b_\pi}{Ex} \int_0^{h_2} dh_1 . F . \ln\left(\frac{h_1}{h_2}\right)$$

$$= \frac{\delta T}{T} \left(\frac{b_\pi}{Ex}\right)^2 \frac{I_0 E^{-\gamma}}{h_2} . \exp\left[- \frac{h_2}{Lx} - \int_{h_2}^{1} \frac{dh}{h} \frac{b_\mu}{\alpha Ex - h + h_2} \right]$$

$$. \int_0^{h_2} dh_1 \left(\frac{h_1}{h_2}\right)^{b_\pi/Ex} \ln\left(\frac{h_1}{h_2}\right)$$

Again, letting $\eta = h_1/h_2$ and $\psi_2 = b_\pi/Ex$, the last factor in the expression above becomes

$$h_2 \int_0^1 d\eta . \eta^{\psi_2} \ln \eta = \frac{- h_2}{(1 + \psi_2)^2}$$

$$\frac{- h_2}{(1 + b_\pi/Ex)^2}$$

so that the complete expression is

$$\frac{- \frac{\delta T}{T} I_0 \left(\frac{b_\pi}{Ex}\right)^2 E^{-\gamma} \exp(-h_2/Lx) \exp(\nu t)}{\left(1 + \frac{b_\pi}{Ex}\right)^2}$$

$$= \frac{- \frac{\delta T}{T} I_0 E^{-\gamma} \exp(-h_2/Lx) \exp(\nu t)}{\left(1 + \frac{Ex}{b_\pi}\right)^2} \qquad (3.41)$$

The total positive temperature effect is then found by adding (3.40) and (3.41):

$$\frac{\frac{\delta T}{T} I_0 E^{-\gamma} \exp(-h_2/Lx) \exp(\nu t)}{1 + \frac{Ex}{b_\pi}} \left\{1 - \frac{1}{1 + \frac{Ex}{b_\pi}}\right\}$$

$$= \frac{\frac{\delta T}{T} I_0 E^{-\gamma} \exp(-h_2/Lx) \exp(\nu t)}{\left(1 + \frac{Ex}{b_\pi}\right)\left(1 + \frac{b_\pi}{Ex}\right)} \qquad (3.42)$$

Finally, integration of the third, *negative* temperature term in (3.37) proceeds as follows:

$$\int_0^{h_2} dh_1 . F \left[- b_\mu \int_{h_2}^{1} \frac{\delta T}{T} \frac{dh}{h} \frac{1}{\alpha Ex - h + h_2} \right]$$

$$= - \int_0^{h_2} dh_1 . F \frac{\delta T}{T} \int_{h_2}^{1} \frac{dh}{h} . \frac{b_\mu}{\alpha Ex - h + h_2}$$

$$= - \frac{\frac{\delta T}{T} I_0 E^{-\gamma} \exp(-h_2/Lx) \exp(\nu t)}{1 + \frac{Ex}{b_\pi}} \int_{h_2}^{1} \frac{dh}{h} . \frac{b_\mu}{\alpha Ex - h + h_2} \qquad (3.43)$$

by virtue of (3.40).

(ii) Integration over E

(a) Positive temperature effect

We require a simplified expression for

$$\int_{E_{min}}^{\infty} dE . \frac{\frac{\delta T}{T} I_0 E^{-\gamma} \exp(-h_2/Lx) \exp(\nu t)}{\left(1 + \frac{Ex}{b_\pi}\right) \left(1 + \frac{b_\pi}{Ex}\right)} \qquad (3.44)$$

Apply again the change of variable $t = \frac{E_{min}}{E}$, and define

$$s = \frac{E_{min} x}{b_\pi} = \frac{1 - h_2 + \Delta E}{\alpha b_\pi} \qquad (3.45)$$

Then (3.44) becomes

$$\frac{\delta T}{T} \cdot I_0 \exp\left(\frac{-h_2}{Lx}\right) \int_0^1 \left(\frac{t}{E_{min}}\right)^{\gamma-1} s\left(\frac{1}{t+s}\right)^2 \exp(\nu t)\,dt$$

$$= \frac{\delta T}{T} \cdot \frac{I_0\ \alpha^{\gamma-2}\, x^{\gamma-1} \cdot \exp(-h_2/Lx)}{b_\pi (1 - h_2 + \Delta E)^{\gamma-2}} \int_0^1 \frac{t^{\gamma-1} \exp(\nu t)\,dt}{(t+s)^2}$$

$$= \frac{\delta T}{T} \cdot \frac{I_0\ \alpha^{\gamma-2}\, x^{\gamma-1} \exp(-h_2/Lx)}{b_\pi (1 - h_2 + \Delta E)^{\gamma-2}} \cdot G_\gamma(s,\nu) \qquad (3.46)$$

where

$$G_\gamma(s,\nu) = \int_0^1 \frac{t^{\gamma-1}}{(t+s)^2} \exp(\nu t)\,dt \qquad (3.47)$$

Thus

$$\delta I_\mu(l,\Delta E,x)_{pos.} = \int_0^1 \frac{W_T^*(h_2,l,\Delta E\ x)}{\delta T} \cdot \delta T\ dh_2 \qquad (3.48)$$

where the numerator W_T^* of the integrand is the expression (3.46). Since variations in intensity are usually expressed as relative changes from the mean, we require an expression for the total directional muon intensity.

To obtain an expression for $I_\mu^{total}(l,\Delta E,x)$, we have

$$I_\mu^{total}(l,\Delta E,x) = \int_{E_{min}}^{\infty} dE \int_0^h dh_2 \int_0^{h_2} dh_1 \cdot F$$

$$= \int_0^1 dh_2 \int_{E_{min}}^{\infty} dE \cdot \frac{I_0 E^{-\gamma} \exp\left(\frac{-h_2}{Lx}\right) \exp(\nu t)}{1 + \frac{Ex}{b_\pi}}$$

$$= I_0 (\alpha x)^{\gamma-1} \int_0^1 dh_2 \frac{\exp\left(\frac{-h_2}{Lx}\right) \cdot H_\gamma(s,\nu)}{(1 - h_2 + \Delta E)^{\gamma-1}}$$

where

$$H_\gamma(s,\nu) = \int_0^1 \frac{t^{\gamma-1}}{t+s} \exp(\nu t)\,dt \qquad (3.49)$$

using the same methods employed in deriving (3.46). Thus

$$I_\mu^{\text{total}}(1,\Delta E,x) = I_0(\alpha x)^{\gamma-1} D_\gamma(1,x) \qquad (3.50)$$

where

$$D_\gamma(1,x) = \int_0^1 \frac{\exp(-h_2/Lx).H_\gamma(s,\nu)}{(1-h_2+\Delta E)^{\gamma-1}}\,dh_2 \qquad (3.51)$$

Finally, dividing (3.48) by (3.50) yields

$$\left[\frac{\delta I_\mu(1,\Delta E,x)}{I_\mu(1,\Delta E,x)}\right]_{\text{pos}} = \int_0^1 W_T^{\text{pos}}(h,1,\Delta E,x)\,\delta T(h)\,dh \qquad (3.52)$$

where

$$W_T^{\text{pos}}(h,1,\Delta E,x) = \frac{\exp(-h/Lx).G_\gamma(s,\nu)}{\alpha T b_\pi (1-h+\Delta E)^{\gamma-2}.H_\gamma(s,\nu)} \qquad (3.53)$$

$W_T^{\text{pos}}(h,1,\Delta E,x)$ is known as the "positive temperature coefficient weighting function" and specifies the temperature influence, due to pion decay, of a differential layer of the atmosphere $[h,h+dh]$. (The "2" subscript on h_2 has been dropped as it is now just a dummy variable.)

(b) Negative temperature effect

A simplified expression is required for

$$\int_{E_{min}}^{\infty} dE \cdot \frac{-\frac{\delta T}{T} I_0 E^{-\gamma} \exp(-h_2/Lx) \exp(\nu t)}{1 + \frac{Ex}{b_\pi}} \int_{h_2}^{1} \frac{dh}{h} \cdot \frac{b_\mu}{\alpha E x - h + h_2}$$

Again using $t = \frac{E_{min}}{E}$ and $s = \frac{E_{min} x}{b_\pi}$, integration of (3.54) over terms dependent on E will be

$$\int_0^1 dt . E_{min} \left(\frac{t}{E_{min}}\right)^{\gamma} \frac{1}{t+s} \frac{1}{1 - h_2 + \Delta E - t(h - h_2)} \exp(\nu t)$$

$$= \left(\frac{\alpha x}{1 - h_2 + \Delta E}\right)^{\gamma-1} \int_0^1 dt \cdot \frac{t^{\gamma}}{t+s} \cdot \frac{1}{h - h_2} \cdot \frac{1}{\left[\frac{1 - h_2 + \Delta E}{h - h_2} - t\right]} \exp(\nu t)$$

$$= \frac{(\alpha x)^{\gamma-1}}{(1 - h_2 + \Delta E)^{\gamma}} \int_0^1 dt \cdot \frac{k t^{\gamma} \exp(\nu t)}{(t+s)(k-t)} \quad \text{where } k = \frac{1 - h_2 + \Delta E}{h - h_2}$$

$$= \frac{(\alpha x)^{\gamma-1}}{(1 - h_2 + \Delta E)^{\gamma}} \cdot K_{\gamma}(s,k,\nu) \tag{3.55}$$

where

$$K_{\gamma}(s,k,\nu) = \int_0^1 \frac{k t^{\gamma} \exp(\nu t)}{(t+s)(k-t)} dt \tag{3.56}$$

Thus

$$\delta I_{\mu}(1,\Delta E,x)_{neg} = -I_0 \frac{\delta T}{T} b_{\mu} \int_0^1 dh_2 \frac{(\alpha x)^{\gamma-1}}{(1-h_2 + \Delta E)^{\gamma}} K_{\gamma}(s,k,\nu) \exp(-h_2/Lx) \int_{h_2}^{1} \frac{dh}{h}$$

This awkward integration is simplified by changing the order and limits of integration, thus:

$$\int_0^1 dh_2 \int_{h_2}^1 dh \rightarrow \int_0^1 dh \int_0^h dh_2$$

Applying this, we get

$$\delta I_\mu(1,\Delta E,x)_{neg} = -\int_0^1 dh \frac{\delta T\, I_0\, q_\mu (\alpha x)^{\gamma-1}}{h} \int_0^h \frac{K_\gamma(s,k,\nu)\, \exp(-h_2/Lx)}{(1-h_2+\Delta E)^\gamma} dh_2 \qquad (3.57)$$

Division of (3.57) by (3.50) gives

$$\left[\frac{\delta I_\mu(1,\Delta E,x)}{I_\mu(1,\Delta E,x)}\right]_{neg} = \int_0^1 W_T^{neg}(h,1,\Delta E,x)\, \delta T(h)\, dh \qquad (3.58)$$

where

$$W_T^{neg}(h,1,\Delta E,x) = \frac{-q_\mu}{D_\gamma(1,x)h} \int_0^h \frac{K_\gamma(s,k,\nu)\exp(-h_2/Lx)}{(1-h_2+\Delta E)^\gamma} dh_2 \qquad (3.59)$$

The complete temperature weighting function is then

$$W_T(h,1,\Delta E,x) = W_T^{pos}(h,1,\Delta E,x) + W_T^{neg}(h,1,\Delta E,x) \qquad (3.60)$$

for muon telescopes at or below sea level. (Again, h_2 becomes h, in the interests of simplicity.)

Case 2: Large Depths Underground

For observations deep underground, ionization losses of muons in the atmosphere are negligible compared with the

threshold energy and we can use the simplified expression for the total directional muon intensity:

$$I_\mu(l,\Delta E,x) = \frac{I_0 L b_\pi x^3}{3} \left(\frac{\alpha}{\Delta E}\right)^3 \qquad (3.28)$$

(a) Positive temperature effect

In (3.38), the second exponential becomes

$$\exp\left[-\int_{h_2}^{l} \frac{dh}{h} \frac{b_\mu}{\alpha E x}\right] = \exp\left[\frac{b_\mu}{\alpha E x} \ln h_2\right]$$

$$= h_2^{\,b_\mu/\alpha E x}$$

$$\simeq 1 \text{ since, for example at Poatina,}$$

$b_\mu/\alpha E x < 5 \times 10^{-12}$ for vertically incident muons.

Thus (3.42) becomes $\dfrac{\frac{\delta T}{T} I_0 E^{-\gamma} \exp(-h_2/Lx)}{\left(1 + \frac{Ex}{b_\pi}\right)\left(1 + \frac{b_\pi}{Ex}\right)}$. Integration over E is then

$$\frac{\delta T}{T} I_0 \exp(-h_2/Lx) \int_{E_{min}}^{\infty} \frac{dE}{E^\gamma \left(1 + \frac{Ex}{b_\pi}\right)\left(1 + \frac{b_\pi}{Ex}\right)}$$

$$= \frac{\delta T}{T} I_0 \exp(-h_2/Lx) \cdot \frac{b_\pi x^2}{3} \left(\frac{\alpha}{\Delta E}\right)^3 \qquad \text{where } \gamma = 3 \qquad (3.61)$$

Division of (3.61) by (3.28) yields

$$W_T^{pos}(h,l,\Delta E \to \infty, x) = \frac{\exp(-h/Lx)}{TLx} \qquad (3.62)$$

(b) Negative temperature effect

Integration of (3.37) over h_1 will be:

$$\int_0^{h_2} dh_1 . F\left[-b_\mu \int_{h_2}^{1} \frac{\delta T}{T} \frac{dh}{h} \frac{1}{\alpha Ex}\right]$$

$$= - \frac{\frac{\delta T}{T} I_0 E^{-\gamma} b_\mu \exp(-h_2/Lx) h_2^{\,b_\mu/\alpha Ex}}{1 + \frac{Ex}{b_\pi}} \int_{h_2}^{1} \frac{dh}{h}$$

Using the change in the order of integration, the integral over h_2 is then

$$- \frac{\frac{\delta T}{T} I_0 E^{-\gamma} b_\mu}{1 + \frac{Ex}{b_\pi}} \int_0^1 \frac{dh}{h} \cdot \frac{1}{\alpha Ex} \int_0^h dh_2 . \exp(-h_2/Lx) h_2^{\,b_\mu/\alpha Ex}$$

Using the change of variable $t = h_2/Lx$, Dorman (1957) shows that the final integral is approximately

$$Lx[1 - \exp(-h/Lx)] \text{ provided } b_\mu/\alpha Ex << 1 .$$

Integration over E then proceeds:

$$- \frac{\delta T}{T} I_0 \, Lx \, [1 - \exp(-h/Lx)] \; \frac{b_\mu}{h\alpha x} \int_{E_{min}}^{\infty} \frac{dE}{E^{\gamma+1}\left(1 + \frac{Ex}{b_\pi}\right)}$$

$$= - \frac{\delta T}{T} I_0 \, Lx \, [1 - \exp(-h/Lx)] \; \frac{b_\mu}{h} \cdot \frac{x^2}{4} \; \frac{b_\pi}{\Delta E} \; \left(\frac{\alpha}{\Delta E}\right)^3 \qquad (3.63)$$

where $\gamma=3$ and using the same integral employed in deriving (3.32).

Division of (3.63) by (3.28) gives

$$W_T^{neg}(h,1,\Delta E \to \infty,x) = -\frac{3}{4}\frac{q_\mu}{h\Delta E}[1 - \exp(-h/Lx)] \qquad (3.64)$$

(c) Asymptotic Behaviour with Energy

From equation 3.62 , the positive temperature weighting function reaches a maximum at $h = 0$ and is independent of ΔE when ΔE is very large. Consider a uniform change in temperature $\delta T = 1$ K over the whole atmosphere. The "integrated" positive temperature coefficient will be

$$\int_0^1 W_T^{pos}(h,1,\Delta E,x)\,dh = -\frac{1}{T}[\exp(-8.3) - 1]$$

$$\simeq \frac{1}{T} K^{-1} \qquad (3.65)$$

where $L = 0.12$ atm $= 120$ g cm^{-2}.

Inserting $T = 217$ K (ICAO Standard Atmosphere) yields an upper limit of 0.46 % K^{-1}.

Meanwhile from (3.64), at high muon threshold energies the negative temperature effect becomes negligible. For example, for $h = 100$ g cm^{-2} and $\Delta E = 100$ GeV, $W_T^{neg}(h) < -7 \times 10^{-15}$ % (g cm^{-2})$^{-1}$ K^{-1}.

(d) Predicted Temperature Coefficients at Poatina and Cambridge

Traditionally, the temperature effect has most often been removed from the muon count rate by using a single temperature coefficient. This method is easy to apply if

a reliable long term coefficient can be obtained via regression analysis. However, representing the temperature effect as a single coefficient assumes that all pion production occurs at some discrete level (such as 100 mb), or over an interval of pressure whose temperature might be represented by a weighted mean, computed from the measured temperature profile. Clearly, this assumption is rather crude since the temperature effect is a continuously varying function of pressure. Therefore the "temperature coefficient" is a somewhat ill-defined concept where the only practicable criterion for selecting the "best" one is to choose the one that gives the highest R^2 value in the regression.

For underground muon telescopes, the effective temperature coefficient will depend on the consistency of temperature variations in the stratosphere. To investigate temperature intercorrelations in the upper atmosphere, Hobart weather data were analysed for the period 1972-77. Using daily mean temperatures, the correlation matrix for 11 levels over the interval [20,300]mb has been computed and the results are shown in graphical form in Figure 3.4. The most important features are that temperatures tend to vary in the opposite sense above and below the tropopause, while consistent behaviour is found in the stratosphere. Thus, for high cut-off energies, it would seem that there is nothing to be gained by using a weighted temperature that includes temperatures from the lower atmosphere. Such a coefficient would be smaller than one computed using stratospheric temperatures only and would therefore account for less of the variation in the muon intensity.

In view of these facts, theoretical prediction of the coefficient is difficult. The temperature weighting function for Cambridge has been computed using the low-energy formulae (3.53) and (3.59), while for Poatina the curve has been calculated using the high-energy formula (3.62) only. The aperture-integrated curves have been obtained using

$$W_T(h,1,\Delta E) = \frac{\int_0^1 W_T(h,1,\Delta E,x)\,RS(x)\,dx}{\int_0^1 RS(x)\,dx}$$

where the radiation sensitivity curves are shown, as functions of θ, in Figures 3.2 - 3.3. The variation of $W_T(h,1,\Delta E,x)$ is shown in Figures 3.5 - 3.7 while the final aperture-integrated curves for the two sites are given in Figures 3.8 - 3.10. Included also, for comparison, is the curve for a vertical semicubical telescope which has operated at Cambridge.

To obtain the Poatina and Cambridge 70° zenith temperature coefficients, the curves in Figures 3.10 and 3.8 respectively have been integrated over the interval [25,200]g cm^{-2}. These values were chosen as acceptable outer limits, based on the behaviour of the upper air correlations in Figure 3.4. The resulting coefficients are shown in Table 3.1.

(e) The Influence of Kaon Decay on the Temperature Coefficient

To this point all calculations have assumed that muons are derived from pions only. However, it is known that the

TABLE 3.1

Temperature coefficients integrated over $h = [25,200] g\,cm^{-2}$.

Units are $\%\ K^{-1}$

	Positive effect	Negative effect	Sum
Cambridge	0.0619	- 0.0397	0.0222
Poatina	0.252	Negligible	0.252

The Poatina value agrees closely with that predicted by the simple method in Section 3.1. However, the negative effect is appreciable at the relatively shallow depth of Cambridge, resulting in an overall coefficient considerably smaller than that previously estimated.

TABLE 3.2

Charged kaon decay modes

Mode	Fraction of decays (%)
$K^{\pm} \rightarrow \mu^{\pm} + \nu$	63
$K^{\pm} \rightarrow \pi^{\pm} + \pi^{0}$	21
$K^{\pm} \rightarrow \pi^{\pm} + \pi^{\pm} + \pi^{\mp}$ $K^{\pm} \rightarrow \pi^{\pm} + \pi^{0} + \pi^{0}$	8
Other	8

proportion of charged kaons produced in primary interactions increases with energy. Burcham (1973) has listed the main decay modes of the kaon; the more important are given in Table 3.2.

At 100 GeV the mean decay length of a $K^{\pm}$ is ~ 0.75 km, compared with ~ 5.4 km for a $\pi^{\pm}$. If the overall kaon parentage of observed muons were large, a reduction in the size of the positive temperature effect would be expected.

The K:π ratio at these energies has been estimated by Barish et al. (1973). A target was bombarded with protons and the resulting secondary hadron beam tuned for positive particles of energy ~ 160 GeV. Of 112 neutrino events, 94 were identified as being of pion parentage and only 18 of kaon parentage. Although the errors are not given, from this evidence it seems reasonable to expect the "kaon effect" to have only a small influence on the positive temperature coefficient.

3.3 A Monte-Carlo Simulation of the Temperature Effect at Poatina.

3.3.1 Introduction

In an alternative estimation of the temperature coefficient at Poatina, a Monte Carlo simulation of the proton-pion-muon chain was carried out. The theory of the method is outlined in Appendix 1. Following standard practice, each run of the computer program begins with the injection of a given number of primary protons on the top of the atmosphere. The history of each subsequent pion and muon is traced down through the

TABLE 3.3

Assumptions used in constructing the Monte Carlo model

Angular distribution of primaries	Isotropic
Form of differential primary spectrum	$E_P^{-2.7}\, dE_P$
Proton interaction length, g cm^{-2}	80
Proton inelasticity	0.5
Charge ratio of pions $\pi^0:\pi^+:\pi^-$	1:1:1
Charged pion multiplicity	$m_{\pi^\pm} = 2\, E_P^{0.25}$
Pion interaction length, g cm^{-2}	100

atmosphere and rock overburden, until the muon is finally absorbed, decays or is detected.

To simulate the temperature effect, a step-wise temperature perturbation of 20°C was applied to the interval [0,150]g cm^{-2} below the top of the atmosphere.

3.3.2 Results

Fifteen simulations were performed, each beginning with the injection of 50,000 primary protons. Each run used a different number to initialize the random number generator. Five runs were performed for zero temperature perturbation, five for + 20°C and five for - 20°C. The resulting weighted mean temperature coefficient was

$$b_{IT} = (0.22 \pm 0.05)\%\ K^{-1}$$

This value is in broad agreement with those predicted in Sections 3.1 and 3.2.

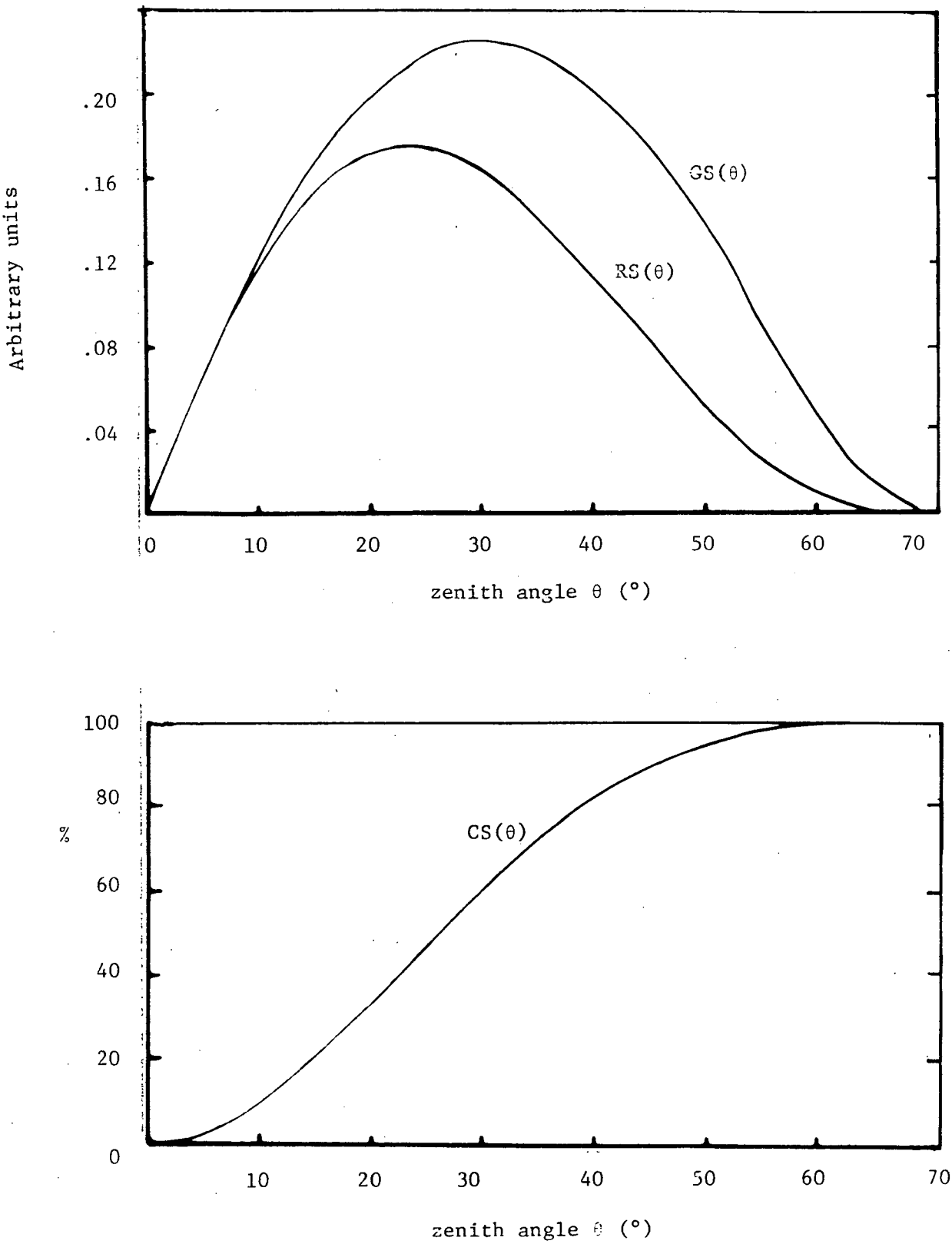

Figure 3.2. Sensitivity functions for a vertical semicubical telescope (Parsons, 1959)

GS(θ) = geometrical sensitivity function
RS(θ) = radiation sensitivity function
CS(θ) = cumulative sensitivity function
= integral under RS(θ) curve

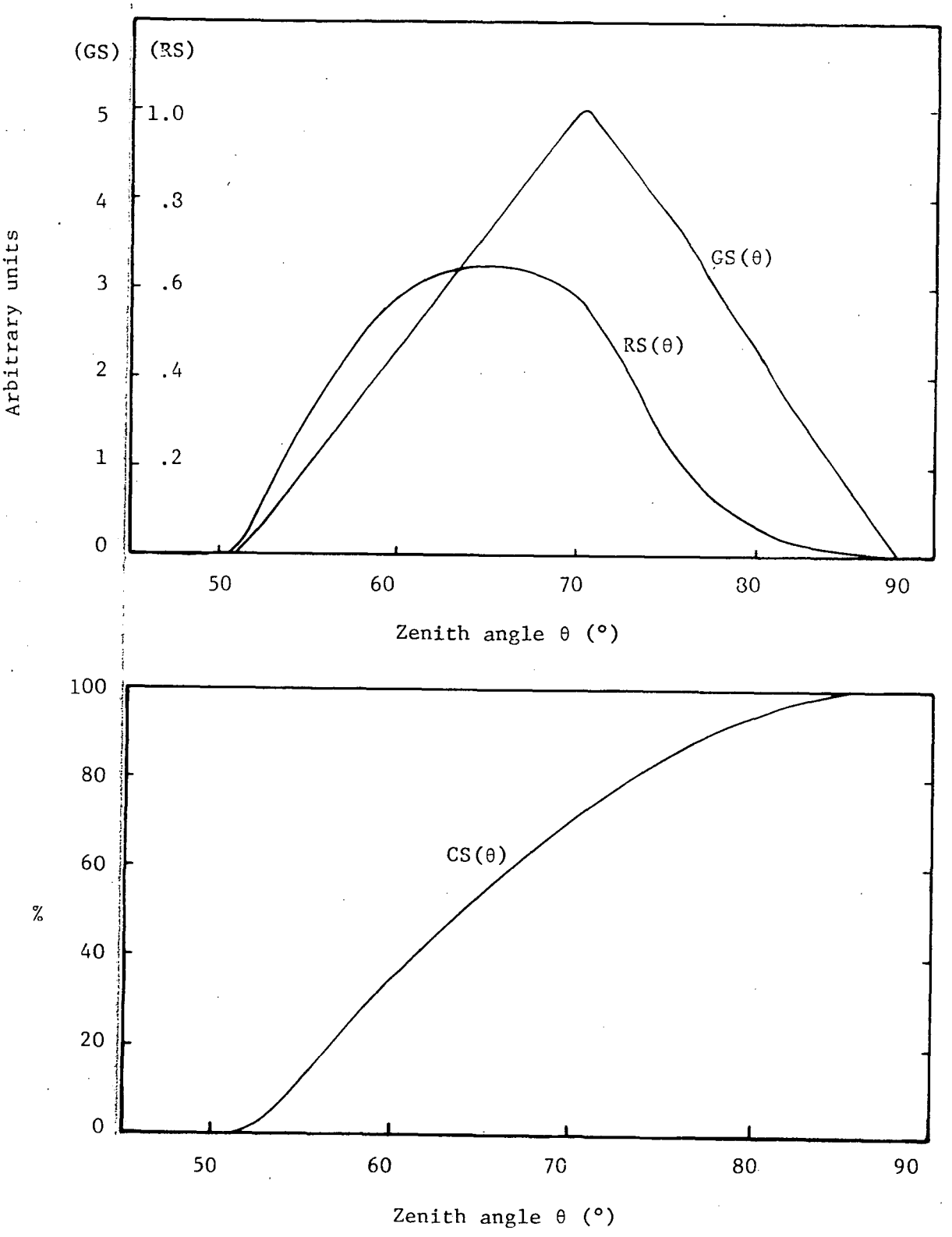

Figure 3.3. Sensitivity functions for a 1 × 1 × 3 m telescope tilted to 70° (calculated using theory of Parsons, 1959).

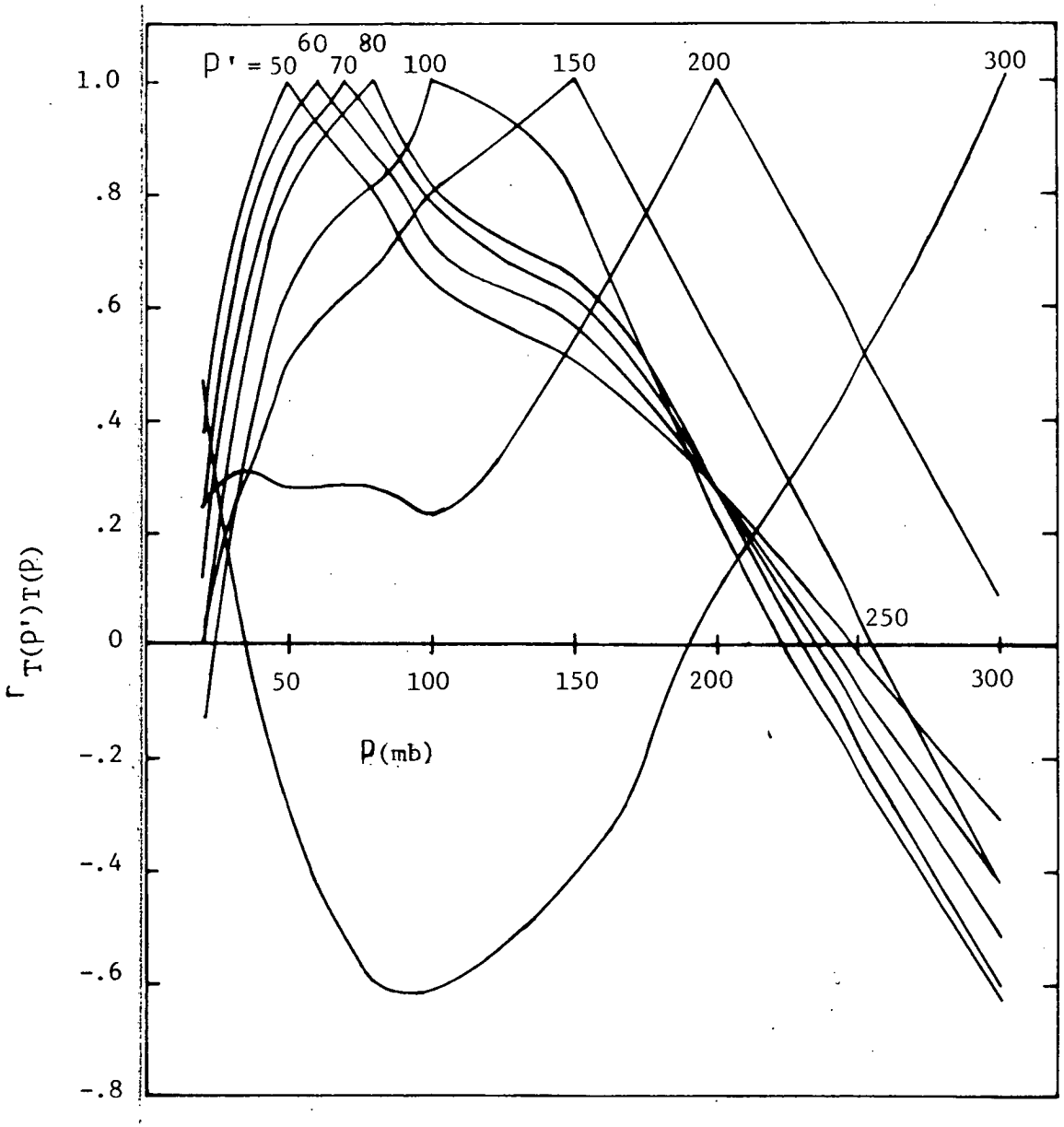

Figure 3.4. Temperature intercorrelations in the upper atmosphere. Source: daily mean temperatures, Hobart Airport radiosonde data, 1972-77.

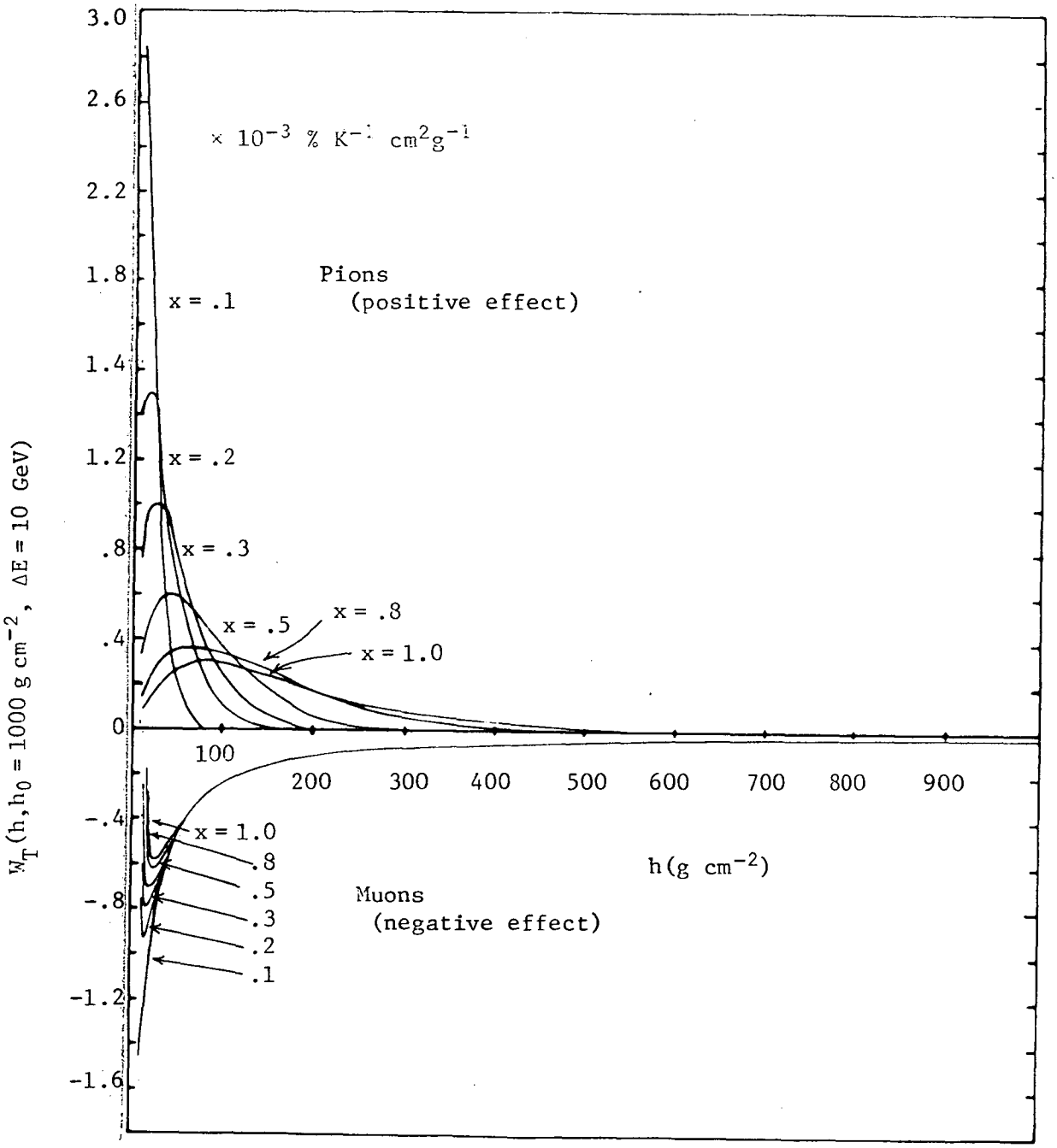

Figure 3.5. Positive and negative temperature coefficient weighting functions for Cambridge ($\Delta E = 10$ GeV)

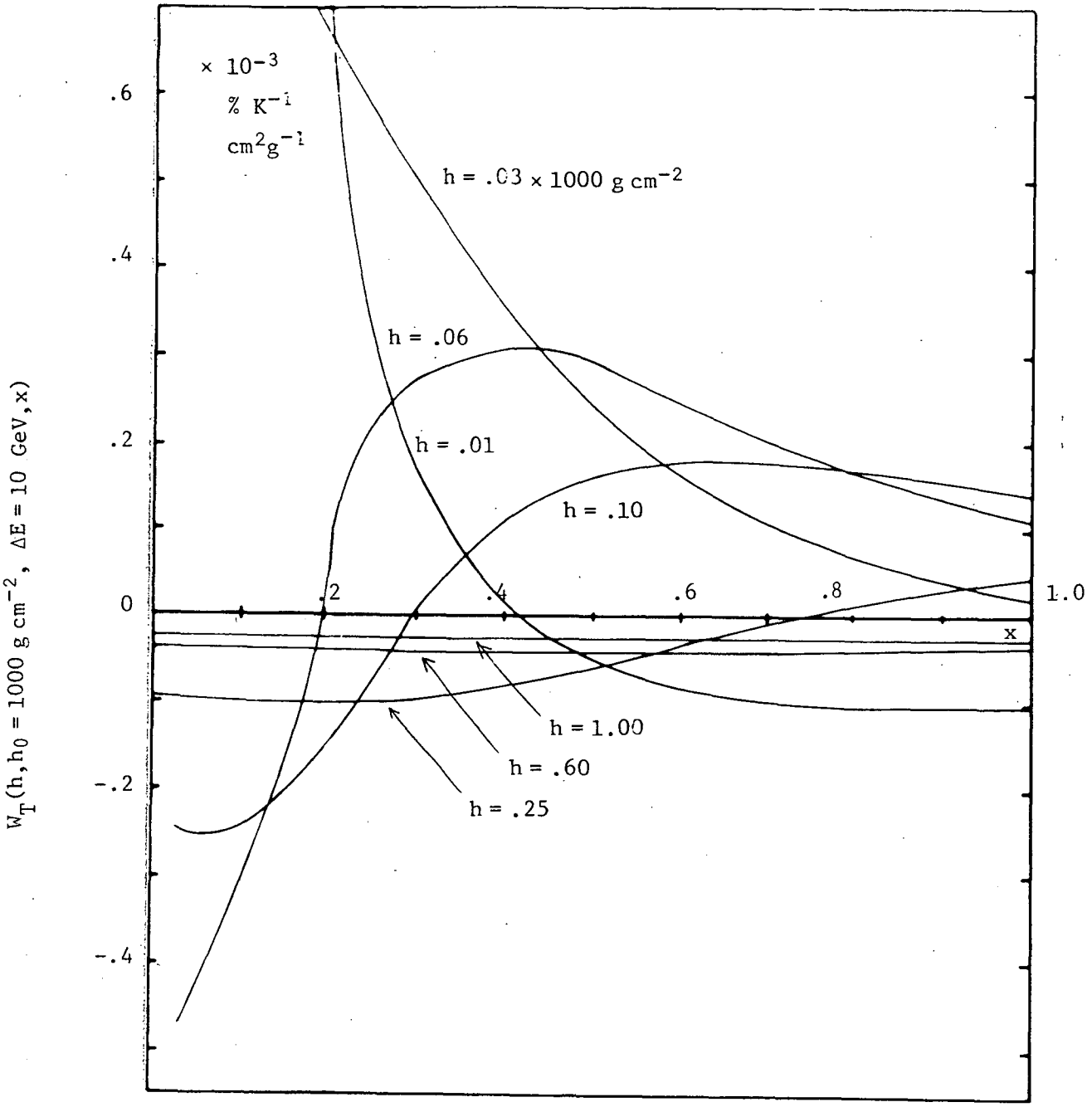

Figure 3.6. Temperature coefficient weighting function for Cambridge ($\Delta E = 10$ GeV). Contours of $W_T(x)$ for various h's.

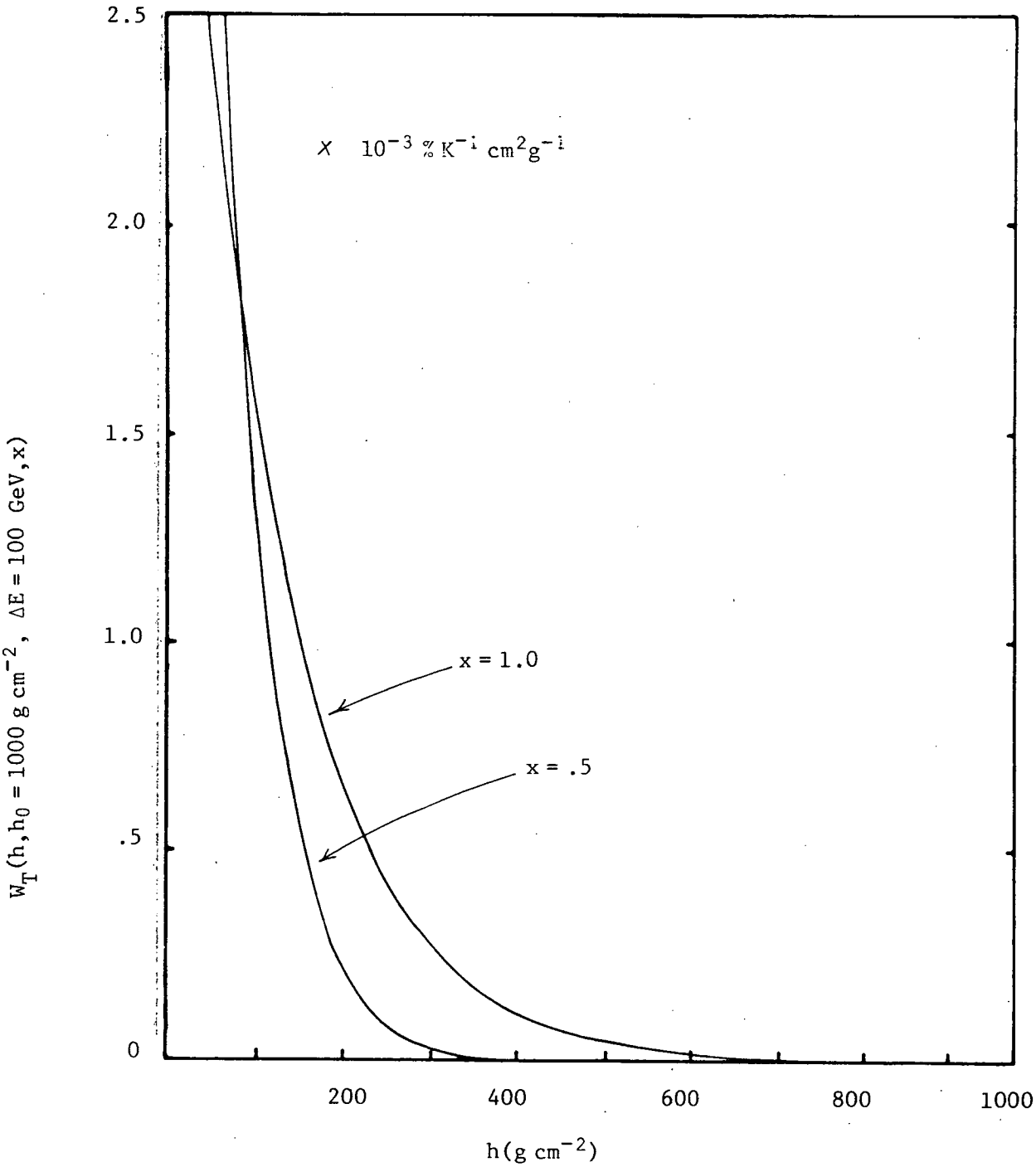

Figure 3.7. Temperature coefficient weighting function for Poatina ($\Delta E = 100$ GeV)

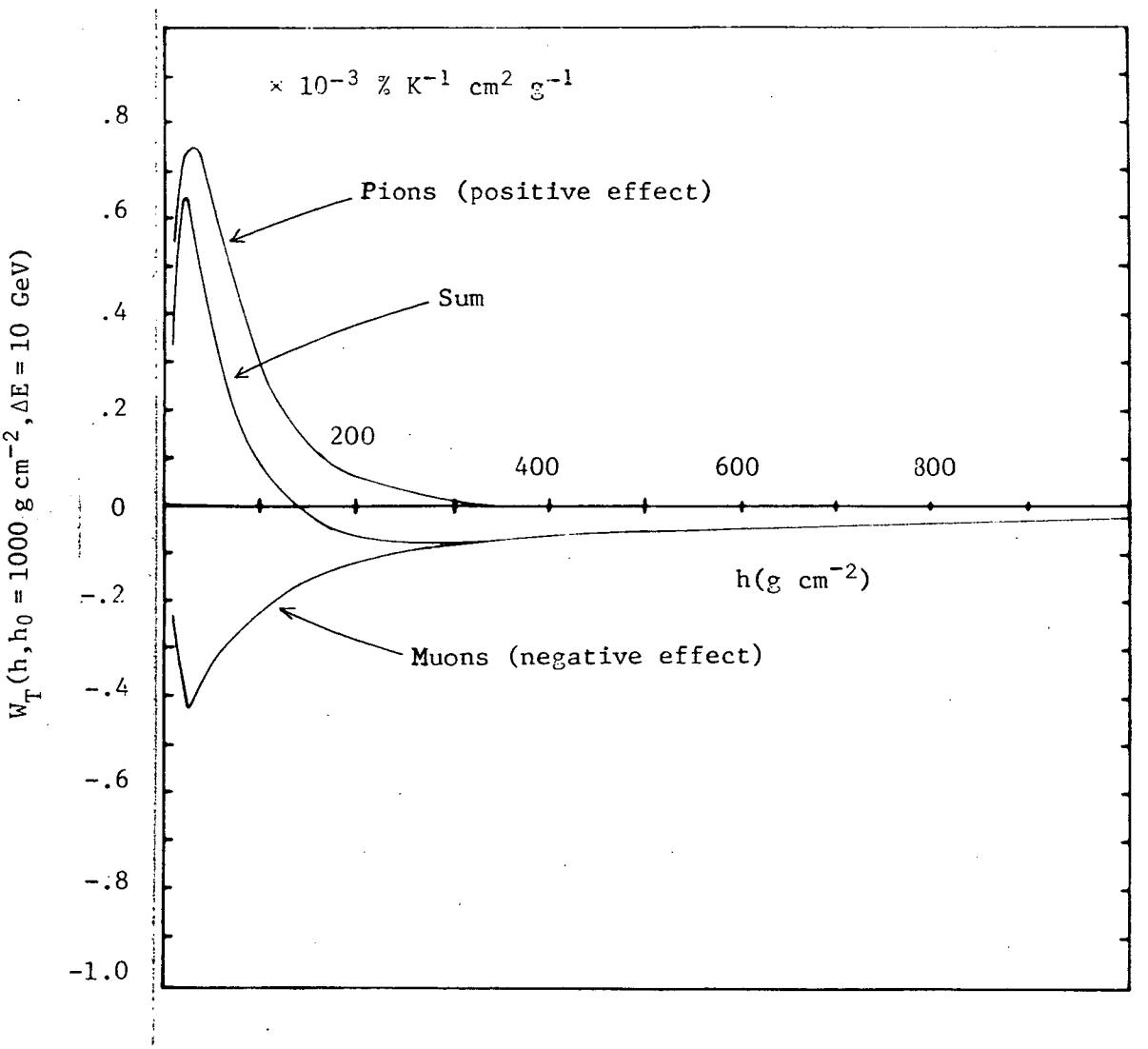

Figure 3.8. Aperture-integrated temperature coefficient weighting functions for the Cambridge 70° zenith angle telescope.

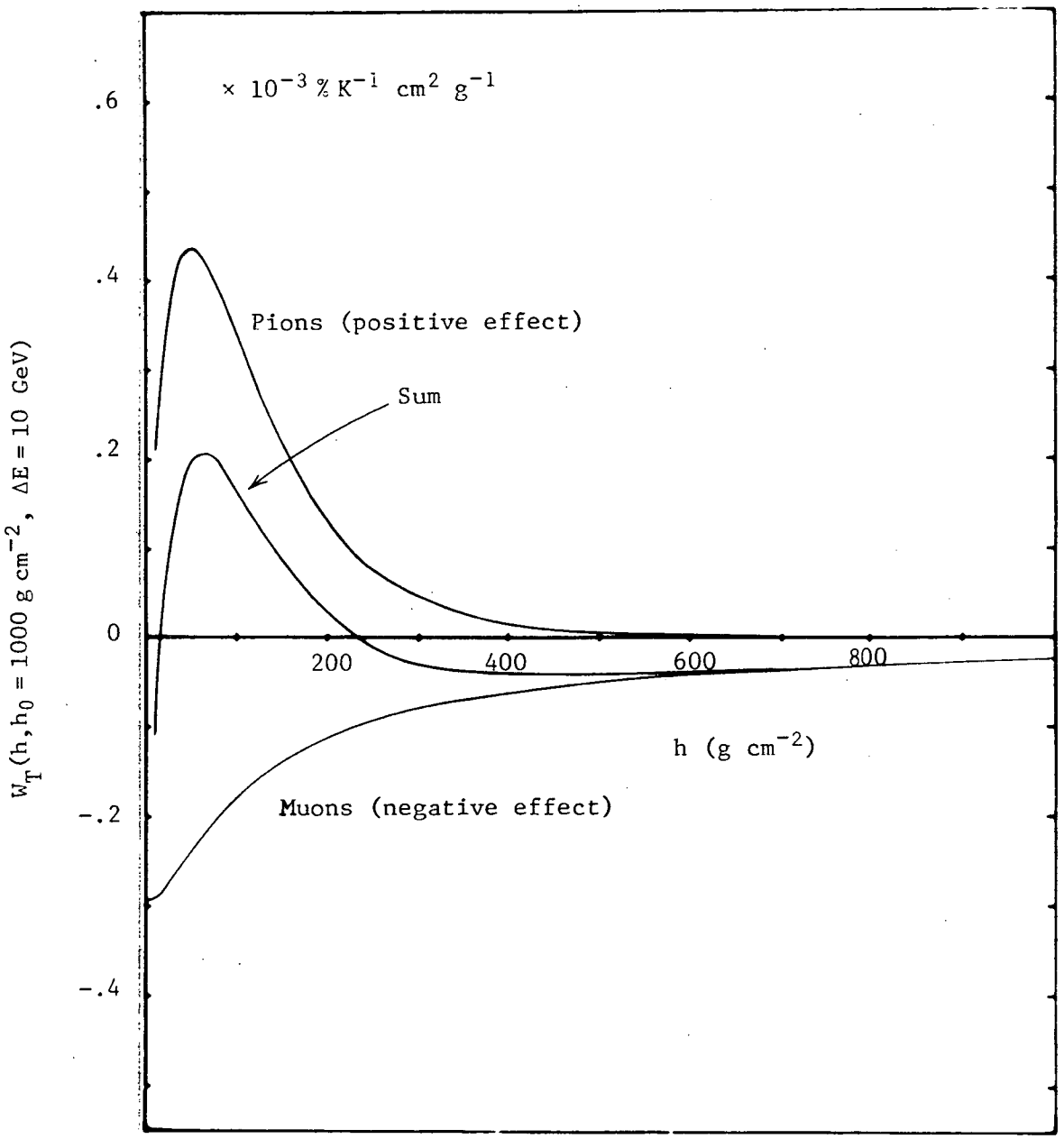

Figure 3.9. Aperture-integrated temperature coefficient weighting function for the Cambridge vertical semicubical telescopes.

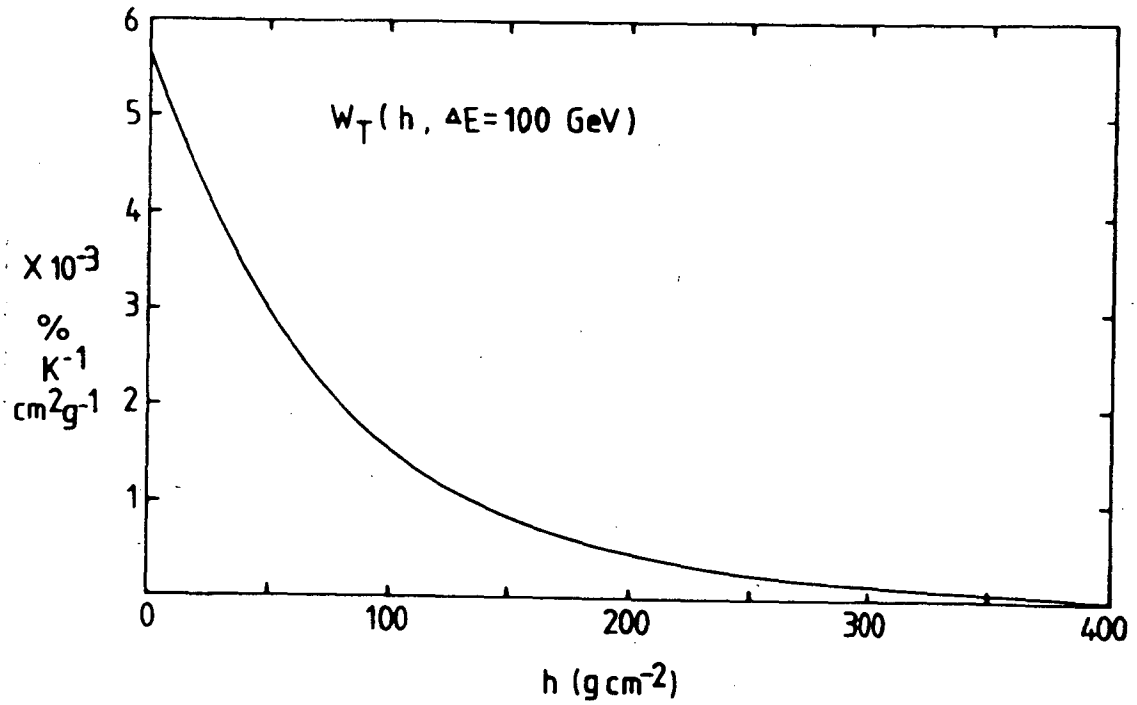

Figure 3.10. Aperture-integrated temperature coefficient weighting function for the Poatina vertical semicubical telescopes.

CHAPTER 4

CALCULATIONS OF ATMOSPHERIC COEFFICIENTS FOR HIGH ENERGY MUONS

4.1 The Equipment

The calculations described in this chapter concern muon observations made on underground detectors located at Poatina and Cambridge, Tasmania. Poatina is located approximately 130 km north of Hobart at latitude 41.8°S, longitude 146.9°E. The equipment is situated in an underground hydro-electric power station at a depth of ~ 357 hg cm^{-1} below the top of the atmosphere (Fujii and Jacklyn , 1979). This corresponds to a median primary energy of ~ 1200 GeV. The muon threshold energy as calculated in Appendix 1 is ~ 101 GeV. The detectors consist of three vertical semicubical Geiger counter telescopes totalling 3 m^2 sensitive area. Continuous observations began in late 1971.

The Cambridge equipment is located in an abandoned railway tunnel 10 km north-east of Hobart at latitude 42.8° S, longitude 147.5° E. The observation depth is ~ 47 hg cm^{-2} which corresponds to a threshold of ~10 GeV. A variety of detectors operate, or have been operated in the station. The calculations in Section 4.4 of this chapter relate to a narrow aperture 70° zenith angle telescope which was operated for the duration of 1964. The inclined depth of this telescope was ~ 140 hg cm^{-2} below the top of the atmosphere, which is equivalent to a threshold energy of ~ 40 GeV.

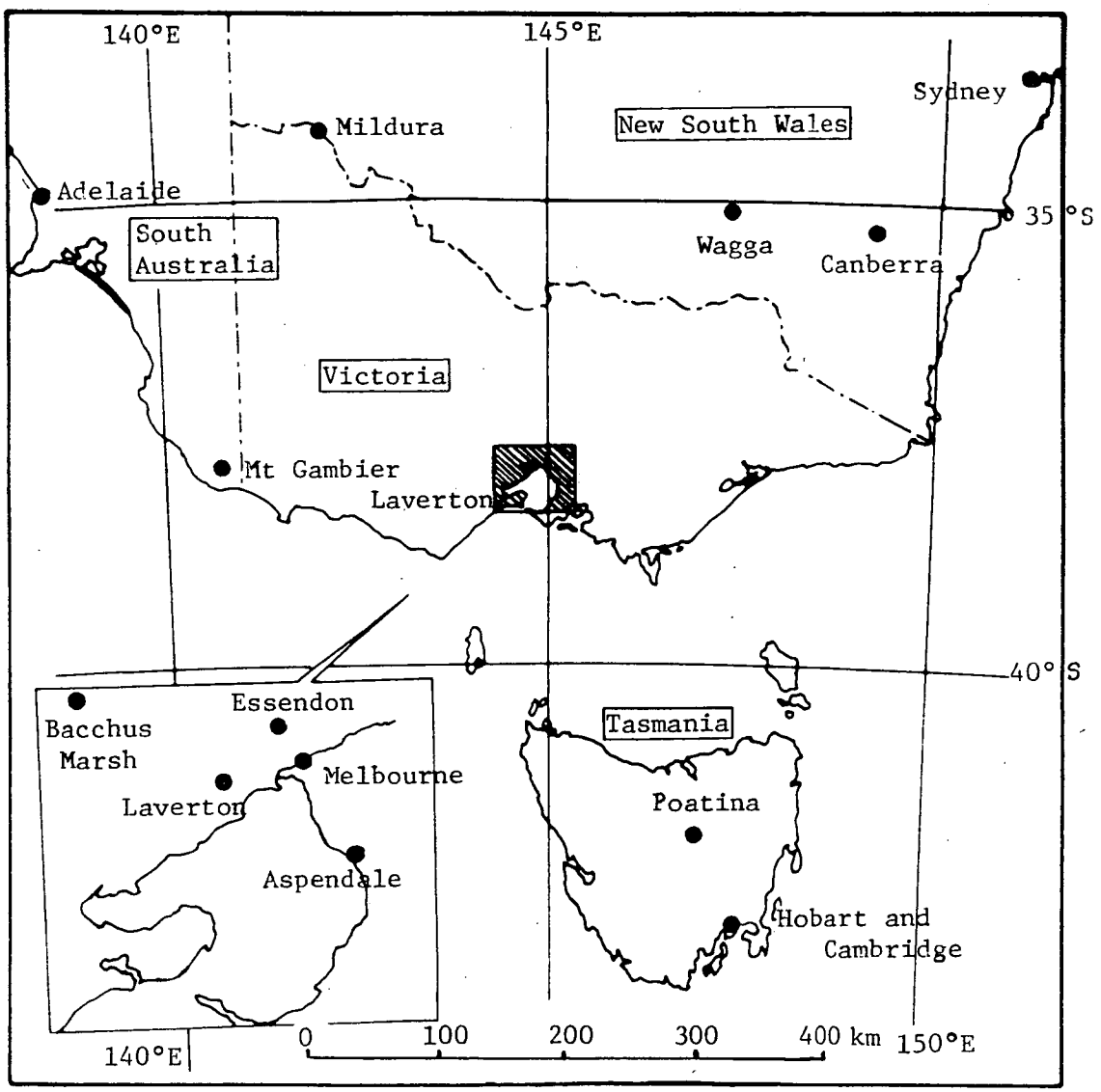

Figure 4.1. South-eastern Australia. Location map.

The location of the stations is shown in the map, Figure 4.1.

4.2 Least Squares Estimation

4.2.1 Two or More Regressor Variables

As a basis for the theory to follow, it is appropriate to review briefly the ordinary least squares (OLS) linear regression model used for calculating atmospheric coefficients. The following theory is summarized mainly from Draper and Smith (1966) and Seber (1977).

Multiple linear regression is a technique used for finding the linear combination of atmospheric variables which best approximates the observed variations in muon intensity. The model then takes the form

$$Y_i = x_{i1}\beta_1 + x_{i2}\beta_2 + \ldots + x_{ip}\beta_p + \varepsilon_i \quad . \qquad (i = 1, \ldots, n) \qquad (4.1)$$

This is far more conveniently expressed in matrix notation as

$$\underline{Y} = X\underline{\beta} + \underline{\varepsilon} \qquad (4.2)$$

where $\underline{Y}$ is an (n×1) column of muon intensity readings, X is an (n×p) matrix of n observations on each of p regressor variables (atmospheric parameters), $\underline{\beta}$ is a (p×1) column of regression coefficients, and $\underline{\varepsilon}$ is an (n×1) column of uncorrelated errors on $\underline{Y}$, distributed with mean zero and variance $\sigma^2_{Poisson}$. Note that (4.1) does not include an intercept term β_0 as this is not normally of interest in the cosmic ray context; we are interested only in changes in $\underline{Y}$ from its mean as a function of changes in X from its

mean. In all further discussion it is assumed that the $\underline{Y}$ and X variables have been "centered" to have zero mean.

The OLS estimator for $\underline{\beta}$ is

$$\hat{\underline{\beta}} = (X^T X)^{-1} X^T \underline{Y} \tag{4.3}$$

where

$$E(\underline{Y}) = \hat{\underline{Y}} = X\hat{\underline{\beta}} \; , \qquad E(\hat{\underline{\beta}}) = \underline{\beta} \tag{4.4}$$

and X^T is the transpose of X, i.e. the estimate of $\underline{\beta}$ is *unbiased*. $\hat{\beta}$ is known as the best linear unbiased estimator of $\underline{\beta}$ and specifies a "plane" in p-space which minimizes the sum of the squared differences of the Y_i from the "plane". This quantity may be specified as follows:

The vector of errors $\underline{\varepsilon}$ is estimated by

$$\begin{aligned} \underline{e} &= \underline{Y} - \hat{\underline{Y}} \\ &= \underline{Y} - Y\hat{\underline{\beta}} \end{aligned} \tag{4.5}$$

called the residual vector, and the minimum residual sum of squares (RSS) is given by

$$\begin{aligned} RSS = \underline{e}^T\underline{e} &= (\underline{Y} - X\hat{\underline{\beta}})^T(\underline{Y} - X\hat{\underline{\beta}}) \\ &= \underline{Y}^T\underline{Y} - \hat{\underline{\beta}}^T X^T \underline{Y} \; . \end{aligned} \tag{4.6}$$

The total sum of squares of the response variable is

$$TSS = \underline{Y}^T\underline{Y} \; . \tag{4.7}$$

By subtraction, the "regression" sum of squares must be

$$\text{Reg SS} = \hat{\underline{\beta}}^T X^T \underline{Y} \; . \tag{4.8}$$

The quantity

$$R^2 = \text{Reg SS/TSS} = 1 - \text{RSS/TSS} \tag{4.9}$$

is known as the coefficient of determination and expresses the fraction of the total variation in $\underline{Y}$ which is accounted for by the model. R is the multiple correlation coefficient between $\underline{Y}$ and X.

The variance-covariance, or dispersion matrix of $\hat{\underline{\beta}}$ is given by

$$D(\hat{\underline{\beta}}) = \sigma^2(X^TX)^{-1} \tag{4.10}$$

and therefore

$$\text{var}(\hat{\beta}_i) = \sigma^2(X^TX)^{-1}_{ii} . \tag{4.11}$$

Estimation of σ^2.

It may readily be shown that

$$s^2 = \text{RSS}/(n - p - 1) \tag{4.12}$$

is an unbiased estimate of σ^2; viz. $E(s^2) = \sigma^2$. If $s^2 \simeq \sigma^2$ the model is inferred as correct and the chosen regressors are regarded as a complete set of explanatory variables. If $s^2 > \sigma^2$ the model is said to suffer from lack of fit. It is important to note that even if $s^2 \simeq \sigma^2$, R^2 may still be poor (low). This merely indicates a large amount of random fluctuation in $\underline{Y}$.

4.2.2 One Regressor Variable

The simplest case is the straight line. Again we are not interested in the intercept β_0 and the model becomes

$$Y_i = \beta_1 x_i + \varepsilon_i , \quad (i = 1,\ldots,n) \tag{4.13}$$

or in matrix terms

$$\underset{(n\times 1)}{\underline{Y}} = \underset{(n\times 1)(1\times 1)}{\underline{x}\ \beta_1} + \underset{(n\times 1)}{\underline{\varepsilon}} \tag{4.14}$$

As before, $\varepsilon_i \sim (0,\sigma^2)$. The OLS estimate of β_1 is

$$\begin{aligned} \hat{\beta}_1 &= (\underline{x}^T\underline{x})^{-1}\ \underline{x}^T\underline{Y} \\ &= \sum_{i=1}^{n} x_i Y_i \Big/ \sum_{i=1}^{n} x_i^2 \end{aligned} \tag{4.15}$$

and its variance is

$$\begin{aligned} \mathrm{var}(\hat{\beta}_1) &= \sigma^2 (\underline{x}^T\underline{x})^{-1} \\ &= \sigma^2 \Big/ \sum_{i=1}^{n} x_i^2 . \end{aligned} \tag{4.16}$$

The coefficient of determination is equal to the squared correlation coefficient between $\underline{Y}$ and $\underline{x}$:

$$\begin{aligned} R^2 = r^2_{xY} &= \underline{x}^T\underline{Y} / (\underline{x}^T\underline{x}\ \underline{Y}^T\underline{Y}) \\ &= \left(\Sigma\, x_i Y_i\right)^2 / \left(\Sigma\, x_i^2\, \Sigma\, Y_i^2\right) . \end{aligned} \tag{4.17}$$

Comparison of (4.15) and (4.17) yields

$$\hat{\beta}_1 = r_{xY}\left(s_Y / s_x\right) \tag{4.18}$$

where s_Y and s_x are the sample standard deviations of $\underline{Y}$ and $\underline{x}$.

Point of Notation

For the remainder of this thesis, when discussing regression coefficients on a conceptual level, the conventional β_i notation is used, as in the previous section. However, in discussing specific estimates obtained from actual calculations, the following system may be used as it is more informative.

Estimates are denoted by a "b" followed by a number of subscripts, as in "$b_{IP.HT}$". This example denotes the partial intensity ~ pressure slope where the remaining explanatory variables are height and temperature. Thus, for example, $b_{IP.T}$ and $b_{IP.HT}$ are readily distinguished as coming from different models, even though they are dimensionally the same. Furthermore, estimates in the "b notation" will be in customary cosmic ray units of % mb^{-1}, % K^{-1}, etc. whilst estimates in "β notation" will usually correspond strictly to the original units in the X and $\underline{Y}$ data. The relationship between the two is then

$$b = \hat{\beta} \left(\frac{100}{\bar{I}}\right) \tag{4.19}$$

where $\bar{I}$ is the mean intensity over the period of data analysed.

4.3 Atmospheric Coefficients at Poatina

4.3.1 The Total Barometer Coefficient

The first calculations of the pressure effect at Poatina were reported by Fenton and Fenton (1975). A straight-line regression was used where daily mean intensities were regressed

against daily mean pressures over a five-month period. In all cases, each daily mean was obtained from 24 hourly readings; missing values were interpolated. The value obtained was $b_{IP} = -0.057$ % mb^{-1}. This is much larger than the value obtained from the depth-intensity curve for muons on the assumption that an increase in pressure is equivalent to taking the muon telescope to an appropriately greater underground depth. The latter method yields -0.007 % mb^{-1} (see Section 3.1).

Alternatively, an estimate may be obtained using the integral theory in Chapter 3. From Equation 3.29 we have, for great underground depths,

$$\beta_P \cong \frac{-0.6\cos\theta}{\Delta E\,(GeV)} \text{ \% } mb^{-1}$$

which for Poatina gives -0.006 % mb^{-1} for vertically incident particles. Integration of the radiation sensitivity curve of a semicubical telescope reduces the value to ~ -0.003 % mb^{-1}, which is very small indeed. A longer-term analysis by Humble et al (1979) for the years 1972-76 yields the value (-0.047 ± 0.002) % mb^{-1}. This figure represents a weighted mean of 60 monthly coefficients. Division of the data into separate monthly intervals was considered necessary to help eliminate the confusing effects of long-term drifts in telescope efficiency. This trend is shown in Figure 4.2.

The estimate obtained above is, again, an order of magnitude "too large". Thus there is a strong suggestion that other atmospheric processes not accounted for in the model are responsible for the inflated coefficient, where these processes may be correlated with surface pressure.

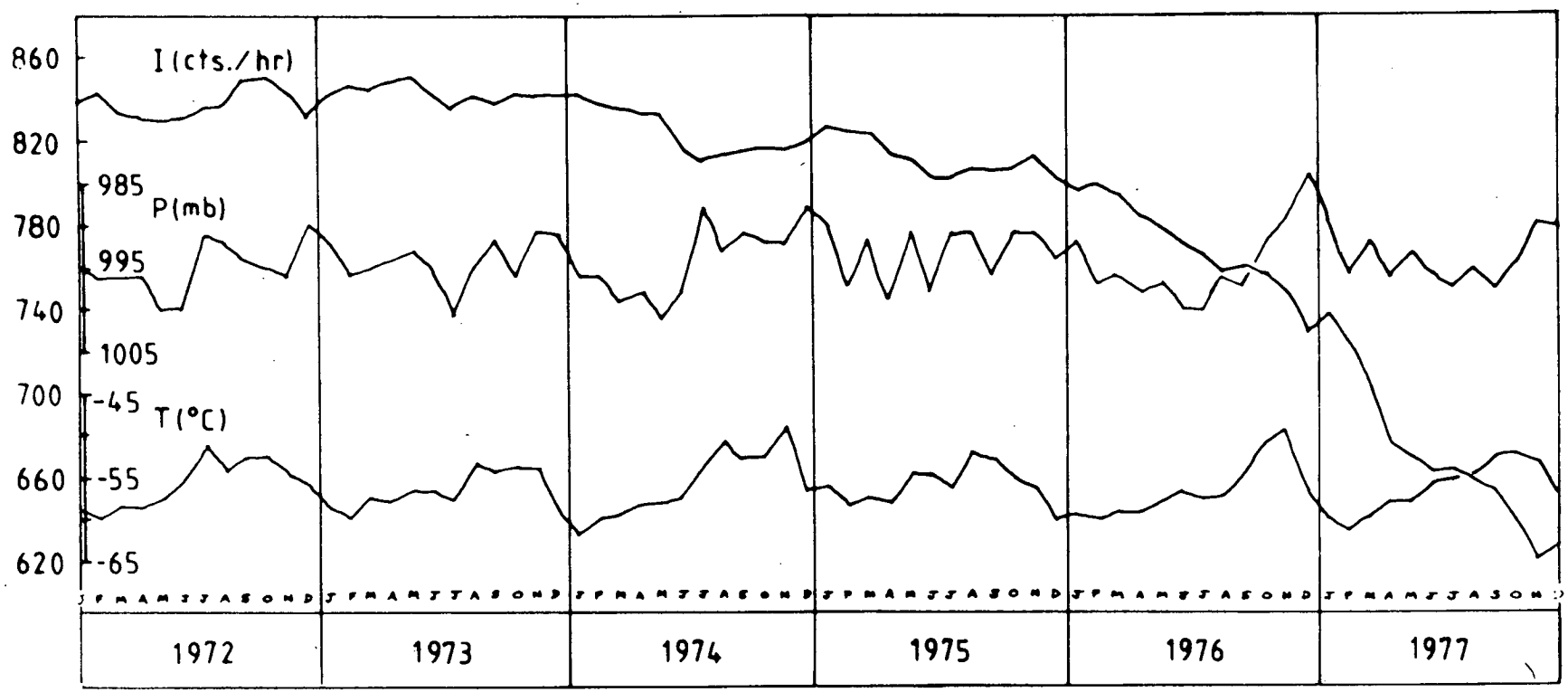

Figure 4.2. Monthly mean muon intensity and surface air pressure at Poatina, plus monthly mean temperature of 80 mb level, Hobart Airport for the years 1972-77. To obtain true intensities, multiply figures by 2.

To investigate this possibility, time variations were examined in the coefficients for the period 1972-76. Figure 4.3 and Table 4.1 show the results of an harmonic analysis, the theory of which is summarized in Appendix 4.

Because of the relatively low count-rate, diurnal and semi-diurnal variations can barely be distinguished. However, there is a very large seasonal variation, confirming that pressure cannot be the only atmospheric parameter responsible for the intensity variations.

4.3.2 Partial Atmospheric Coefficients

Under the assumption that a Duperier-type multiple regression model is appropriate, a four-fold model using the following regressor variables was tried:

1. Surface pressure, P
2. Geopotential height of the 100 mb level, H_{100}
3. Temperature of the 100 mb level, T_{100}.

The aerological data were obtained from the Bureau of Meteorology computer records, which are compiled from radiosonde flights made at Hobart Airport at ~ 1100 UT and ~ 2300 UT daily. The average maximum height of ascent is about 40 mb for these flights, which typically last for two hours. The launch site is about 135 km from Poatina. Thus there is a possibility of regressor error resulting from this separation. This question is examined in Section 5.3.3.

Weighted running means from three successive readings of H_{100} and T_{100} were used to calculate the daily means of these variables, whilst 24-hour daily means were used for

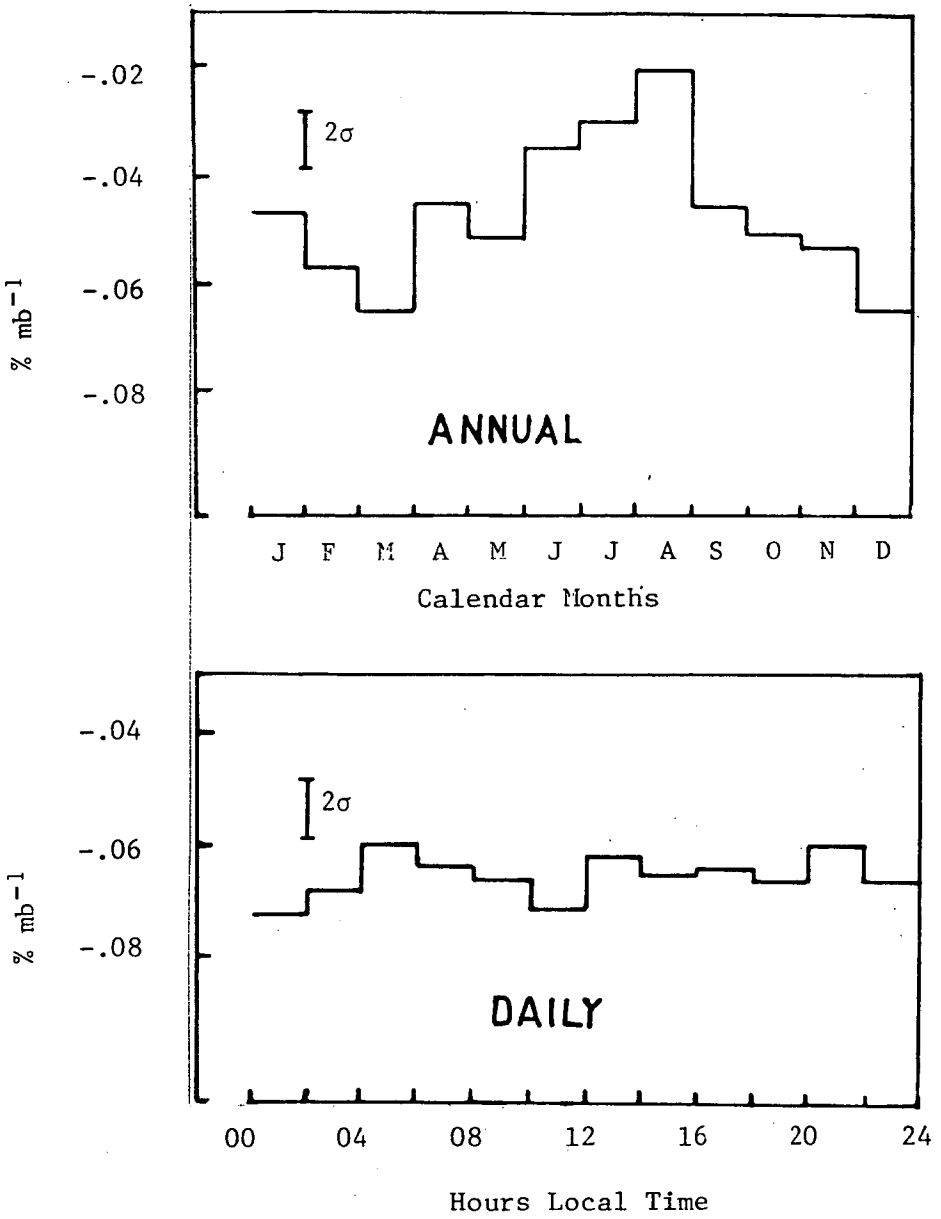

Figure 4.3 Variations in the total barometer coefficient at Poatina.

TABLE 4.1

Harmonics found in the total barometer coefficient at Poatina. Amplitudes are given as percentage departures from the mean; phases as times of maxima.

Variation	First Harmonic		Second Harmonic	
	Ampl.(%)	Phase	Ampl.(%)	Phase
Annual	30.3 ±5.1	Jul.(25±9)	15.1 ±5.1	Jan.(26±10)
Daily	1.55±4.77	Indeterminate	6.14±4.77	0634 ± 0178

I and P. As with the total pressure coefficient, a separate analysis was carried out for each month. The resulting coefficients were then multiplied by $100/\bar{I}$, when $\bar{I}$ is the mean monthly intensity. Weighted mean figures for the years 1972-77 are shown in Table 4.2.

From these results it is clear that $b_{IP.HT}$ is very nearly the same as b_{IP} obtained earlier. Thus the multiple regression analysis has failed to reduce the apparent dependence of muon intensity on pressure. In addition, as the cut-off energy for Poatina is ~ 100 GeV, its partial height coefficient should be negligible. Since muons of energy $\gtrsim$ 100 GeV have a mean path length before decay of $\gtrsim$ 600 km, fluctuations in their production height should have almost no effect on their intensity. Using the theory in Section 3.1, a value of -0.15 % km^{-1} may be predicted. Instead, $b_{IH.PT}$ has a large positive value. Finally, the value of the temperature coefficient $b_{IT.PH}$ is lower than the expected figure of ~ 0.25 % K^{-1} (see Sections 3.1, 3.2).

Revised estimation of the coefficients

In a more refined investigation of the partial coefficients, the data for Poatina have been re-analysed for the period 1972-76. The 1977 data were omitted on the grounds of excessive decline in telescope efficiency. This may be seen in Figure 4.1. Three height reference levels were tried: 100, 150 and 200 mb. In addition, the temperature reference level was changed to 80 mb. This was seen as a reasonable compromise between improved muon correlation with the higher

level and worsened temperature measurement error. The latter effect is seen in Table 5.1.

As before, weighted means were obtained from the results of 60 months' data. These are shown in Table 4.2, along with analysis of variance information.

Once again, the estimates differ considerably from those expected. In particular the sudden change in the 100 mb height coefficient from (2.41 ± 0.50) to (3.96 ± 0.41)% km^{-1} (approximately 95% confidence limits) is rather disconcerting, considering the fact that the H regressor was not altered and the T regressor was changed only slightly. A yearly breakdown of the values is also given and shows that the H and T estimates fluctuate markedly from year to year. The low R^2 values imply that only some of the intensity variation is accounted for by the regression.

To test the goodness of fit of the model, the residual standard deviation, s, is compared with the Poisson error, σ_{Pois}, in the count-rate. The results for 1972 are given in Table 4.3, where moderate agreement is seen. The fairly serious discrepancy for some months suggests an inadequacy in the four-fold model. However, even those months with σ_{Pois}/s ratios approaching unity display anomalous coefficients.

4.4 Atmospheric Coefficients at Cambridge

As a means of comparison, data for the Cambridge 70° narrow angle telescope have been analysed. Since the inclined threshold energy is about 40 GeV, it seems

reasonable that some of the anomalous trends present in the Poatina coefficients might also exist in those for Cambridge, if they are systematic.

The chosen regressors were P, H_{100} and $\bar{T}_{80-100}$ (mean temperature). The results are shown in Table 4.4.

It is clear that the temperature estimate agrees fairly well with that predicted in Chapter 3. However, the pressure and height coefficients are, respectively, lower and higher than expected. Reasonable agreement is obtained between σ_{Pois} and s.

From these results a clear trend emerges where the partial coefficients tend to differ increasingly from those expected, as the muon threshold energy is increased. The search for a reason for this behaviour is the subject of the next chapter.

TABLE 4.2

Various OLS regression coefficients for Poatina

Regressor	P(surface) (% mb^{-1})	H(200) (% km^{-1})	H(150) (% km^{-1})	H(100) (% km^{-1})	T(80) (% K^{-1})	R^2 (%)
Theory	-0.007		~ - 0.15		~0.25	
Total coeffs. 1972-76	-0.047±0.002*				0.088±0.005	16.0 6.3
Partial coeffs. 1972-77	-0.050±0.003			2.41±0.25	0.063±0.008 (100 mb)	9.0
Partial coeffs. 1972-76	-0.057±0.002 -0.058±0.002 -0.057±0.002	 2.690±0.183	 3.460±0.195	3.955±0.206	0.080±0.006 0.103±0.007 0.108±0.007	39.4 38.4 37.3
R_j 1972-76 (see Sect. 5.2)	0.53			0.67	0.63	

* Humble, 1979

TABLE 4.3

OLS regression coefficients for Poatina

January - December 1972

Month	P(surface) (% mb^{-1})	H(100) (% km^{-1})	T(80) (% K^{-1})	σ_{Pois}	s	R^2 (%)
January	-0.0546 ± 0.0234	-2.3288 ± 2.6577	-0.0331 ± 0.0558	4.18	4.88	14.9
February	-0.0692 ± 0.0187	-1.2675 ± 2.1735	-0.0394 ± 0.0653	4.19	4.83	58.5
March	-0.0236 ± 0.0156	2.8008 ± 1.4527	0.1479 ± 0.0540	4.17	5.97	17.4
April	-0.0332 ± 0.0152	1.0363 ± 1.0776	0.0505 ± 0.0583	4.16	4.66	31.0
May	-0.0463 ± 0.0168	4.6706 ± 2.2567	0.0607 ± 0.0412	4.16	5.89	19.7
June	-0.0362 ± 0.0128	3.4944 ± 1.2511	0.1487 ± 0.0502	4.16	5.87	60.3
July	-0.0280 ± 0.0163	0.9095 ± 1.5099	0.1224 ± 0.0448	4.18	5.52	51.5
August	-0.1158 ± 0.0200	4.7238 ± 0.9042	0.1449 ± 0.3026	4.18	7.44	66.5
September	-0.0599 ± 0.0173	2.5602 ± 1.2500	0.1007 ± 0.0509	4.21	7.16	47.6
October	-0.0997 ± 0.0137	2.9579 ± 1.8908	0.0050 ± 0.0430	4.21	9.54	62.4
November	-0.0711 ± 0.0221	2.9913 ± 2.4301	0.1236 ± 0.0663	4.19	6.36	43.5
December	-0.0598 ± 0.0190	-1.4304 ± 2.2863	-0.0120 ± 0.0637	4.16	6.85	34.8

TABLE 4.4

OLS regression coefficients for Cambridge, (70° narrow angle), January - December 1964

Month	P(surface) (% mb^{-1})	H(100) (% km^{-1})	$\bar{T}$(80-100) (% K^{-1})	σ_{Pois}	s	R^2 (%)
Theory	-0.07	-1.3	0.022			
January	-0.0374 ± 0.0168	-3.5354 ± 2.3212	0.0500 ± 0.0449	0.439	0.554	48.9
February	-0.0250 ± 0.0160	-3.6765 ± 2.4155	0.0224 ± 0.0483	0.437	0.503	20.4
March	-0.1065 ± 0.0160	0.0279 ± 1.9984	-0.0490 ± 0.0332	0.441	0.749	51.6
April	-0.0819 ± 0.0262	2.4649 ± 2.4404	0.0241 ± 0.0595	0.443	0.461	46.1
May	-0.0668 ± 0.0182	-1.1126 ± 1.7572	0.0784 ± 0.0640	0.444	0.456	53.4
June	-0.0498 ± 0.0099	-2.9252 ± 2.5811	0.0481 ± 0.0432	0.444	0.424	71.6
July	-0.0439 ± 0.0122	-2.0789 ± 1.3035	-0.0398 ± 0.0767	0.446	0.469	63.8
August	-0.0717 ± 0.0143	-3.3421 ± 1.1730	0.0732 ± 0.0492	0.444	0.515	72.4
September	-0.0543 ± 0.0145	-0.6978 ± 2.3649	-0.0549 ± 0.0388	0.444	0.428	45.6
October	-0.0259 ± 0.0168	-2.2380 ± 1.9773	0.0977 ± 0.0407	0.442	0.850	15.6
November	0.0911 ± 0.0169	-9.3973 ± 2.4266	0.1029 ± 0.0442	0.441	0.992	35.6
December	-0.0870 ± 0.0210	0.2247 ± 1.1475	0.0792 ± 0.0345	0.442	1.160	12.3
mean	-0.0447 ± 0.0044	-2.1835 ± 0.4980	0.0297 ± 0.0129			

CHAPTER 5

EXPLAINING THE ANOMALOUS COEFFICIENTS

5.1 Possible Reasons

It is conceivable that the empirical atmospheric coefficients are genuine and that they are caused by some unknown physical mechanism. This possibility should not be dismissed outright, as, historically, anomalies in the absorption of secondary particles have played an important role in the development of cosmic ray physics. For example, studies of the temperature effect by Cini Castagnoli et al. (1967) at 70 hg cm^{-2} helped to disprove the early assumption that the absorption length for pions is less than that of primary protons. However, in recent years the production of nucleons, charged pions and kaons in accelerator fireball collisions has become well understood and agrees well with the cosmic ray evidence.

If the physical model is correct, the observed coefficients could still be wrong if other influential factors have not been included in the regression. As mentioned in Section 4.3.1, the most serious of these - change in Geiger tube efficiency - was minimized as far as possible by analysing the data in separate one-month blocks. Ambient temperature variations around the detectors were not considered important as they amount to only several degrees C (at most) throughout the year for both stations.

A third possibility is that the regression coefficients are anomalous because of problems with the OLS technique resulting from the nature of the data. The evidence for this is very strong and will now be presented.

5.2 Correlations Among the Regressor Variables

Dorman (1957) has pointed out that conventional regression methods are meaningful only when the variation of each explanatory variable is statistically independent of other factors which may influence the cosmic ray intensity. To see whether this condition was being violated, each explanatory variable was regressed against the remaining two for the period 1972-76. The resulting "partial" multiple correlation coefficients R_P, R_H and R_T were found to be significant and are shown in Table 4.2 (last row). Such interdependence between the regressor variables is known in econometrics as collinearity. In its most extreme form - perfect association between two or more variables - it renders a unique solution for $\hat{\underline{\beta}}$ impossible. This corresponds to the X^TX matrix being singular (less than full rank).

Thus, strong evidence exists of a data problem which may be causing misleading regression coefficients. This question will be returned to in Section 5.5.

5.3 Measurement Errors in the Aerological Data

5.3.1 Introduction

As long ago as 1904, Spearman showed that random errors in the explanatory variables will affect the expected values of the regression coefficients. The OLS estimates are no longer unbiased, so that

$$E(\hat{\underline{\beta}}) = \underline{\beta} - \underline{\theta} \qquad (5.1)$$

where $\underline{\theta}$ is some non-zero vector. In the cosmic ray context, Trefall and Nordö (1959) studied the problem from a theoretical viewpoint. In a four-fold analysis using the sea level muon intensity, they showed that the differences between the empirical estimates and their theoretical values could be attributed to uncertainties in the atmospheric variables.

In the general regression model, Hodges and Moore (1972) and Davies and Hutton (1975) have derived expressions for computing the bias in each coefficient which is due solely to scatter in the regressors. The bias is particularly misleading, as the dispersion matrix $\sigma^2(X^TX)^{-1}$ is hardly effected by the errors in X, so that the estimates *appear* reliable (Seber , 1977).

For a given X matrix, the bias is systematic and analytically related to the error on each regressor. Expressions are derived in Section 5.4.1.

5.3.2 The Effect of Pressure and Temperature Errors

The twice-daily balloon flights at Hobart Airport give temperature as a function of pressure. The chosen pressure

reference levels are at the surface and then 1000, 900, 850 mb, etc. up to about 20 mb effective maximum. The geopotential heights of these levels are calculated from the following equation, which is derived by assuming that the atmosphere obeys the perfect gas law and is in hydrostatic equilibrium:

$$H_2 - H_1 = -\frac{R'}{Mg}\int_{P_1}^{P_2} T \cdot \frac{dP}{P}$$

$$\simeq R\,\bar{T}\,\ln(P_1/P_2) \qquad (5.2)$$

where $H_2 - H_1$ is the height difference between the levels at pressure P_1 and P_2, $\bar{T}$ is the mean temperature over $[P_1,P_2]$ and $R = 2.925 \times 10^3\ \mathrm{cm\,K^{-1}}$. (Equation 3.13.)

The accuracy of each $H_j - H_{j-1}$ evaluated from (5.2) depends on calculating the appropriate $\bar{T}$ for that layer. An erroneous pressure measurement distorts the limits over which $\bar{T}$ should be determined; an erroneous temperature measurement affects $\bar{T}$ directly. The second error has the most serious effect on the absolute height of a given level. The higher the level, the greater the cumulative error which results from repeated use of (5.2).

5.3.3 Previous and Current Studies of Errors

The assessment of bias requires *a priori* knowledge of the error variances and covariances in the X matrix. These errors are comprised of up to three components:

(a) a "real", instrumental component due to the actual measurement errors associated with each flight,

(b) a possible component resulting from the effect of distance from the radiosonde station, and

(c) a spurious component which is due to the low sampling rate of the atmospheric parameters.

These effects are now described in turn.

(a) Instrumental Errors. The problem has been studied by Raab and Rodskjer (1950), Rossi (1952), Nyberg (1952), Leviton (1954), Eliassen (1954) and Trefall and Nordö (1959). The general method used was to release two closely-space balloons simultaneously and compare results.

Leviton's study was semi-theoretical; he assumed a ±1 K error in T at all levels (probably an underestimate), a pressure error of ±3 mb up to the 100 mb level and ±1.5 mb above that level. Using these values, he calculated the total error on H for various heights in the stratosphere.

The results of the last three groups of workers are given in Table 5.1. The error *covariances* (shown as off-diagonal terms) are seen to be non-zero. This arises from the fact that any error in T at a given level will contribute to the error in the integrated height of that level. Thus, the T vs. H error covariance is strictly positive while the measured T vs. H covariance may be of either sign, depending on the levels chosen. For the 100 mb level, the T vs. H error covariance has been calculated using Trefall and Nordö's error correlation coefficient of 0.56. They do not quote a correlation for the 200 mb level, but a likely covariance has been based on the value of 0.5.

TABLE 5.1

Estimated variance-covariance matrix for errors in aerological data. Units are:

T in K^2, H in m^2, P in mb^2. Figures apply to *single flights*.

	H_{300}	T_{300}	H_{200}	T_{200}	H_{100}	T_{100}
H_{300}	Eliassen: 2092 T & N[1] : 1898					
T_{300}		T & N : 2.56 Leviton: 1				
H_{200}			T & N: 2772			
T_{200}			T & N: 57*	T & N : 4.69 Leviton: 1		
H_{100}					T & N : 5074 Leviton: 5800	
T_{100}					T & N : 90	T & N : 5.04 Leviton: 1

[1]Trefall and Nördo (1959)

*Inferred; see Section 5.3.3

The figures in Table 5.1 indicate reasonable agreement amongst the results of different studies. The error variances and covariances increase rapidly with height, largely because the steep lapse rate of temperature in the stratosphere exacerbates the effect of pressure error.

Accuracy of the Hobart Radiosonde

Australian radiosondes are manufactured to Bureau of Meteorology specification A570 and carry temperature, pressure and humidity sensors. Temperature is measured with a rod thermistor using a low radiation absorptivity coating. Pressure is measured using a temperature-compensated aneroid capsule. The quoted accuracies are ±1 K and ±5 mb respectively (Upper Air Statistics 1957-75 [April 1977]).

To the best of my knowledge, no detailed figures of the type in Table 5.1 are available for Australian radiosondes. However, the appreciable errors quoted above imply that the Table 5.1 figures are probably applicable to Hobart as well.

(b) Effect of Distance from the Radiosonde Station. As pointed out in Section 4.1, Poatina is about 130 km north of Hobart Airport where the weather balloons are launched. The possibility of regressor error resulting from this separation must therefore be investigated.

Carmichael et al. (1967) calculated various atmospheric coefficients for muon data at Deep River, Canada, which is 120 km west of the radiosonde station at Maniwaki. Their weather is known to travel from west to east and they found that an average time delay of $\sim$ 3 hours, when built into the weather data, resulted in a very small improvement in R^2.

Barrett et al. (1952), in an early study of the muon intensity at 1574 hg cm^{-2} underground, also considered this possible source of error. They compared weather data from three radiosonde stations all situated within 250 km of the cosmic ray observatory at Ithaca, New York. In particular, the separation of Ithaca and Rome (N.Y.), whose radiosonde figures were used in their regression analysis, is ~ 150 km, much the same as the distance from Hobart to Poatina. Close agreement was seen in the temperature variations for the three centres. They therefore concluded that no significant error resulted from using the Rome data in their analysis.

Tasmania is situated in a band of latitude known as the Roaring Forties and, as in the Canadian case, its weather also generally approaches from the west. As the longitude of Hobart Airport is almost the same as that of Poatina, there should be negligible time delay in atmospheric conditions between the two sites. Thus there should be very little error resulting from this effect.

The spatially-caused error at Poatina may be investigated by comparing the Hobart radiosonde data with those of the nearest other radiosonde station at Laverton, Victoria, which is 400 km northwest of Hobart at latitude 37.9° S and longitude 144.8° E (see map: Figure 4.1).

Figure 5.1 shows monthly mean values of H_{100} and T_{80} for the two centres. These data were drawn from "Upper Air Statistics, Australia 1957-75" (April 1977). Although the annual means differ, this does not matter as the constant term $\hat{\beta}_0$ in the regression equation is of no interest. The

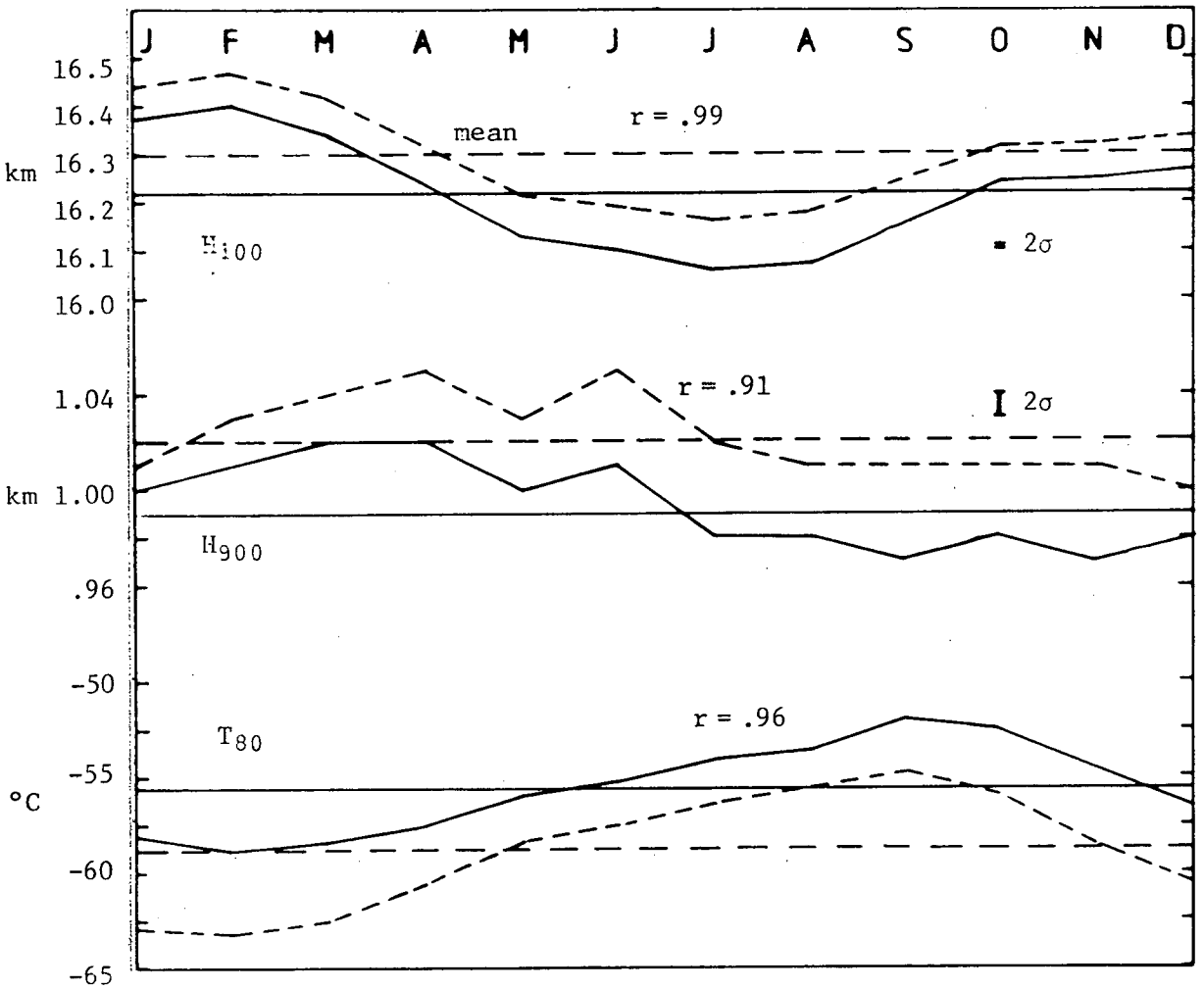

Figure 5.1. Temperature and height correlations in the atmosphere. Mean geopotential of 100 and 900 mb levels and temperature of 80 mb level. Dotted lines: Laverton, Victoria; solid lines: Hobart Airport, Tasmania. 2σ on T_{80} is too small to show.

Source: Upper Air Statistics, Australia, 1957-75 (1977).

calculated correlation coefficients are all high and significant at > 99.9 % level. As Poatina is much closer to Hobart than Laverton, we may conclude that variations in the stratosphere over Poatina closely follow those over Hobart.

From these considerations, it is reasonable to rule out the distance between Hobart and Poatina as a significant source of regressor error.

(c) Errors resulting from the method of sampling. The effective sampling rate for H and T, at three times per day, is much slower than the fluctuations in these parameters. Cutler (1980) cites this error source in an analysis of muon variations at Utah (506 hg cm^{-2}). In the case of Poatina, the muon intensities were averaged over 24 hour periods, whereas any rapid fluctuations in T and H during the period would introduce scatter into the (so-called) means of T and H. Dyring and Lindgren (1962) have shown that this type of error imposes an upper limit on the accuracy of the regression coefficients. The limit is shown to be a function of the stretch of time for which the data are representative. As this amounts to a few hours, at most, the scarcity of aerological data may be a serious problem.

5.3.4 Previous Applications of Bias Corrections

Trefall and Nordö found that the partial three-fold coefficients differed significantly from their theoretical values. In particular, their pressure estimate was "too large" and their height estimate "too small".

Using the theory explained in the next section, better agreement was obtained. The serious influence of regressor

errors was emphasized by the results of Bachelet and Conforto (1956). They found better agreement between their estimates and theory when monthly means, rather than daily means, were used in the regression analysis. This trend is to be expected, as the relative error variance is smaller for monthly means than for daily means.

5.4 Bias in the Regression Coefficients

5.4.1 Two or More Regressor Variables

Bias due to measurement errors.

Suppose the observed regressor matrix is subject to measurement error so that we observe

$$X_\Delta = X + \Delta \tag{5.3}$$

where X is the true matrix and Δ is an unbiased error matrix. The j^{th} column of X_Δ is

$$\underline{x}_{\delta j} = \underline{x}_j + \underline{\delta}_j \ . \tag{5.4}$$

Denote the covariance of $\underline{\delta}_i$ and $\underline{\delta}_j$ by

$$\sigma_{ij} = (\underline{\delta}_i^T \underline{\delta}_j)/n$$

and the variance of $\underline{\delta}_j$ by σ_j^2. The OLS estimator of $\underline{\beta}$ is

$$\begin{aligned} \hat{\underline{\beta}}_\Delta &= (X_\Delta^T X_\Delta)^{-1} X_\Delta^T \underline{Y} \\ &= [(X+\Delta)^T(X+\Delta)]^{-1} (X+\Delta)^T \underline{Y} \\ &= (X^T X + \Delta^T\Delta)^{-1} X^T \underline{Y} \end{aligned} \tag{5.5}$$

where Δ is assumed uncorrelated with X and $\underline{Y}$. Equation (5.5) defines a biased estimator, where

$$\Delta^T\Delta = nS = n \begin{pmatrix} \sigma_1^2 & \sigma_{12} & \cdots & \sigma_{1p} \\ \sigma_{21} & \sigma_2^2 & \cdots & \sigma_{2p} \\ \vdots & \vdots & & \vdots \\ \sigma_{p1} & \sigma_{p2} & \cdots & \sigma_p^2 \end{pmatrix}$$

Seber (1977), in a development of the treatment of Davies and Hutton (1975), shows that the expected value of $\hat{\underline{\beta}}_\Delta$ is

$$E(\hat{\underline{\beta}}_\Delta) \simeq \underline{\beta} - n(X_\Delta^T X_\Delta)^{-1} S \underline{\beta} \quad . \tag{5.6}$$

Thus $\underline{\beta}$ is no longer unbiased, but is shifted by the column bias vector

$$\hat{\underline{\theta}} = n(X_\Delta^T X_\Delta)^{-1} S \underline{\beta} \quad . \tag{5.7}$$

Unfortunately, we usually do not know $\underline{\beta}$ and must use $\hat{\underline{\beta}}_\Delta$ in its place.

In the approximations of Hodges and Moore (1972), the off-diagonal elements of S are ignored, so that

$$\hat{\underline{\theta}} = (n-p-1)(X_\Delta^T X_\Delta)^{-1} S \underline{\beta} \tag{5.8}$$

where

$$S = \text{diag}(\sigma_1^2, \sigma_2^2, \ldots, \sigma_p^2) \quad . \tag{5.9}$$

Comparison of (5.8) with (5.7) shows that even if the regressor errors are intercorrelated, for $n >> p$ the bias is increased very little.

Since $X_\Delta^T X_\Delta = X^T X + nS$, the "true" vector of coefficients is then

$$\hat{\underline{\beta}}^{*} = [X_{\Delta}^{T} X_{\Delta} - nS]^{-1} X^{T}\underline{Y} \ . \qquad (5.10)$$

Equation (5.10) was used by Trefall and Nordö to obtain their corrected coefficients.

Standard errors.

Seber (1977) shows that for large n and small S, the apparent dispersion matrix $D(\hat{\underline{\beta}}_{\Delta}) = \sigma^{2}(X_{\Delta}^{T} X_{\Delta})^{-1}$ of the estimates is not much in error. The reader is referred to the source if detail is desired.

Composition of the bias vector.

We note that (5.8) gives the user no prior idea whether the corrected coefficients will be bigger or smaller than their biased values. The answer to this question is provided by the following:

Since

$$D(\hat{\underline{\beta}}_{\Delta}) = \sigma^{2}(X_{\Delta}^{T} X_{\Delta})^{-1} \simeq D(\hat{\underline{\beta}})$$

we have, by (5.7),

$$\hat{\underline{\theta}} \simeq n.D(\hat{\underline{\beta}}_{\Delta}) S \underline{\beta} / \sigma^{2} \ . \qquad (5.11)$$

For simplicity, we drop the Δ subscript, assume S is diagonal, and then expand the j^{th} row of (5.11):

$$\hat{\theta}_{j} \simeq \frac{n}{\sigma^{2}} [\mathrm{var}(\hat{\beta}_{j}) \sigma_{j}^{2} \beta_{j} + \sum_{\substack{k=1 \\ k \neq j}}^{p} \mathrm{cov}(\hat{\beta}_{j}, \hat{\beta}_{k}) \sigma_{k}^{2} \beta_{k}] \ . \qquad (5.12)$$

If the X matrix is orthogonal, $D(\hat{\underline{\beta}})$ will be diagonal and $\hat{\theta}_{j}$ will be given by the first term (only) in the square

brackets. Thus, random errors in a regressor variable always tend to *reduce* the absolute value of the corresponding regression coefficient. However, if some of the regressors are intercorrelated, the situation becomes very complicated and the bias could be of either sign. Therefore the net size and direction of bias is highly dependent on the *conditioning* of the X matrix as well as any errors it may contain. This matter is returned to in Section 5.9.1.

Bias due to underfitting.

Recall that if the postulated model $\underline{Y} = X\beta + \underline{\varepsilon}$ is the true model then $E(\hat{\underline{\beta}}) = \underline{\beta}$, viz. the estimates are unbiased. Suppose, however, that some variables have been incorrectly omitted so that the true model is really

$$\underline{Y} = X\underline{\beta} + Z\underline{\gamma} + \underline{\varepsilon} \; . \tag{5.13}$$

Then

$$\begin{aligned} E(\hat{\underline{\beta}}) &= (X^TX)^{-1} X^T.E(\underline{Y}) \\ &= (X^TX)^{-1} X^T(X\underline{\beta} + Z\underline{\gamma}) \\ &= \underline{\beta} + (X^TX)^{-1} X^T Z \underline{\gamma} \end{aligned}$$

i.e.

$$E(\hat{\underline{\beta}}) = \underline{\beta} + A\underline{\gamma}$$

where

$$A = (X^TX)^{-1} X^TZ \; . \tag{5.14}$$

Thus, underfitting introduces a bias vector $A\underline{\gamma}$ where A is called the alias matrix. The bias will be zero if $X^TZ = 0$, i.e. if the included and omitted variables are not

correlated with each other. Under these conditions, underfitting does not matter.

Seber (1977) shows that underfitting causes s^2 to be biased, so that $E(s^2) > \sigma^2_{Poisson}$ strictly.

5.4.2 One Regressor Variable

If the regressor variable is measured with error, we observe

$$x_{\delta i} = x_i + \delta_i \ . \tag{5.15}$$

Let σ_δ^2 be the variance in $\underline{\delta}$, such that $\delta_i \sim N(0,\sigma_\delta^2)$. For large n and using a little algebra, (5.6) simplifies to

$$E(\hat{\beta}_{1\delta}) = \beta_1 - \beta_1 \cdot \frac{\sigma_\delta^2 n}{\Sigma(x_i - \bar{x}) + n\sigma_\delta^2}$$

$$\simeq \beta_1[1 - \sigma_\delta^2/(s_x^2 + \sigma_2^2)]$$

$$= \beta_1[1 - \sigma_\delta^2/s_{x\delta}^2]$$

where

$$s_{x\delta}^2 = s_x^2 + \sigma_\delta^2$$

i.e.

$$E(\hat{\beta}_{1\delta}) = \beta_1[1 - R^*]$$

where

$$R^* = \frac{\sigma_\delta^2}{s^2_{x\delta}} \ . \tag{5.16}$$

$s^2_{x\delta}$ is the sample variance of $\underline{x}_\delta$, evaluated from the measurable $x_{\delta i}$. Thus the *relative error variance* R^*

determines the *bias factor* $1-R^*$. If $\sigma_\delta^2 = 0$, $E(\hat{\beta}_{1\delta})$ is unbiased. We see that non-zero errors δ_i always reduce the absolute value of $E(\hat{\beta}_{1\delta})$ below its potential value, viz. "shrink" it towards zero.

If β_1 is known, we may use (5.16) to evaluate σ_δ^2:

$$\sigma_\delta^2 = s_{x_\delta}^2 R^* = S_{x_\delta}^2 [1 - E(\hat{\beta}_{1\delta})/\beta_1] \tag{5.17}$$

by assuming that $\hat{\beta}_{1\delta}$ approximates $E(\hat{\beta}_{1\delta})$. (5.16) may also be derived in the following way:

$$\begin{aligned}
\hat{\beta}_{1\delta} &= (\underline{x}_\delta^T \underline{x}_\delta)^{-1} \underline{x}_\delta^T \underline{Y} \\
&= (\underline{x}^T \underline{x} + \underline{\delta}^T \underline{\delta})^{-1} \underline{x}^T \underline{Y} \\
&= \frac{\Sigma x_i Y_i}{\Sigma x_i^2 + \Sigma \delta_i^2} \\
&\leq \frac{\Sigma x_i Y_i}{\Sigma x_i^2} = \hat{\beta}_1 \text{ since } \Sigma \delta_i^2 \geq 0 \text{ strictly.}
\end{aligned}$$

Thus

$$\begin{aligned}
\hat{\beta}_{1\delta} &= \hat{\beta}_1 \cdot \frac{\Sigma x_i^2}{\Sigma x_i^2 + \Sigma \delta_i^2} \\
&= \hat{\beta}_1 \cdot \frac{1}{1 + \Sigma \delta_i^2 / \Sigma x_i^2} \\
&\simeq \hat{\beta}_1 (1 - \Sigma \delta_i^2 / \Sigma x_i^2) \text{ provided } \Sigma \delta_i^2 << \Sigma x_i^2 \\
&= \hat{\beta}_1 (1 - \sigma_\delta^2 / s_x^2) \\
&\simeq \hat{\beta}_1 (1 - \sigma_\delta^2 / s_{x_\delta}^2) \ .
\end{aligned}$$

Taking expected values of both sides,

$$E(\hat{\beta}_{1\delta}) \simeq \beta_1 (1 - \sigma_\delta^2 / s_{x_\delta}^2) \ . \tag{5.18}$$

The effect of errors in the variables on the correlation coefficient.

Let

$$\underline{x}_\delta = \underline{x} + \underline{\delta}, \qquad \underline{Y}_\varepsilon = \underline{Y} + \underline{\varepsilon}.$$

Then

$$r_{x_\delta Y_\varepsilon} = \underline{x}_\delta^T \underline{Y}_\varepsilon \Big/ \left[\left(\underline{x}_\delta^T \underline{x}_\delta \right) \left(\underline{Y}_\varepsilon^T \underline{Y}_\varepsilon \right) \right]^{\frac{1}{2}}$$

$$= \underline{x}^T \underline{Y} \Big/ \left[\left(\underline{x}^T \underline{x} + \underline{\delta}^T \underline{\delta} \right) \left(\underline{Y}^T \underline{Y} + \underline{\varepsilon}^T \underline{\varepsilon} \right) \right]^{\frac{1}{2}}$$

provided

$$\underline{x}^T \underline{\delta} = \underline{\delta}^T \underline{x} = \underline{Y}^T \underline{\varepsilon} = \underline{\varepsilon}^T \underline{Y} = \underline{x}^T \underline{\varepsilon} = \underline{\delta}^T \underline{Y} = \underline{\delta}^T \underline{\varepsilon} = 0$$

i.e.

$$r_{x_\delta Y_\varepsilon} = r_{xY} \left\{ \underline{x}^T \underline{x} \; \underline{Y}^T \underline{Y} \Big/ \left[\left(\underline{x}^T \underline{x} + \underline{\delta}^T \underline{\delta} \right) \left(\underline{Y}^T \underline{Y} + \underline{\varepsilon}^T \underline{\varepsilon} \right) \right] \right\}^{\frac{1}{2}} \tag{5.19}$$

Therefore non-zero errors in either variable "shrink" the apparent correlation coefficient towards zero.

Estimation of the Temperature Error for Poatina

Since upper air temperature is expected to be the only significant atmospheric influence on the Poatina muon intensity, equation 5.17 provides a means of estimating the temperature error variance at Poatina.

The measured temperature standard deviation for the years 1972-76 was $s_T = 2.70$ K; thus $s^2_\delta = s^2_T = 7.29$. Using $\hat{\beta}_{1\delta} = 0.088$ % K^{-1} (Table 4.2) and $\beta_1 = 0.25$ % K^{-1} (Section 3.2.3), we obtain $\sigma_\delta^2 = \sigma_T^2 = 4.72$ K^2. This error variance agrees well with Trefall and Nordö's value of 4.69 K^2 at the 200 mb level, given in Table 5.1. The corresponding standard deviation is $\sigma_T = 2.17$ K.

5.5 The Effect on the Coefficients of Collinearity Among the Atmospheric Variables

5.5.1 A Complete Model

In Table 4.2 it was shown that significant correlations were present among the Poatina (P, H_{100}, T_{80}) weather data. The conclusion was based on large values of R_P, R_H and R_T, the multiple correlation coefficients within the X matrix.

To see the effect of these correlations on the regression coefficients, from (4.21) it may be shown that

$$\begin{aligned} \text{var}(\hat{\beta}_j) &= \sigma^2 (X^T X)^{-1}_{jj} \\ &= \frac{\sigma^2}{(1-R_j^2)\underline{x}_j^T \underline{x}_j} \end{aligned} \qquad (5.20)$$

where the R_j are mentioned above. Marquardt (1970) terms the quantity $1/(1-R_j^2)$ the *variance inflation factor* of the j^{th} estimate (VIF_j). Clearly, $VIF_j \to \infty$ as $R_j \to \pm 1$. However, the moderate R_j observed for the Poatina weather data imply VIF_j of only ~ 1.3, which is not serious.

It is clear that provided the model is complete, data collinearity alone cannot cause bias in the coefficients. However, a large amount of Poisson noise (σ^2) or a small data sum of squares ($\underline{x}_j^T \underline{x}_j = \sum_i x_{ij}^2$) will increase the variance. Consider the "signal-to-noise" ratio of the j^{th} term in the model (4.1):

$$\omega_j = \frac{\text{signal due to } \beta_j}{\text{random noise}} = \frac{(\underline{x}_j \beta_j)^T (\underline{x}_j \beta_j)}{(n-1)\sigma^2_{Pois}}$$

$$\frac{\beta^2 \, \underline{x}_j^T \underline{x}_j}{(n-1)\sigma^2_{Pois}} \qquad (5.21)$$

Combining (5.20) and (5.21) yields

$$\frac{\text{var}(\hat{\beta}_j)}{\beta_j^2} = \frac{VIF_j}{(n-1)\omega_j} \qquad (5.22)$$

Thus the relative error in β_j depends only on the ratio VIF_j/ω_j.

5.5.2 An Underfitted Model

In Section 5.4.1 it was shown that underfitting will cause the variables which *are* included in the regression to have biased coefficients, if the included and omitted variables are correlated. In this situation, data

collinearity alone can cause bias. It seems highly likely that the total barometer coefficient, calculated in Chapter 4, is severely biased through omission of upper air temperature. The latter variable has already been shown to be correlated with P and H_{100}. Further analyses of this effect are considered in Section 5.7.

5.6 Revised Coefficients After Corrections for Data Errors

5.6.1 Introduction

Theory

We recall from Section 5.4.1 that an unbiased estimate of $\underline{\beta}$ may be obtained by calculating

$$\begin{aligned} \hat{\underline{\beta}}^* &= (X_\Delta^T X_\Delta - \Delta^T \Delta)^{-1} X^T \underline{Y} \\ &= (X_\Delta^T X_\Delta - nS)^{-1} X^T \underline{Y} \end{aligned} \tag{5.23}$$

The success of this method relies on having a complete model, an accurate estimation of $S = \text{diag}[\sigma_1^2, \sigma_2^2, \ldots \sigma_p^2]$ and on Δ being uncorrelated with both X and $\underline{Y}$. The implementation of (5.23) for Poatina data will now be described.

5.6.2 The Poatina (P,T,I) Model

Since only P and T are expected to be applicable to the Poatina data, corrections for this case were tried first. We assume certain error variances in P and T but zero error *covariance* (a reasonable assumption). Then $S = \text{diag}[\sigma_P^2, \sigma_T^2]$.

Without loss of generality, let X_Δ' and $\underline{Y}'$ denote data matrices whose columns have been centered to have zero mean and unit length:

$$\begin{aligned} \sum_i x'_{ij} &= 0 , & \sum_i x'_{ij} &= 1 \\ \sum_i Y'_i &= 0 , & \sum_i Y'^2_i &= 1 \end{aligned} \tag{5.24}$$

The OLS coefficients are then

$$\underline{\hat{\alpha}} = \left(X_\Delta'^T X_\Delta'\right)^{-1} X_\Delta'^T \underline{Y}'$$

$$\begin{bmatrix} 1 & r_{PT} \\ r_{TP} & 1 \end{bmatrix}^{-1} \begin{bmatrix} r_{IP} \\ r_{IT} \end{bmatrix} \tag{5.25}$$

where r_{ij} is the simple correlation between the i^{th} and j^{th} variables. In normal units, the coefficients are then

$$\underline{\hat{\beta}} = \operatorname{diag}\left[\frac{s_I}{s_P}, \frac{s_I}{s_T}\right] \underline{\hat{\alpha}} \tag{5.26}$$

The dispersion matrix of $\underline{\hat{\alpha}}$ is

$$D(\underline{\hat{\alpha}}) = \sigma^2_{Pois}\left(X_\Delta'^T X_\Delta'\right)^{-1}$$

$$= \sigma^2_{Pois}\begin{bmatrix} 1 & r_{PT} \\ r_{TP} & 1 \end{bmatrix} \tag{5.27}$$

so that

$$\operatorname{var}(\hat{\beta}_P) = \frac{\operatorname{var}(\hat{\alpha}_P)}{n\, s_P^2}, \quad \operatorname{var}(\hat{\beta}_T) = \frac{\operatorname{var}(\hat{\alpha}_T)}{n\, s_T^2} \tag{5.28}$$

In (5.26) and (5.28), s_I, s_P and s_T denote the sample standard deviations in original units. The diagonal elements of $X_\Delta'^T X_\Delta'$ are inflated due to the nS' matrix, where

$$S' = \text{diag}\left[\frac{\sigma_P^2}{s_P^2}, \frac{\sigma_T^2}{s_T^2}\right]$$

An estimate of $\underline{\alpha}$, corrected for measurement errors, is then

$$\begin{aligned}\hat{\underline{\alpha}}^* &= (X_\Delta'^T X_\Delta' - nS')^{-1} X_\Delta'^T \underline{Y}' \\ &= \begin{bmatrix} 1 - \sigma_P^2/s_P^2 & r_{PT} \\ r_{TP} & 1 - \sigma_T^2/s_T^2 \end{bmatrix}^{-1} \begin{bmatrix} r_{IP} \\ r_{IT} \end{bmatrix}\end{aligned} \qquad (5.29)$$

and the error-corrected variances are, by analogy with (5.27),

$$D(\hat{\underline{\alpha}}^*) = \sigma_{Pois}^2 (X_\Delta'^T X_\Delta' - nS')^{-1} \qquad (5.30)$$

Conversely, if $\underline{\alpha}$ is known and is substituted for $\hat{\underline{\alpha}}^*$ in (5.29), we obtain estimates for σ_P^2 and σ_T^2:

$$\left.\begin{aligned}\sigma_P^2 &= s_P^2 \left[1 - \frac{r_{IP} - r_{PT}\alpha_P}{\alpha_P}\right] \\ \sigma_T^2 &= s_T^2 \left[1 - \frac{r_{IT} - r_{PT}\alpha_T}{\alpha_T}\right]\end{aligned}\right\} \qquad (5.31)$$

Since $\beta_j = \alpha_j \left(\frac{s_I}{s_j}\right)$, (5.31) may be re-written

$$\sigma_j^2 = \frac{1}{\beta_j}\left(\beta_j s_j^2 + \beta_k s_{jk} - s_{Ij}\right), \quad k \neq j \qquad (5.32)$$

Provided S is diagonal, (5.32) generalizes for any number of regressors as

$$\sigma_j^2 = \frac{1}{\beta_j} \left(\sum_{k=1}^{p} \beta_k s_{jk} - s_{Ij} \right) \qquad (5.33)$$

Cutler (1980) shows that the standard error in σ_j may be estimated by

$$\varepsilon(\sigma_j) = \frac{s_j}{2\sigma_j n^{\frac{1}{2}} |\beta_j|} \left[\sum_{k=1}^{p} \beta_k^2 s_k^2 + s_I^2 \right]^{\frac{1}{2}} \qquad (5.34)$$

This expression may be derived from the variance of the product of two normal distributions.

If the chosen model is the true one and $\underline{\beta}$ is the true coefficient vector, equations (5.31) and (5.34) should yield estimates of σ_p^2 and σ_T^2 consistent with the values predicted in Section 5.3.2.

Implementation

The 1972-76 data were divided into 30 bi-monthly periods, and bi-daily means of the variables were used in the regression analysis, in an effort to reduce their error variances. The pressures were assumed to be well-determined and therefore σ_p^2 was set to zero. The chosen temperature variable was the mean of the 80-200 mb interval. The inclusion of the lower level is justified on two grounds:

(i) Temperature variations generally occur in the same sense above the tropopause (Figure 3.4).

(ii) The results in Table 5.1 indicate smaller temperature errors at greater depths in the atmosphere.

Results

Table 5.2 gives the results for a range of assumed values of σ_T.

TABLE 5.2

Error-corrected coefficients for Poatina, 1972-76

Assumed temp. error σ_T (K)	P(surface) (% mb^{-1})	$\bar{T}$(80-200) (% K^{-1})
0	-0.0257 ± 0.0019	0.0660 ± 0.0056
2	-0.0248 ± 0.0020	0.0699 ± 0.0057
4	-0.0214 ± 0.0020	0.0848 ± 0.0063

It is seen that the error-corrected results do not differ significantly from the unadjusted (OLS) figures when $\sigma_T = 2$ K. Choosing $\sigma_T = 4$ K causes some hint of bias toward the predicted theoretical coefficients, but such a temperature error is unrealistically large. It is, however, significant that the pressure coefficient has been halved from its typical value in Table 4.2. This suggests that the bi-monthly treatment *is* reducing the effective error variance(s) to some extent.

These results indicate that the observed pressure and temperature coefficients cannot be the result of temperature

noise alone. If the (P,T,I) model really is complete, the only other possible influence on $\hat{\underline{\beta}}$ would be non-zero pressure error.

To check this possibility, equations (5.33) - (5.34) were implemented for the 1972-76 data. Table 5.3 shows the results which correspond to various assumed $\underline{\beta}$'s.

TABLE 5.3

Inferred σ_P and σ_T using equations (5.33) and (5.34) for various assumed $\underline{\beta}$'s.

$T^I \equiv T(80)$, $T^{II} \equiv \bar{T}(80\text{-}200)$

β_P (% mb^{-1})	Resulting σ_P (mb)	No. of Months	β_T (% K^{-1})	Resulting σ_T (K)	No. of Months
- 0.003	24.53 ± 2.85	20	0.25	(T^I) 2.16 ± 0.06	59
- 0.003	28.16 ± 1.95	31	0.25	(T^{II}) 2.17 ± 0.06	58
- 0.006	20.24 ± 1.30	33	0.25	(T^{II}) 2.19 ± 0.06	59
- 0.010	14.79 ± 1.40	30	0.20	(T^{II}) 2.20 ± 0.08	58
- 0.020	11.13 ± 0.62	36	0.20	(T^{II}) 2.29 ± 0.07	57

At times, σ_j could not be estimated as σ_j^2 turned out to be negative. The table lists the number of months which contribute to the quoted weighted means.

The results indicate a value of σ_T in very good agreement with that found in Section 5.4.2, which was calculated from the total temperature coefficient. However, the pressure error σ_P is absurdly large, even in the last row of the table. This is puzzling, especially in view of the thoroughly

reasonable values obtained for σ_T by two different methods. It is possible that the formula (5.34) for $\varepsilon(\sigma_j)$ is somehow not appropriate for this particular set of data.

Cutler (1980) has performed a similar analysis for muons at 506 hg cm^{-2} in the Heber gold mine at Utah. Using surface pressure and an "effective" weighted mean temperature T_{eff} (see Section 5.7.2), he has obtained pressure and temperature errors of (4.7 ± 4.1)mb and (1.61 ± 0.09)K respectively. These values seem reasonable.

5.7 An Alternative Calculation of the Total Barometer Coefficient at Poatina

5.7.1 Theory of the Method

From Section 4.3.1, the total barometer coefficient for Poatina over 1972-76 was (-0.047 ± 0.002) % mb^{-1}. Yasue et al. (1981) in an analysis of muons underground at Matsushiro (220 hg cm^{-2}) obtained a virtually identical result, (-0.045 ± 0.005) % mb^{-1}. As these figures have been obtained from straight line regressions, there are only two possible sources of bias in the coefficients:

(i) pressure measurement error

(ii) bias due to underfitting.

Intuitively we expect that there is negligible error in the pressures. In fact, if the errors were non-zero, the theory of Section 5.4.2 (equation 5.18) shows that the true coefficient would be even larger! However, underfitting

resulting from the omission of T (which is correlated with P) will be expected.

From (5.13) - (5.14), the true model is probably

$$E(\underline{Y}) = X\underline{\beta} + Z\,\underline{\gamma}$$

i.e. $$E(\underline{I}) = \underline{P}\beta_P + \underline{T}\,\beta_T \quad \text{in this case.}$$

Thus

$$E(\hat{\beta}_P) = (\underline{P}^T\underline{P})^{-1}\,\underline{P}^T(\underline{P}\beta_P + \underline{T}\beta_T)$$

$$= \beta_P + (\underline{P}^T\underline{P})^{-1}\,\underline{P}^T\underline{T}\,\beta_T$$

By virtue of (4.15), the alias matrix is just the scalar $(\underline{P}^T\underline{P})\underline{P}^T\underline{T} = \hat{\beta}_{TP}$, the simple straight-line slope of T against P. Thus

$$E(\hat{\beta}_P) = \beta_P + \hat{\beta}_{TP}\cdot\beta_T \qquad (5.35)$$

Since both terms on the righthand side of (5.35) are strictly negative, the underfitting should result in an inflated pressure coefficient. Furthermore, as β_T increases with muon threshold energy, the bias (second) term in (5.35) would be expected to increase rapidly with depth underground.

5.7.2 Implementation and Results

To test this theory, the T vs. P slope was estimated for Poatina weather data, 1972-76. Several weighted temperature variables were tried and the results

are given in Table 5.4. The "effective" temperature T_{eff} was calculated by weighting the temperature profile of the atmosphere by the probability function

$$p(h) = (h/\lambda)e^{-h/\lambda}$$

due to Cutler (1980), where $\lambda \approx 130\ g\,cm^{-2}$. (This expression gives the probability that a muon will be produced at a depth h. The rather long interaction length has been derived by J. Elbert (private communication to Cutler) and takes into account both pion and kaon parents.)

TABLE 5.4

Mean T vs P slope, Poatina 1972-76

Temp. variable	T vs. P slope ($K\ mb^{-1}$)	T vs P correlation coefficient
T(80)	-0.151 ± 0.006	- 0.45
$\bar{T}$(80-200)	-0.150 ± 0.006	- 0.45
T_{eff}	-0.149 ± 0.006	- 0.44

It is seen that the actual choice of the temperature variable makes no difference to the observed link between pressure and upper air temperature.

Using $\hat{\beta}_{TP} \equiv -0.15\ K\,mb^{-1}$, $\beta_T \equiv 0.25\ \%\ K^{-1}$ (Section 3.2.3) and $\beta_P \equiv -0.003\ \%\ mb^{-1}$ (Section 3.2.2) we obtain $E(\hat{\beta}_P) \equiv -0.041\ \%\ mb^{-1}$. This value is in very good agreement with the observed barometer coefficient.

We may also estimate the theoretical limit to the total barometer coefficient. From Chapter 3, $\beta_T \to 0.46\ \%\ K^{-1}$ as $\Delta E \to \infty$, and $\beta_P \to 0$. Therefore the upper limit to $\hat{\beta}_P$ should be about $-0.15 \times 0.46 = -0.069\ \%\ mb^{-1}$.

As a further check of these results, the form of equation 5.35 suggested the following procedure: if the I vs. P regression is performed subject to a constraint of constant temperature, the bias term in (5.35) should tend to zero, so that $E(\hat{\beta}_P) \simeq \beta_P$. To achieve this, the Poatina total pressure coefficient was computed for days when the temperature of the 80 mb level was within $\pm \Delta T$ of a chosen value, T. The extrema of T employed were 208 and 224 K. T was scanned over this range with step size $2\Delta T$ and a value of $b_{IP} = \hat{\beta}_P \times 100/\bar{I}$ was computed in each case. The weighted mean value of b_{IP} was then derived over all ΔT's. It was found in practice that the sample for each b_{IP} was too small when the data were analysed on a monthly basis, so bi-monthly periods were used instead. The results are shown in Figure 5.2.

From the diagram it is clear that a reduction in the allowed temperature variation is accompanied by a reduction in the empirical pressure coefficient. For a tolerance $\Delta T = \pm 0.05$ K, the resulting value of $(-0.005 \pm 0.002)\ \%\ mb^{-1}$ does not differ significantly from the figure expected.

It may at first seem reasonable that holding P constant and calculating $E(\hat{\beta}_T)$ should yield a negligible temperature coefficient, as, after all, P and T are linked. However, the equivalent of (5.35) for the temperature estimate is

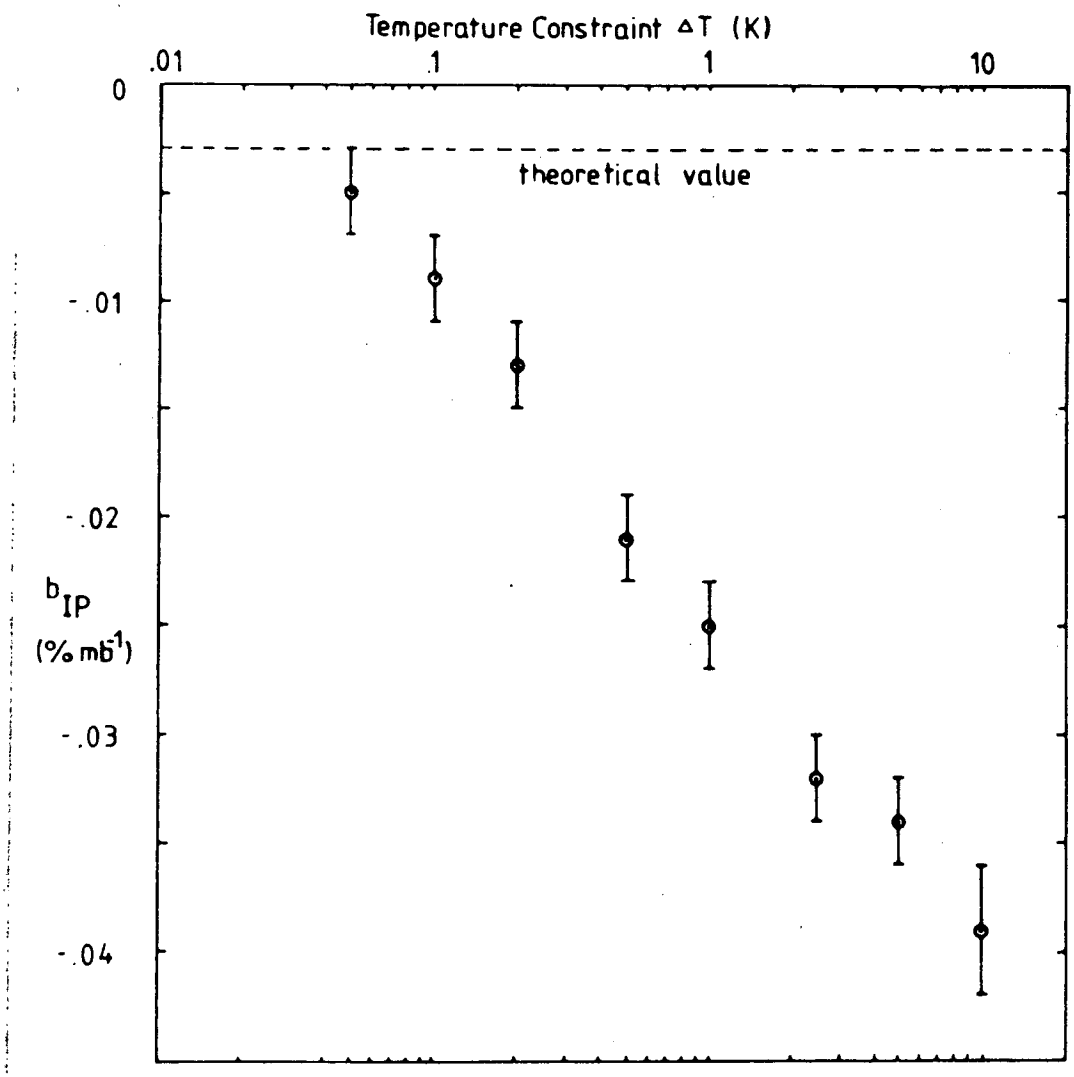

Figure 5.2. Total barometer coefficient at Poatina, 1972-76, subject to a temperature constraint ΔT during the regression.

$$E(\hat{\beta}_T) = \beta_T + \hat{\beta}_{PT}\beta_P \qquad (5.36)$$

Since both terms on the right hand side are strictly positive, forcing the bias to zero will still leave a significant temperature effect. This prediction was confirmed by $E(\hat{\beta}_T) \equiv (0.084 \pm 0.060)\ \%\ K^{-1}$, corresponding to $\Delta P = \pm 0.1$ mb. This temperature coefficient does not differ significantly from the value of $(0.088 \pm 0.005)\ \%\ K^{-1}$ in Table 4.2.

[N.B. Equation 5.36 assumes that the only bias in $E(\hat{\beta}_T)$ is due to the $\hat{\beta}_{PT}\beta_P$ term. In fact, since T is now the regressor and is measured with error, (5.36) should really include a second bias term on the R.H.S. This is the reason $E(\hat{\beta}_T)$ does not equal the predicted value of $0.25\ \%\ K^{-1}$ after $\hat{\beta}_{PT}$ has been forced to zero.]

5.8 Assessing the Seriousness of the Bias Introduced by Regressor Errors

5.8.1 Introduction

So far, it has been shown that the collinearity and data errors in the weather data are probably responsible for the anomalous coefficients at Poatina. However these problems also afflict the data used to calculate the Cambridge coefficients. Why then are the Cambridge coefficients less biased? The results for any sea-level muon telescope show even better agreement between theory and observation. For comparison, Table 5.5 contrasts the results for three

different muon threshold energies. The standard errors have been normalized so that they correspond to values that would have been obtained using one month's data (~ 30 observations).

From the table it is clear that the bias in the coefficients increases with threshold energy. Consider the bias vector, given by equation (5.7):

$$\underline{\hat{\theta}} \simeq n(X_{\Delta}^{T} X_{\Delta})^{-1} S\underline{\beta}$$

This is independent of Poisson noise and therefore of detector size, depending entirely on the X_{Δ} matrix and the true coefficients, $\underline{\beta}$. What is required, however, is some criterion for deciding whether the bias introduced by Δ is likely to be serious. For a given set of data $(X,\underline{Y})$ we might say that the bias in an estimate is serious if it is larger than the standard error of the estimate. This is illustrated in Figure 5.3. Following Davies and Hutton

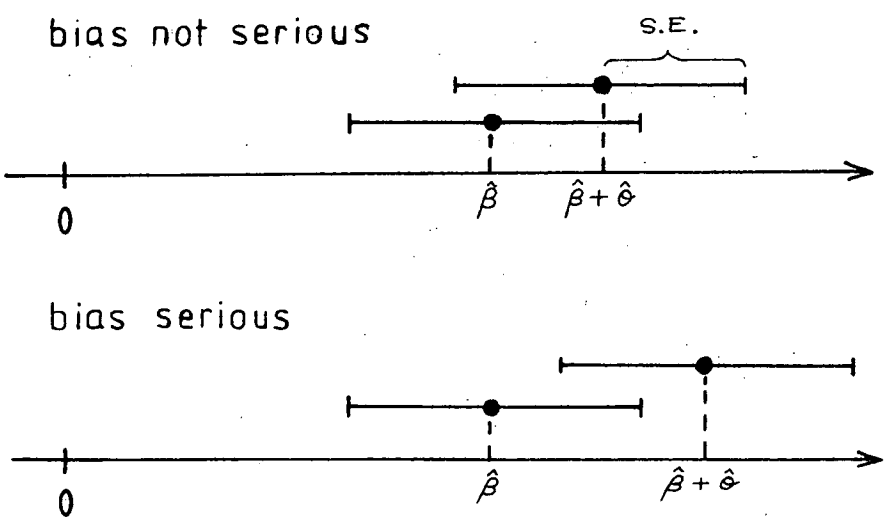

Figure 5.3. Serious and non-serious bias in a regression coefficient estimate.

TABLE 5.5

Predicted and Observed partial coefficients at Poatina (357 hg cm^{-2}), Cambridge 70° narrow angle (47 hg cm^{-2}) and Hobart (sea level cubical). Predicted coefficients are in brackets.

Regressors used: Poatina (P, H_{100}, T_{80}) 1972-76
Cambridge $(P, H_{100}, \bar{T}_{80-100})$ 1964
Hobart $(P, H_{100}, \bar{T}_{100-200})$ 1972

Location	Muon threshold energy (GeV)	Muon intensity I_{sc} (scaled counts per hour)	Scale factor	Poisson error (daily) σ_{Pois}	Pressure coeff. (% mb^{-1})	Height coeff. (% km^{-1})	Temp. coeff. (% K^{-1})
Poatina (PHTI model)	100	850	2	4.2	-0.057 ± 0.015 (-0.003)	3.955 ± 1.596 (-0.15)	0.080 ± 0.039 (0.25)
Poatina (PTI model)	100	850	2	4.2	-0.042 ± 0.015 (-0.003)		0.045 ± 0.039 (0.25)
Cambridge	10	75	16	0.44	-0.045 ± 0.014 (-0.07)	-2.139 ± 1.725 (-1.3)	0.030 ± 0.045 (0.022)
Hobart	0.3	500	256	0.29	-0.1185 ± 0.0017 (-0.12)*	-3.610 ± 0.145 (-6.7)*	0.061 ± 0.003 $(+0.06)$*

*Trefall (1956)

(1975) we quantify this idea in the following way:

Suppose $\underline{a}\,\hat{\underline{\beta}}$ estimates $\underline{a}\,\underline{\beta}$ where $\underline{a}$ is some row vector with p elements. Then the bias of $\underline{a}\,\hat{\underline{\beta}}$ might be considered serious if it exceeds the standard error of $\underline{a}\,\hat{\underline{\beta}}$, namely $\sigma_{Pois}[\underline{a}(X_\Delta^T X_\Delta)^{-1}\underline{a}^T]^{\frac{1}{2}}$. Let $|\underline{x}|$ denote the sum of the absolute values of the elements in some general vector $\underline{x}$. Then we may regard the bias introduced by Δ as unimportant if the "relative bias"

$$c = \sup_{\underline{a}}\{|\underline{a}[E(\hat{\beta}) - \underline{\beta}]|/\sigma_{Pois}[\underline{a}(X_\Delta^T X_\Delta)^{-1}\underline{a}^T]^{\frac{1}{2}}\} \qquad (5.37)$$

is less than about one.

Davies and Hutton show that this condition may be simplified as

$$c = \frac{\sum_j^n \sigma_j|\beta_j|}{\sigma_{Pois}} \leq 1 \qquad (5.38)$$

The quantity c is a measure of the "total" relative bias, summed over all the regression coefficients. Since $\underline{\beta}$ is generally unknown we have to use $\hat{\underline{\beta}}$ in its place. (In any case, to be open-minded, $\underline{\beta}$ should not be pre-supposed!). Of course it is possible that the errors in X_Δ are so bad that $\hat{\underline{\beta}}$ is meaningless and hence so is the estimate of c. However, the length of $\hat{\underline{\theta}}$ is related to how close $X_\Delta^T X_\Delta$ is to being singular. To investigate this, a singular value decomposition was performed on the $X_\Delta^T X_\Delta$ for the three sites. This is described in Appendix 3 , where it is shown that the collinearity and errors in the matrices are not sufficient to render them "close" to being singular. We

may therefore regard c as a valid indicator of the relative bias in $\hat{\underline{\beta}}$.

Before the parameter c can be used to compare atmospheric coefficients seen by different detectors, it must be "normalized" to the same value of σ_{Pois}. This is necessary, since, otherwise, an improvement in counting statistics will make c appear worse (larger). The effective daily Poisson errors in Table 5.5 have been obtained using the formula

$$\sigma_{Pois} = \sqrt{\frac{I_{sc}}{24f}}$$

where I_{sc} is the scaled muon intensity and f is the recording scale factor. Thus $f\,I_{sc}$ is the absolute intensity in particles per hour.

5.8.2 Implementation for Poatina, Cambridge and Hobart Data

The parameter c was calculated for the three stations using data standard errors $\sigma_P = 0$, $\sigma_H = 50$ m and $\sigma_T = 2.2$ K. The results are shown in Table 5.6.

TABLE 5.6

c-parameter calculated for Poatina, Cambridge and Hobart Data. The Poisson errors have been taken from Table 5.5.

Location	Normalization factor $\frac{\sigma_{Pois}(site)}{\sigma_{Pois}(poatina)}$	Relative bias, c	
		Unnormalized	Normalized (with respect to Poatina)
Poatina (PHTI)	1	18.3	18.3
(PTI)	1	6.8	6.8
Cambridge	0.105	9.0	0.94
Hobart	0.069	10.2	0.70

It is seen that the c-values for Cambridge and Hobart are considerably lower than for Poatina. This is entirely consistent with the much lower bias observed for the first two locations. It is also interesting to note the drop in the relative bias at Poatina when height is omitted from the model. This implies that the height measurement errors are responsible for severe bias in the Poatina (P,H,T,I) model.

In an isolated situation, where we are presented with a single set of coefficients and we need to know whether they are significantly biased or not, consideration must also be given to the relative standard error of each estimate: $S.E.(\hat{\beta}_j)/\hat{\beta}_j$. If this quantity is large, then even a small value of c (say, 2) will mean that $\hat{\beta}_j$ is severely biased. This situation exists for the Poatina results and, to a lesser extent, for Cambridge (see Table 5.5). On the other hand, the *relative* accuracy of the Hobart coefficients is good enough to allow a large value of c to be tolerated.

The dependence on $\underline{\beta}$ of bias in $\underline{\hat{\beta}}$ has been emphasized by the results of Cutler (1980). He has obtained partial coefficients for P and T_{eff} at 506 hg cm^{-2} which also are strongly biased from his predicted values (Table 5.7). This is despite a much lower daily Poisson error (0.15 % vs. 0.5 % at Poatina).

Thus it is seen that an acceptable threshold for c is a matter for judgment in each case. The c-parameter, used in conjunction with the observed standard errors in $\underline{\hat{\beta}}$, should provide a powerful tool in the interpretation of regression coefficients where data errors are known to be present.

TABLE 5.7

Partial coefficients obtained by Cutler (1980) at 506 hg cm^{-2} underground

Regressor	P ($\% \ mb^{-1}$)	$T_{eff.}$ ($\% \ K^{-1}$)
Predicted	- 0.0054	0.29
Observed	- 0.023 ±0.003	0.121± 0.007

5.9 Correction of the Poatina Muon Intensity for Atmospheric Effects

5.9.1 Optimization of R^2

By this stage, we see that the empirical regression coefficients may furnish a very poor means of discovering the true relative influence of the atmospheric variables. A short $\underline{\beta}$ vector will most likely result in a biased $\underline{\hat{\beta}}$ vector if the regressors are intercorrelated or measured with error. However, the OLS coefficients still give the highest R^2 value despite the fact that they may be meaningless physically.

To optimize R^2 for the Poatina muon intensity, an exhaustive series of regressions was tried, using up to three explanatory variables. Since H_{100} is correlated with P, it is interesting to try H_{100}-H_{1000}, which is more a measure of the mean temperature over the corresponding pressure interval (following Equation 3.13). This *may* reduce the bias in $\underline{\hat{\beta}}$. Four different temperature variables were tried, including T_{eff} which was used in Section 5.7.2. Table 5.8 shows the

results, which may be summarized thus:

(i) Barometric pressure P is a poor predictor to use on its own. This agrees with the theory.

(ii) Upper air temperature T_{80} is even worse on its own, but only because it is not well determined. (Its relative error variance may be estimated from Section 5.4.2 as $(2.17/2.70)^2 = 0.896$).

(iii) P and T together are better, and there is nothing to choose between the various forms of T used: $R^2 \simeq 30\ \%$. However, T_{eff} gives the least bias in $\hat{\underline{\beta}}$.

(iv) The addition of H improves R^2 to $\sim 40\ \%$. Again it does not matter which T is used. However, two facts are evident. First, the $H_{100}-H_{1000}$ variable halves the bias in $\hat{\beta}_P$. This confirms that, from a mathematical viewpoint, it is a better variable to use than just H_{100}. Second, the best overall agreement between $\underline{\beta}$ and $\hat{\underline{\beta}}$ is obtained using $(P,H_{100}-H_{1000},T_{eff})$ and the worst with (P,H_{100},T_{80}). A singular value decomposition, as described in Appendix 3, has been carried out on the $X_\Delta^T X_\Delta$ matrices for the two cases. The results in Table 5.9 show that the variables in the former set are less interdependent than those in the latter. Therefore the observed coefficients are not surprising.

By normal standards, $R^2 = 40\ \%$ is not a very good figure, but probably cannot be improved upon in view of the large Poisson error and the measurement errors in the regressors. Cutler (1980) has performed an analysis using P and T_{eff} for muons at 506 hg cm^{-2}. Their counting rate was approximately 17000 h^{-1} (10 times that of Poatina) but R^2

TABLE 5.8

Extended table of regression coefficients for Poatina, 1972-76.

Key: $T^{I} \equiv T_{80}$, $T^{II} = (T_{100} + T_{200})/2$, $T^{III} = (0.5T_{200} + T_{150} + T_{100} + T_{80} + 0.5T_{60})/4$, T_{eff} = "effective" temperature (Section 5.7.2).

Regressor	P(surface)	H_{100}	$H_{100}-H_{1000}$	T^{I}	T^{II}	T^{III}	T_{eff}	R^2
	% mb^{-1}	(% km^{-1})	(% km^{-1})	(% K^{-1})	(% K^{-1})	(% K^{-1})	(% K^{-1})	(%)
Predicted coeff.	- 0.003	- 0.15	—	~ 0.25				
Total coeffs. 1972-76	- 0.047 ± 0.002							16.0
				0.088 ± 0.005				6.3
Partial coeffs. 1972-76 (PTI model)	- 0.042 ± 0.002			0.045 ± 0.005				29.8
	- 0.041 ± 0.002				0.079 ± 0.007			31.9
	- 0.038 ± 0.002					0.060 ± 0.006		29.6
	- 0.035 ± 0.002						0.115 ± 0.008	31.4
Partial coeffs. 1972-76 (PHTI model)	- 0.057 ± 0.002	3.955 ± 0.205		0.080 ± 0.006				39.4
	- 0.024 ± 0.002		3.813 ± 0.203	0.079 ± 0.006				39.3
	- 0.058 ± 0.002	3.397 ± 0.214			0.083 ± 0.008			39.1
	- 0.030 ± 0.002		3.186 ± 0.211		0.079 ± 0.008			39.0
	- 0.052 ± 0.002	3.482 ± 0.198				0.083 ± 0.007		39.1
	- 0.021 ± 0.002		3.325 ± 0.195			0.082 ± 0.007		39.1
	- 0.048 ± 0.002	2.718 ± 0.194					0.112 ± 0.009	39.3
	- 0.023 ± 0.002		2.615 ± 0.191				0.110 ± 0.009	39.3

TABLE 5.9

Variance decomposition proportions of X matrix for

(1) Poatina (P, H_{100}, T_{80}) 1972-76 (upper figures)

(2) Poatina ($P, H_{100}-H_{1000}, T_{eff}$) 1972-76 (lower figures)

The theory of the method is contained in Appendix 3.

Proportion of	Associated singular value		
	μ_1	μ_2	μ_3
	$= \begin{cases} 1.38 \\ 1.18 \end{cases}$	$= \begin{cases} 0.876 \\ 0.912 \end{cases}$	$= \begin{cases} 0.535 \\ 0.682 \end{cases}$
$var(\hat{\beta}_p)$	0.091 0.136	0.513 0.472	0.396 0.392
$var(\hat{\beta}_H)$	0.114 0.082	0.158 0.274	0.729 0.644
$var(\hat{\beta}_T)$	0.102 0.065	0.282 0.201	0.615 0.734
η_k	1.00 1.00	1.57 1.32	2.57 2.04

was still only 47 %. Therefore, regressor errors remain a serious impediment to removing atmospheric effects from the high energy muon intensity.

5.9.2 Application of Corrections

The muon intensity, corrected for atmospheric effects, is given by

$$I_{corr} = I_{obs} - \Delta I$$

$$= I_{obs} - 10^{-2}\,\bar{I}\left(\sum_j b_j\,\Delta A_j\right) \qquad (5.39)$$

where the b_j are the various regression coefficients and the ΔA_j are the deviations in the corresponding atmospheric variables from their means. Since Table 5.8 shows that R^2 is not improved by using regressors which are themselves complicated linear combinations of the basic meteorological quantities, corrections have been applied using simply P, H_{100} and T_{80}. Table 5.10 gives the results for 1972. Two methods were employed:

(i) using the 60-month averaged coefficients

(ii) using the actual coefficients calculated from the particular month's data.

These results indicate that the averaged coefficients are at times quite inappropriate for correcting the data. This reflects the fact that the bias in each $\hat{\beta}_j$ is an unstable quantity (see Table 4.3). In comparison, the individual monthly coefficients give consistently better values of R^2.

TABLE 5.10

Percentage of variation R^2 removed from the Poatina intensity, for 1972.

Month	Jan	Feb	Mar	Apr	May	Jun	Jul	Aug	Sep	Oct	Nov	Dec	Mean
R^2 (using averaged coeffs.)	1.5	37.5	0.8	-3.0	17.8	44.6	43.8	50.8	39.8	54.3	34.7	15.7	28.2
R^2 (using individual month's coeffs.)	15.0	58.5	17.3	30.7	19.6	60.5	51.6	66.3	47.5	62.0	43.3	34.8	42.3

In order to gauge the success of the partial coefficients in removing atmospheric effects, the corrected muon data may be compared with pressure-corrected neutron data from a nearby neutron monitor. Thus it is assumed that any residual variations in the two components are due only to variations in the primary intensity. The neutron correction is based on the fact that temperature effects on the nucleon component are negligible.

The objection to this procedure is that the nucleon and meson components do not cover the same part of the primary spectrum. For example, neutron data show a greater sensitivity to Forbush events than do muons. However, the results of Ehmert (1958) and Lindgren and Lindholm (1961) have shown that most of the non-atmospheric variation in the muon intensity may be inferred using pressure-corrected neutron data.

Figure 5.4 shows the daily mean intensity at Poatina after correction using the individual monthly coefficients, for the period January to June 1972. Plotted alongside are pressure-corrected neutron data from the Mt. Wellington IQSY neutron monitor. The detector is situated near Hobart at 725 metres above sea level (950 g cm^{-2} atmospheric depth).

The correspondence between the two plots is not strong. Apart from the effects already discussed, the Poatina plots show a large Poisson scatter and reflect the low R^2 values given in Table 5.9. In a similarly-motivated comparison, Yasue et al. (1981) have plotted the muon intensity at Matsushiro (220 hg cm^{-2} underground) where the data have

been corrected for pressure *only*. Figure 5.5 shows their results, together with the pressure-corrected Tokyo neutron intensity. The correlation between the two plots appears better than for Poatina, partly because of their high counting rate ($\sim$ 21,000 h^{-1}) which yields a daily Poisson error of $\sim$ 0.14%. Yasue et al. found that their muon pressure coefficient removed $\sim$ 40% of the variation in the muon intensity, a figure which is much the same as that achieved in the Poatina (P,H,T,I) model.

Since temperature is believed to be the *real* cause of the atmospheric effects, it is reasonable to assume that if a temperature coefficient, based on accurate and frequent temperature measurements, were introduced into the correction procedure, most of the atmospheric effects could be removed from the high energy muon intensity.

Detection of Sidereal Anisotropies

As mentioned in Section 1.1, muon variations in sidereal time should become discernable at the high primary rigidities seen by detectors deep underground. Harmonic analyses have been performed on data from Poatina (Fenton and Fenton, 1976), Holborn (Elliot, 1979) and Utah (Cutler, 1980). The cut-off rigidities of the three stations are $\sim$ 1200, 500 and 1500 GV, respectively. After correction for motion relative to the local interstellar medium, first harmonic amplitudes in the range 0.02 to 0.05% have been detected. No significant second harmonics were found at Poatina or Holborn but a figure of $\sim$ 0.02% was seen at Utah.

Comparison of these figures with the temperature coefficients at Poatina and Utah (0.2 - 0.3% K^{-1}) suggests a serious problem in separating out these effects. However, after applying a barometer correction of - 0.057% mb^{-1}, Fenton and Fenton found no significant change in the amplitude of the observed first sidereal harmonic at Poatina. Against this it must be remembered that the barometer coefficient alone accounts for very little of the muon intensity variations. Thus it is not possible to say, from this result alone, that sidereal variations are not obscured by atmospheric influences.

Fenton and Fenton have also examined the solar daily variation in the Poatina intensity. Data uncorrected for pressure showed little variation but, after correction, the first harmonic disappeared while the second harmonic was enhanced, to ~ 0.04%. This suggests the influence of the pressure-upper air temperature link.

From these results, it appears that the true size of the sidereal variation will only be known once an effective atmospheric correction has been applied. This re-emphasizes the need for a noise-free temperature variable.

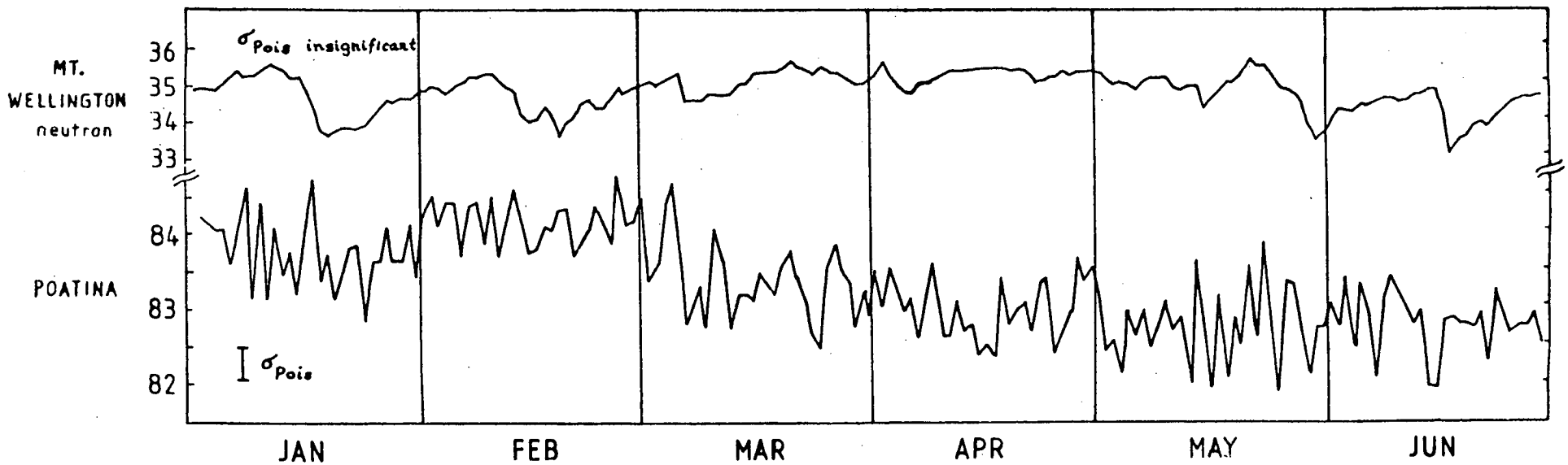

Figure 5.4. Top: pressure-corrected neutron data from Mt. Wellington for January to June, 1972.
Bottom: corrected muon data from Poatina for the same period. For correction method, see text.
Scale factors: neutron, ×6400
muon , × 20

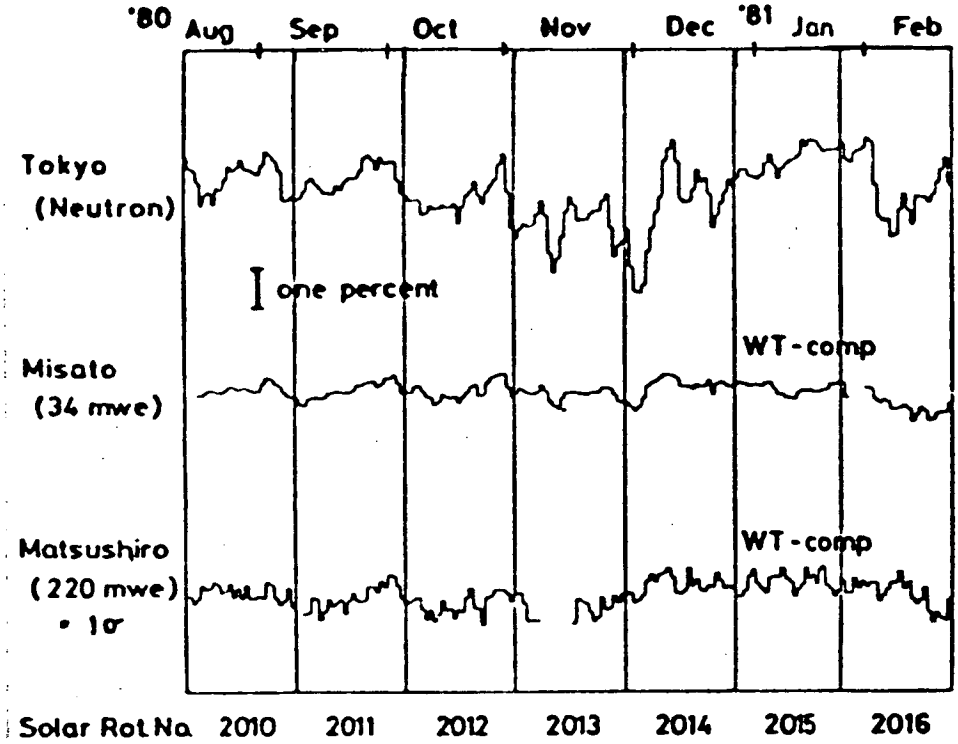

Figure 5.5. Pressure-corrected neutron and muon data from Yasue et al. (1981).

5.10 A Future Possibility - The Method of Instrumental Variables

It has been shown that errors in the atmospheric variables can cause serious bias in the OLS coefficients. An alternative method of estimation, which may yield unbiased coefficients under these conditions, is the method of "instrumental variables". This has been described by Kmenta (1971), Johnston (1972) and others. To understand the technique, consider the straight line case where x is measured with error (Section 5.4.2):

The *true* regression is

$$Y_i = x_i \beta_1 + \varepsilon_i$$

but because we measure $x_{\delta i} = x_i + \delta_i$, this is equivalent to

$$Y_i = (x_{\delta i} - \delta_i)\beta_1 + \varepsilon_i$$

i.e.

$$Y_i = x_{\delta i}\beta_1 + \omega_i \qquad (5.40)$$

where $\omega_i = \varepsilon_i - \delta_i \beta_1$. The covariance of $\underline{x}_\delta$ and $\underline{\omega}$ is

$$\begin{aligned} S_{x_\delta \omega} &= E\{(x_i + \delta_i)(\varepsilon_i - \delta_i \beta_1)\} \\ &= E\{x_i \varepsilon_i - \beta_1 \delta_i x_i + \delta_i \varepsilon_i - \beta_1 \delta_i^2\} \\ &= -\beta_1 E(\delta_i^2) \\ &= -\beta_1 \sigma_\delta^2 \end{aligned}$$

In other words, the error term ω_i in our *effective* regression (5.40) is correlated with $x_{\delta i}$, one of the measured

variables. This violates one of the basic OLS assumptions. The technique of instrumental variables involves the search for a new variable, v say, which is both highly correlated with x but also uncorrelated with w. Then instead of calculating

$$\hat{\beta}_{1\delta} = \frac{\Sigma x_i' Y_i}{\Sigma x_i^2 + \Sigma \delta_i^2}$$

we calculate

$$\begin{aligned}\tilde{\beta}_1 &= \frac{\Sigma v_i Y_i}{\Sigma x_{\delta i} v_i} \\ &= \frac{\Sigma(v_i \beta_1 x_{\delta i} + v_i w_i)}{\Sigma x_{\delta i} v_i} \\ &= \frac{\beta_1 \Sigma v_i x_{\delta i} + \Sigma v_i w_i}{\Sigma x_{\delta i} v_i} \qquad (5.41)\end{aligned}$$

If v_i and w_i are uncorrelated, $\Sigma v_i w_i \to 0$ for large samples. Then $\tilde{\beta}_1 \to \beta_1$, the true slope.

The multidimensional analogue of (5.40) is

$$\underline{Y} = X_\Delta \underline{\beta} + \underline{W} \qquad (5.42)$$

where $\underline{\beta}$ is estimated by

$$\tilde{\underline{\beta}} = (V^T X_\Delta)^{-1} V^T \underline{Y} \qquad (5.43)$$

which has the dispersion matrix

$$D(\tilde{\underline{\beta}}) = s^2 (V^T X_\Delta)^{-1} (V^T V) (X_\Delta^T V)^{-1} \qquad (5.44)$$

where s^2 estimates σ^2.

A requirement for a good "instrument* matrix" V is that is be uncorrelated with the error term

$$\left(\underset{n\to\infty}{\text{plim}} \quad \frac{V^T W}{n} = 0\right)$$

but correlated with the variable that replaces it

$$\left(\underset{n\to\infty}{\text{plim}} \quad \frac{V^T X_\Delta}{n} \neq 0\right)$$

From the dispersion matrix above, it is seen that the "larger" $V^T X_\Delta$, the smaller the variances of the $\tilde{\beta}_j$. Thus the efficiency of the instrumental variables estimator increases with the correlation between V and X_Δ. If some of the columns of X_Δ are uncorrelated with W, then these can be used as instruments for themselves. If all the columns are uncorrelated with W, the instrumental variables estimator becomes OLS.

The problem in calculating the partial pressure and temperature coefficients is then to find good "instruments" to use for these variables. There is no real problem with pressure as measurements can be made very accurately and whenever desired. However, it should be possible to derive a better variable for temperature by suppressing frequency components in the variation which are outside the main region of interest. Cutler (1980) has performed a discrete Fourier transform on the variable T_{eff}, and found that the spectrum is fairly flat for frequencies $\gtrsim 0.5\ \text{day}^{-1}$. Therefore, much of the noise probably occurs with a period

*the word "instrument" has nothing to do with the equipment used to measure the muon intensity, or radiosonde hardware.

of 2 days or less. Although he sampled once per 12 hours instead of using a running mean of three readings per 24 hours, it is clear that the "fast" variations are responsible for much of the measurement error. The remaining jitter could only be removed by improving the accuracy of the radiosonde's thermistor.

In summary, the combined use of spectral analysis to filter out noise in the atmospheric regressor(s) and the implementation of the method of instrumental variables may yield coefficients which are unbiased and also achieve high values of R^2. This approach should be well worth pursuing.

APPENDIX 1

THE MONTE CARLO METHOD AND ITS APPLICATION TO SIMULATING THE TEMPERATURE EFFECT AT .357 hg cm^{-2}

Introduction

The name "Monte Carlo" as applied to mathematical methods generally means the use of random sampling in the treatment of deterministic or probabilistic problems, the outcomes of which are decided by random numbers. These are chosen so that they directly simulate the random physical processes of the real situation.

The first example of the use of Monte Carlo methods was in Buffon's famous "Needle Problem" in 1777. In the experiment, random tossings of a needle onto a parallel-ruled plane gave an unexpected method for finding π. In 1950, Volser obtained the value 3.1596 for π after an experiment involving 1000 trials.

Monte Carlo modelling requires a succession of truly random numbers, R, equidistributed in some interval (a,b), such that

$$p(R)dR = \frac{dR}{b-a} \qquad \text{(A1.1)}$$

Usually, (a,b) is the unit interval (0,1) so that $p(R) = 1$.

Modern computers generally contain a pseudo-random number generator in their library of intrinsic functions.

The numbers produced have a finite periodicity, which is however long compared with the number of values of R required in a calculation. Algorithms for generating random numbers have been described by Hammersley and Hanscomb (1964). The following summary of selection methods has been drawn partly from Quang (1970, 1974).

Basic Selection Techniques

A basic technique in the Monte Carlo method is the selection of the occurrence of an event or finite quantity from a given probability distribution.

(i) Selection from a discrete distribution. Consider a discrete distribution - i.e. one in which there is a number of mutually exclusive, exhaustive events, labelled, $1,2,\ldots,n$ of which the i^{th} has a probability of occurrence P_i. Let there be associated with a random number $R \in (0,1)$ the event I such that

$$\sum_{i=1}^{I-1} P_i < R \leq \sum_{i=1}^{I} P_i \quad . \tag{A1.2}$$

Then each event I has probability P_I. For example, if P_π and $Q_\pi = 1 - P_\pi$ are the probabilities that a muon escapes interaction before decay and interacts before decay respectively, then for R such that $R < P_\pi$, the event is termed a survival.

(ii) Selection from an arbitrary function. Let f(x) be some arbitrary distribution where

$$\int_{-\infty}^{\infty} f(x)dx = 1 .$$

Corresponding to a random number R_j, we may select a random variable X_j from f(x) by solving

$$\int_{-\infty}^{X_j} f(x)dx = \int_{0}^{R_j} dy = R_j \qquad \text{(A1.3)}$$

In some cases, the use of Equation A1.3 will necessitate a very large number of histories being simulated before the jitter in the final answer is reduced to an acceptable level. This is particularly critical if the difference between two successive answers (in separate runs of the simulation) is required. The error is caused by statistical fluctuations in the distribution of sampled values of X. A histogram plot of frequency vs. sampled X's will undoubtedly contain some intervals of x with more, or less, values than predicted by the distribution f(x). However, if the number N of X's to be selected is known in advance, it is possible to reduce the variation by using the so-called systematic sampling biasing technique. This is done by solving

$$\int_{-\infty}^{X_j} f(x)dx = \frac{j - R_j}{N} \qquad \text{(A1.4)}$$

where $j = 1,2,\ldots,N$.

This biasing technique ensures that successive values of X_j will lie within successive $\frac{1}{N}$ - intervals of the cumulative distribution for x. However, the position of X_j

within each interval is selected at random. Since the number of sampled X_j's within a given interval of x will then correspond more closely to the number predicted by the distribution function, statistical fluctuations from one run to another will be reduced. Thus the variance in the output data will also be decreased.

The Main Steps in the Monte Carlo Simulation

(i) Selection of the primary proton energy

Except at very low energies, the differential primary intensity follows the power law spectrum

$$I(E)dE = K E^{-2.7} dE \qquad (A1.5)$$

(from Wolfendale, 1963). To select a value of E from the spectrum, the condition (A1.3) must hold. Thus

$$\int_{-\infty}^{\infty} K E^{-2.7} dE = 1 \qquad (A1.6)$$

Clearly, non-positive values of E are impermissible. In addition, the selection of primaries of too low an energy to produce muons detectable at Poatina will waste computer time on "dead-end" histories. To calculate the lower limit in the integral (A1.6) and therefore to find the value of the constant K, the mean multiplicity of charged and neutral pions has been calculated using the expression of Hook and Turver (1974):

$$m_\pi = 3.85(K E_p)^{0.25} \qquad (A1.7)$$

where E_p is the proton energy in GeV. The constant K is the proton collision inelasticity, which they take to be rectangularly distributed in the interval [0.25,0.75]. For the Monte Carlo simulation, the mean value of 0.5 has been used, so that

$$m_\pi = 3.24\, E_p^{0.25} \qquad \text{(A1.8)}$$

To a first approximation, it has been assumed that positive, negative and neutral pions are produced in equal numbers, so that

$$m_{\pi^\pm} = 2.16\, E_p^{0.25} \qquad \text{(A1.9)}$$

If we assume that the energy is shared equally among the secondaries, each charged pion will have a production energy of

$$E_\pi = \frac{2}{3}\,\frac{K\, E_p}{m_{\pi^\pm}}$$

$$= \frac{E_p^{0.75}}{6.48}\,, \quad \text{using (A1.9)} \quad . \qquad \text{(A1.10)}$$

Therefore

$$E_p = (6.48\, E_\pi)^{4/3} \qquad \text{(A1.11)}$$

Each pion of energy E_π gives rise to a muon of energy $E_\mu = 0.787\, E_\pi$, on the average (see Appendix 2). Since the muon threshold energy at Poatina is $\sim$ 100 GeV, we require a minimum pion energy at production of $\sim$ 127 GeV. (Ionization energy losses have been ignored.) Inserting this value in

(A1.11) yields a minumum allowed proton energy of ~ 7000 GeV. (This value is much greater than the accepted median energy of 1200 GeV quoted in Section 4.1. The overestimation is probably partly due to the approximation used for the proton inelasticity distribution and the fact that the constant α in $E_\mu = \alpha E_\pi$ actually varies over the interval [0.574,1.000]). We then require K such that

$$\int_{7000}^{\infty} K E^{-2.7}\, dE = 1 \qquad \text{(A1.12)}$$

The solution to this is $K = 5.85 \times 10^6$. Using systematic sampling, we then solve

$$\int_{7000}^{E_j} 5.85 \times 10^6\ E^{-2.7}\ dE = \frac{j - R_j}{N}$$

to obtain

$$E_j = [3.44 \times 10^6 N/(N - j + R_j)]^{1/1.7} \qquad \text{(A1.13)}$$

(ii) Selection of zenith angle

The angular distribution is assumed isotropic so that $f(\theta)$ = const. for $0° \leq \theta < 90°$. Since we must have

$$\int_{-\infty}^{\infty} f(\theta)d\theta = 1\ ,$$

the analytic form for $f(\theta)$ is

$$f(\theta)d\theta = d\theta/\theta_{co} , \quad 0 < \theta \leq \theta_{co}$$
$$= 0 , \quad \theta > \theta_{co} \qquad \text{(A1.14)}$$

where θ_{co} is the aperture cut-off angle for the muon telescope. For a semicubical telescope, $\theta_{co} = 70°32'$ (see Figure 3.2). Using systematic sampling we solve

$$\int_0^{\theta_j} \frac{d\theta}{\theta_{co}} = \frac{j - R_j}{N}$$

to obtain

$$\theta_j = \left(\frac{j - R_j}{N}\right) \theta_{co} \qquad \text{(A1.15)}$$

(iii) Selection of atmospheric depth of proton collision

The mass of air traversed by a proton follows the distribution

$$f(\ell_p)d\ell_p = \frac{1}{\lambda_p} \exp\left(-\frac{\ell_p}{\lambda_p}\right) d\ell_p$$

where λ_p, the interaction length, has been assumed 80 g cm^{-2} (Hook & Turver, 1974). Again using systematic sampling, the chosen value of ℓ_p will be

$$\ell_p = \frac{1}{\lambda_p} \ln[N/(N - j + R_j)] \qquad \text{(A1.16)}$$

so that the atmospheric depth of the collision is

$$h_1 = \ell_p \cos\theta \qquad \text{(A1.17)}$$

(iv) Selection of the pion decay length

Since the pion multiplicity is not known in advance, it is not possible to use systematic sampling. The lifetime of a pion follows the distribution

$$f(t_\pi)dt_\pi = \frac{1}{\tau_\pi} \exp\left(-\frac{t_\pi}{\tau_\pi}\right) dt_\pi \qquad \text{(A1.18)}$$

where $\tau_\pi = 2.55 \times 10^{-8}$s. The solution to the integral

$$\int_0^{t_\pi} \frac{1}{\tau_\pi} \exp\left(-\frac{t_\pi}{\tau_\pi}\right) dt_\pi = R$$

is $t_\pi = -\tau_\pi \ln(1-R)$ but since R is equidistributed in the interval (0,1) it is simpler to just use $t_\pi = -\tau_\pi \ln R$. The decay length of the pion is then

$$z_\pi = -\tau_\pi c \gamma_\pi \ln R \qquad \text{(A1.19)}$$

where $\gamma_\pi = 1 + E_\pi/m_\pi c^2$ and c is the speed of light.

(v) Probability of pion capture

The air mass traversed by the pion over its flight is

$$\ell_\pi = \int_{z(h_1)}^{z(h_2)} \rho(z)dz / \cos\theta \qquad \text{(A1.20)}$$

where

$$h_2 = h_1 + \ell_\pi \cos\theta$$

and where $\rho(z)$ is the density obtained from the ICAO Standard Atmosphere. Since this is only given to the 12 mb level, the

data were augmented by an extension to the 1 mb level, obtained from the Cospar International Reference Atmosphere (1965). The probability that the pion escapes collision is then

$$P_\pi = \exp(-\ell_\pi/\lambda_\pi) \qquad \text{(A1.21)}$$

where $\lambda_\pi \simeq 100\ \mathrm{g\,cm^{-2}}$ (Hook and Turver, 1974). As mentioned earlier, for selected R such that $R < P_\pi$, the pion is counted as having escaped interaction.

(vi) Probability of muon survival

For a muon to be detected at Poatina, the pion production energy must be $\gtrsim$ 127 GeV and so its energy loss over ℓ_π is insignificant. Each pion of energy E_π given by (A1.10) results in a muon of energy $E_\mu = 0.787\ E_\pi$. If $E_\mu < \Delta E/\cos\theta$, the detector threshold energy, the history is terminated. The energy loss of the muon between $z(h_2)$ and the ground is negligible as it amounts to $\lesssim$ 2% of the Poatina threshold energy.

In exact analogy with the pion, the distribution of muon lifetimes is

$$f(t_\mu)dt_\mu = \frac{1}{\tau_\mu} \exp\left(\frac{-t_\mu}{\tau_\mu}\right) dt_\mu \qquad \text{(A1.22)}$$

where $\tau_\mu = 2.2 \times 10^{-6}$ s. The decay length of the muon is

$$z_\mu = -\tau_\mu c \gamma_\mu \ln R \qquad \text{(A1.23)}$$

where $\gamma_\mu = 1 + E_\mu/m_\mu c^2$ and $t_\mu = -\tau_\mu \ln(1-R)$ is the

sampled value of t_μ; again we substitute lnR for ln(1-R).

The probability that the muon will not decay before reaching the ground is then

$$P_\mu = \exp\left(-z\,(h_2)/z_\mu\right) \qquad \text{(A1.24)}$$

To allow for the geometrical sensitivity function of the telescope, let

$$\omega_G = GS(\theta)$$

where $GS_{max}(\theta) = GS(30°)$ has been normalized to unity (see Figure 3.2). Then for sampled R such that $R < P_\mu\,\omega_G$, the muon is counted as having reached the detector. [Note that the geometric depth of the detector has been ignored also. For Poatina, this is ~ 140 m which is about 1% of the average muon production height.]

Calculation of Detector Threshold Energies

George (1952) gives the following expression for the rate of energy loss in rock where z = 10 and A = 20:

$$\frac{dE}{dx} = d + bE \quad \text{where} \quad b = 5.1 \times 10^{-6}\ \text{cm}^2\,\text{g}^{-1}$$
$$d = 2.66\ \text{MeV cm}^2\,\text{g}^{-1} \qquad \text{(A1.25)}$$

(In (A1.25), x denotes range, not the cosine of the zenith angle θ). Integrating the reciprocal of (A1.25) yields

$$x = \int_0^E \frac{dE}{d + bE}$$

$$= \frac{1}{b} \ln \left(1 + \frac{bE}{d}\right) \qquad \text{(A1.26)}$$

This expression may then be inverted to give E in terms of x. We find

$$E = \frac{d}{b} [\exp(bx) - 1]$$

i.e.

$$E[\text{GeV}] = 5.22 \times 10^2 [\exp(5.1 \times 10^{-4} x[\text{hg cm}^{-2}] - 1] \qquad \text{(A1.27)}$$

The Cambridge detector is located at a depth of 47 hg cm^{-2} below the top of the atmosphere, or 37 hg cm^{-2} below the surface. Equation (A1.27) then yields for the muon threshold energy

$$\Delta E_{\text{Camb.}} \simeq 9.94 \text{ GeV}$$

For Poatina, x = 357 hg cm^{-2} below the top of the atmosphere, or 347 hg cm^{-2} below the surface. We then find

$$\Delta E_{\text{Poa.}} \simeq 101.1 \text{ GeV}$$

APPENDIX 2

PION-MUON DYNAMICS AND ENERGY TRANSFER

Consider a relativistic charged pion, which decays according to the process

$$\pi^{\pm} \rightarrow \mu^{\pm} + \nu$$

We desire an expression for the kinetic energy of the muon in terms of that of the pion, in the laboratory system.

For the pion: let E_π = total energy in lab system

T_π = kinetic energy in lab system

p_π = momentum in lab system

m_π = rest mass of pion

For the muon: let E_μ^* = total energy in centre-of-mass (CM) system

E_μ = total energy in lab system

T_μ^* = kinetic energy in CM system

T_μ = kinetic energy in lab system

p_μ^* = momentum in CM system

p_μ = momentum in lab system

m_μ = rest mass of muon

For the neutrino: let

E_ν^* = total energy in CM system

p_ν^* = momentum in CM system

Now

$$m_\pi c^2 = 139.88 \text{ MeV} \qquad \text{(A2.1)}$$

$$m_\mu c^2 = 105.89 \text{ MeV} \qquad \text{(A2.2)}$$

From conservation of energy and momentum it follows that the muon and neutrino momenta must cancel vectorially, while their total energies must add up to the rest energy of the original pion. Then

$$p_\mu^* = p_\nu^* \tag{A2.3}$$

$$E_\mu^* + E_\nu^* = 139.88 \text{ MeV} \tag{A2.4}$$

From (A1.4) it follows that

$$T_\mu^* + m_\mu c^2 + T_\nu^* + m_\nu c^2 = 139.88$$

$$\therefore T_\mu^* + T_\nu^* = 33.99 \text{ MeV} \tag{A2.5}$$

since $m_\mu c^2 = 105.89$ and $m_\nu c^2 = 0$. Now

$$E_\nu^{*2} = c^2 p_\nu^{*2} \quad \text{since} \quad m_\nu c^2 = 0 \tag{A2.6}$$

Thus

$$\frac{E_\nu^{*2}}{c^2} = p_\nu^{*2} \tag{A2.7}$$

from (A2.3). We also have

$$E_\mu^{*2} = c^2 \left(p_\mu^{*2} + m_\mu^{\ 2} c^2 \right)$$

$$\therefore \quad p_\mu^{*2} = \frac{E_\mu^{*2}}{c^2} - m_\mu^{\ 2} c^2 \tag{A2.8}$$

Equating (A2.7) and (A2.8),

$$E_\nu^{*2} = E_\mu^{*2} - (m_\mu c^2)^2 \tag{A2.9}$$

(A2.4) implies

$$E_\nu{}^{*2} = (m_\pi c^2)^2 - 2E_\mu{}^* m_\pi c^2 + E_\mu{}^{*2} \qquad \text{(A2.10)}$$

Equating (A2.9) and (A2.10),

$$E_\mu{}^* = \frac{(m_\pi c^2)^2 + (m_\mu c^2)^2}{2m_\pi c^2}$$

Thus

$$T_\mu{}^* = E_\mu{}^* - m_\mu c^2$$

$$= \frac{(m_\pi c^2 - m_\mu c^2)^2}{2m_\pi c^2}$$

i.e. $$T_\mu{}^* = 4.13 \text{ MeV} \qquad \text{(A2.11)}$$

Now the CM frame is moving at speed βc relative to the laboratory frame along the direction shown in Figure A2.1. The Lorentz energy transformation for E_μ in terms of $E_\mu{}^*$ yields

$$E_\mu = \frac{E_\mu{}^* + \beta c\, p_\mu{}^* \cos\theta^*}{(1-\beta^2)^{\frac{1}{2}}}$$

where θ^* = angle of emission of the muon in CM system relative to pion trajectory.

Then

$$E_\mu{}^* = \frac{E_\pi}{m_\pi c^2} E_\mu{}^* + \frac{p_\pi}{m_\pi} p_\mu{}^* \cos\theta^*$$

whence

$$(E_\mu)_{\substack{\max \\ \min}} = \frac{E_\pi}{m_\pi c^2} E_\mu{}^* \pm \frac{p_\pi}{m_\pi} p_\mu{}^* \qquad \text{(A2.12)}$$

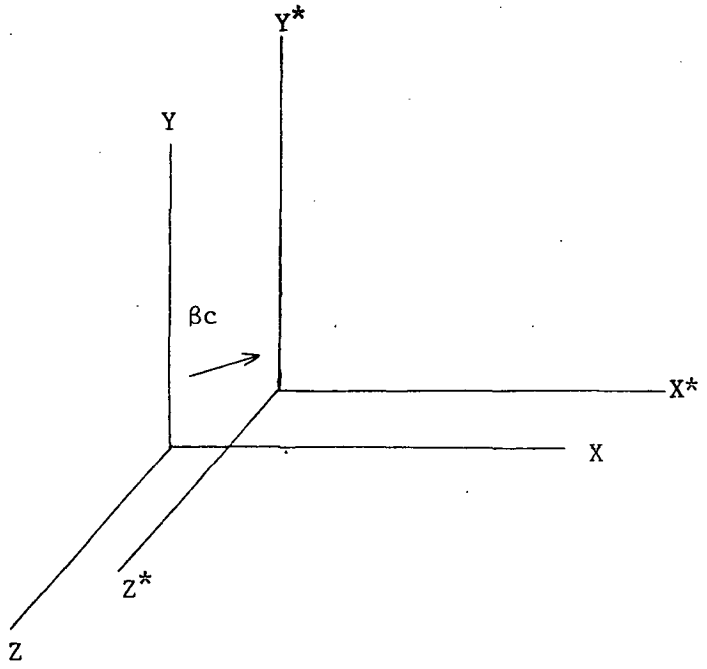

Figure A2.1. Laboratory and centre-of-mass frames.

In the CM frame, the probability of emission of the muon is the same in all directions. Thus

$$\langle \cos\theta^* \rangle = 0$$

and

$$\langle E_\mu \rangle = \frac{E_\pi E_\mu^*}{m_\pi c^2} \qquad \text{(A2.13)}$$

We then have an expression for $\frac{\langle T_\mu \rangle}{T_\pi}$:

$$\frac{\langle T_\mu \rangle}{T_\pi} = \frac{\langle E_\mu - m_\mu c^2 \rangle}{E_\pi - m_\pi c^2}$$

$$\simeq \frac{\langle E_\mu \rangle}{E_\pi} \quad \text{provided} \quad E_{\mu,\pi} >> m_{\mu,\pi} c^2$$

$$= \frac{E_\mu^*}{m_\pi c^2} \quad \text{from (A2.13)}$$

$$= \frac{T_\mu^* + m_\mu c^2}{m_\pi c^2}$$

i.e. $\langle T_\mu \rangle \simeq 0.787\, T_\pi$ (A2.14)

It is easily shown that the second term on the R.H.S. of (A2.12) is

$$\frac{p_\pi}{m_\pi} p_\mu^* = \frac{p_\mu^*}{m_\pi c} T_\pi \quad \text{provided} \quad E_\pi >> m_\pi c^2$$

$$= \frac{T_\mu^* (E_\mu^* + m_\mu c^2)^{\frac{1}{2}}}{m_\pi c^2} \cdot T_\pi$$

$$= 0.213\, T_\pi \qquad \text{(A2.15)}$$

Thus

$$(T_\mu)_{\substack{\max \\ \min}} = (0.787 \pm 0.213) T_\pi \qquad \text{(A2.16)}$$

Since $T_{\mu,\pi} >> m_{\mu,\pi} c^2$ for muons observed underground ($\gtrsim 40$ hg cm^{-2}), we may use T and E interchangeably with negligible error.

APPENDIX 3

METHODS FOR DETECTING COLLINEARITY IN THE REGRESSOR MATRIX

To decide whether bias or variance inflation is likely to be serious in a set of regression coefficients, a number of techniques have commonly been used in an attempt to detect collinearity amongst the explanatory variables. The following is a summary of these methods, drawn chiefly from Belsley, Kuh and Welsch (1980).

(i) Examine the correlation matrix X^TX, or its inverse $(X^TX)^{-1}$

If the columns of X have been centered to have zero mean and unit length (Section 5.6.2) the matrix of correlation coefficients is simply X^TX.

In the simple (P,T,I) model, collinearity is indicated by "large" values of r_{PT}, the simple pressure-temperature correlation coefficient. However, the addition of a third regressor such as H to the model means there are now three simple and three partial correlations amongst the columns of X. While high correlations between columns in X may point to damaging collinearity, it is possible for all variables to be collinear and yet no single r_{ij} to be very large.

The inverse matrix $(X^TX)^{-1}$ is more useful. From (4.11) we have

$$\begin{aligned} \text{var}(\hat{\beta}_j) &= \sigma^2 (X^TX)^{-1} \\ &= \sigma^2/(1 - R_j^2) \end{aligned} \qquad \text{(A3.1)}$$

The variance inflation factors $1/(1 - R_j^2)$ have been shown in Section 5.5.1 to be small for atmospheric data at Poatina. However, a better insight into the "distribution" of the dependencies in the X matrix may be achieved by the following methods:

(ii) Examine the eigensystem of X^TX

It is well known that the more ill-conditioned a matrix becomes, the smaller are some of its eigenvalues. Using this property, Kendall (1957) and Silvey (1969) suggest examination of the eigenvalues of X^TX as a key to the presence of collinearity. Hoerl and Kennard (1976) show that the expectation of the length of $\hat{\underline{\beta}}$ is given by

$$E\left(\hat{\underline{\beta}}^T\hat{\underline{\beta}}\right) = \underline{\beta}^T\underline{\beta} + \sigma^2 tr(X^TX)^{-1}$$

$$\underline{\beta}^T\underline{\beta} + \sigma^2 \sum_j \lambda_j^{-1}$$

where the λ_j are the eigenvalues of X^TX. Therefore the more orthogonal X is, the shorter $\hat{\underline{\beta}}$ will be. In other words, wild bias in $\hat{\underline{\beta}}$ will be unlikely. However, it is not so much the presence of "small" - that is, near-zero, eigenvalues which implies serious collinearity, as the ratio between the smallest and the largest eigenvalues. If this ratio is large, a problem exists. The presence of large eigenvectors of X^TX also points to collinearity. To see this, we note that if the atmospheric variables are uncorrelated with each other, $X^RX = I_p$, the identity matrix, which by definition has p eigenvalues, each equal to one, and scalar eigenvectors, each equal to one. The less orthogonal X becomes, the more

non-uniform the "spectrum" of eigenvalues and the larger the eigenvectors of X^TX.

The logical refinement of this method of analysis is now explained.

(iii) The singular value decomposition of X

The key to a sophisticated collinearity diagnostic is the singular value decomposition (SVD) of the X matrix. A more complex description is given by Golub and Reinsch (1970), Hanson and Lawson (1969), Belsley, Kuh and Welsch (1980), and others.

Any n×p matrix X, considered here as a matrix of n observations on each of p atmospheric variables, may be decomposed as

$$\underset{(n\times p)}{X} = \underset{(n\times p)}{U}\ \underset{(p\times p)}{D}\ \underset{(p\times p)}{V^T} \qquad \text{(A3.2)}$$

where $U^TU = V^TV = I_p$ and $D = \text{diag}(\mu_1, \mu_2, \ldots, \mu_p)$. The μ_i are non-negative and are known as the *singular values* of X. Other dimensional formulations of (A3.2) are possible; see Belsley, Kuh and Welsch (1980). The squares of the singular values are the eigenvalues of X^TX. Furthermore, it may be shown that the columns of V are the p eigenvectors of X^TX, while the columns of U are the p eigenvectors of XX^T associated with its p non-zero eigenvalues.

The values of the μ depend on the scaling of the X matrix. Although it does not matter physically whether H is measured in metres or kilometres, for example, such a change in column scaling will result in a different set of singular values. Since two such data sets are physically equivalent, it is customary to remove the ambiguity in the μ_j by scaling all the columns in X to have unit length. Belsley, Kuh and Welsch examine this question and conclude that such scaling is close

to the optimal, especially when p is small (as in our case). We recall that the columns in X have already been centred to have zero mean as the constant β_0 is of no interest in the cosmic ray context.

The singular value decomposition of X is to be preferred to the eigensystem of X^TX as X is, after all, the focus of our concern. One might think it adequate merely to compute the eigenvalues of X^TX (after the appropriate scaling) and then take their square roots. However, Golub and Reinsch (1970) show that this indirect process may involve needless inaccuracy.

Given the set of singular values, ordered such that $\mu_1 \geq \mu_2 \geq \ldots \geq \mu_p$, we define the k^{th} condition index by

$$\left.\begin{aligned} \eta_k &\equiv \frac{\mu_{max}}{\mu_k} = \frac{\mu_1}{\mu_k}, \quad k = 1,\ldots,p \\ \text{and the condition number of X as} \\ K(X) &\equiv \frac{\mu_{max}}{\mu_{min}} = \frac{\mu_1}{\mu_p} \end{aligned}\right\} \qquad \text{(A3.3)}$$

Clearly, $1 \leq \eta_k \leq K(X)$.

We then say that there are as many *near-dependencies* among the columns of X as there are *high condition indices*. This criterion overcomes the problem that even well-conditioned matrices can have arbitrarily low singular values (see Belsley, Kuh and Welsch). The distribution of the η_k is then a good indicator of the extent of collinearity present.

The Regression Coefficient Variance Decomposition

To ascertain which estimates may be affected by collinearity, we note that using the SVD of X,

$$D(\hat{\underline{\beta}}) = \sigma^2(X^TX)^{-1}$$

$$= \sigma^2[(UDV^T)^T(UDV^T)]^{-1}$$

$$= \sigma^2 VD^{-2}V^T \qquad \text{(A3.4)}$$

and the variance of the j^{th} estimate is then

$$\text{var}(\hat{\beta}_j) = \sigma^2 \sum_{k=1}^{p} \frac{v_{jk}^2}{\mu^2_k} \quad \text{where} \quad V \equiv (v_{jk}) \ . \qquad \text{(A3.5)}$$

We see that (A3.5) decomposes $\text{var}(\hat{\beta}_j)$ into a sum of components, each associated with one singular value μ_k. The smaller a given μ_k, the larger will be the term in which it appears (other things being equal). Now define

$$\phi_{jk} \equiv \frac{v_{jk}^2}{\mu^2_k} \quad \text{and} \quad \phi_j \equiv \sum_{k=1}^{p} \frac{v_{jk}^2}{\mu^2_k}$$

$$= \sum_{k=1}^{p} \phi_{jk} \ . \qquad \text{(A3.6)}$$

Then

$$\pi_{jk} = \frac{\phi_{jk}}{\phi_j} \ , \qquad j,k = 1,\ldots,p \qquad \text{(A3.7)}$$

is known as the (j,k) *variance decomposition proportion* (VDP) of $\text{var}(\hat{\beta}_j)$. Using (A3.7), we may draw up a variance decomposition proportion table, of dimensions p×p. This is shown in Table A3.1 for the 3×3 case.

To see the value of the VDP table in diagnosing collinearity, consider the case of a perfectly orthogonal X matrix - viz., atmospheric variables uncorrelated with each other. Then

TABLE A3.1

Format of variance decomposition proportion table

PROPORTIONS OF:	ASSOCIATED SINGULAR VALUE μ_1	μ_2	μ_3
$var(\hat{\beta}_P)$	π_{P1}	π_{P2}	π_{P3}
$var(\hat{\beta}_H)$	π_{H1}	π_{H2}	π_{H3}
$var(\hat{\beta}_T)$	π_{T1}	π_{T2}	π_{T3}
CONDITION INDEX	η_1	η_2	η_3

$$X^TX = I_p \Rightarrow (X^TX)^{-1} = I_p$$

$$\therefore \quad v_{jk} = \begin{Bmatrix} 1 , & j = k \\ 0 , & j \neq k \end{Bmatrix} \quad j,k = 1,\ldots,p \ .$$

Furthermore, all the μ_k will be unity. Thus each variance is associated with one, *and only one*, singular value, μ_ℓ say. The variance is therefore composed of a single VDP, which by definition is equal to unity.

Now let X tend away from orthogonality. The off-diagonals v_{jk} in V increase in magnitude and some $var(\hat{\beta}_j)$ may be built up of components ϕ corresponding to *several* μ_k. The variance is then composed of several VDP's.

From these considerations, the following practical procedure has been evolved by Belsley, et al.:

Degrading (i.e. potentially harmful) collinearity is said to exist if:

(i) a singular value is judged to have a high condition index, and is associated with

(ii) high variance decomposition proportions of at least two regression coefficient variances.

Empirically, $\eta_k \gtrsim 30$ and $\pi_{jk} \gtrsim 0.5$ have been considered reasonable thresholds.

Implementation of the Singular Value Decomposition on Poatina, Cambridge and Hobart Atmospheric data.

To investigate the variance decompositions applying to atmospheric data used at different locations, figures for the following stations have been analysed using their singular value decomposition

(1) Poatina (P, H_{100}, T_{80}), 1972-76

(2) Cambridge 70° zenith angle $(P, H_{100}, \bar{T}_{80-100})$, 1964

(3) Hobart sea level $(P, H_{100}, \bar{T}_{100-200})$, 1972.

The averaged results are shown in Table A3.2. The observed and expected coefficients and the norms of the $\underline{\beta}$ ("true") vectors have been included for the benefit of the following discussion.

In all three sets of results it is seen that whilst μ_3 is associated with large ($\gtrsim 0.5$) variance decomposition proportions in at least two estimate variances, none of the η_k come anywhere near threshold of ~ 30 suggested previously. As Belsley, Kuh and Welsch (1980) observe, the choice of

TABLE A3.2

Mean variance decompositions proportions of X matrix for

(1) Poatina (P, H_{100}, T_{80}) 1972-76

(2) Cambridge 70° zenith angle ($P, H_{100}, \bar{T}_{80-100}$), 1964

(3) Hobart sea level ($P, H_{100}, \bar{T}_{100-200}$), 1972

POATINA

Proportion of	Associated singular value		
	$\mu_1 = 1.38$	$\mu_2 = 0.876$	$\mu_3 = 0.535$
$var(\hat{\beta}_P)$	0.091	0.513	0.396
$var(\hat{\beta}_H)$	0.114	0.158	0.729
$var(\hat{\beta}_T)$	0.102	0.282	0.615
η_k	1.00	1.57	2.57

CAMBRIDGE

Proportion of	Associated singular value		
	$\mu_1 = 1.32$	$\mu_2 = 0.943$	$\mu_3 = 0.577$
$var(\hat{\beta}_P)$	0.123	0.290	0.587
$var(\hat{\beta}_H)$	0.141	0.111	0.749
$var(\hat{\beta}_T)$	0.086	0.503	0.410
η_k	1.00	1.40	2.29

TABLE A3.2 (continued)

HOBART

Proportion of	Associated singular value		
	$\mu_1 = 1.43$	$\mu_2 = 0.823$	$\mu_3 = 0.494$
$var(\hat{\beta}_P)$	0.081	0.220	0.699
$var(\hat{\beta}_H)$	0.081	0.294	0.625
$var(\hat{\beta}_T)$	0.097	0.402	0.501
η_k	1.00	1.73	2.89

this level is somewhat akin to choosing a test size (α) in standard hypothesis testing, where only practical experience indicates a reasonable value for the conditions. However, as none of the η_k exceed 3 we may safely conclude that the collinearity present is weak and could not, by itself, be responsible for the anomalous coefficients at Poatina and Cambridge.

APPENDIX 4

THE METHOD OF HARMONIC ANALYSIS

The General Case

It is assumed that the variation in the observed quantity is periodic in time and may be represented by the function

$$\beta(\theta) = \sum_{k=1}^{m} \left(a_k \cos k\theta + b_k \sin k\theta\right) \qquad \text{(A4.1)}$$

The number of harmonics being fitted is m and we solve for the a_k and b_k such that the function provides the best fit to n experimental points corresponding to times given by

$$\theta = 0, \ \frac{2\pi}{n}, \ \frac{4\pi}{n}, \ \ldots, \ (n-2)\ \frac{2\pi}{n}, \ (n-1)\ \frac{2\pi}{n}.$$

The n experimental points might be monthly values of β over one year, or hourly values over one day. It is found that the coefficients in (A4.1) take the following values under conditions of best fit:

$$a_k = \frac{2}{n} \sum_{\ell=0}^{n-1} u_\ell \cos\left\{\frac{2k\ell\pi}{n}\right\}$$

$$b_k = \frac{2}{n} \sum_{\ell=0}^{n-1} u_\ell \sin\left\{\frac{2k\ell\pi}{n}\right\} \qquad \text{(A4.2)}$$

where the u_ℓ are successive values of β. The amplitude of the k^{th} harmonic component is

where the u_ℓ are successive values of β. The amplitude of the k^{th} harmonic component is

$$R_k = \left(a_k^2 + b_k^2\right)^{\frac{1}{2}} \qquad \text{(A4.3)}$$

and the phase angle of maximum is

$$f_k = \arctan\left(\frac{b_k}{a_k}\right) \qquad \text{(A4.4)}$$

These two quantities may be visualized on an harmonic dial as shown below.

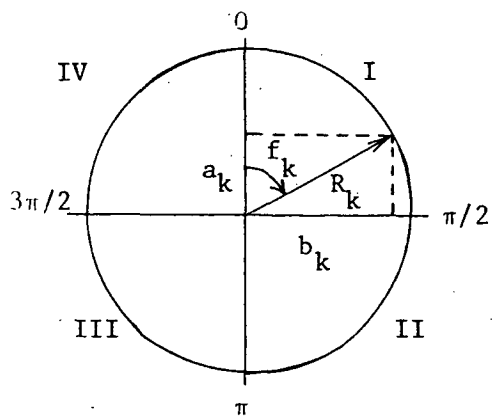

The phase angle f_k is measured clockwise from 0° ("12 o'clock") position. In this scheme, the a_k are measured on the ordinate, not the abscissa. To see this, we note that the first harmonic (k=1) is expressed as a cosine wave of the form

$$\beta_1(\theta) = R_1\cos(\theta - f_1)$$
$$= a_1\cos\theta + b_1\sin\theta \quad \text{where} \quad a_1 = R_1\cos f_1$$
$$b_1 = R_1\sin f_1$$

Thus,

$$f_1 = \arctan\left(\frac{b_1}{a_1}\right) \quad . \qquad \text{(A4.5)}$$

Amplitude and Phase Corrections for Time-Averaged Data

As shown by Humble (1971), Parsons (1959) and others, corrections must be applied if the u_ℓ are averaged figures accumulated over a finite interval of time. Such corrections will apply to cosmic ray data.

Let $\omega = \frac{k\pi}{n}$, where k = harmonic number.

It may be shown that the amplitude of the k^{th} component becomes

$$R_k = \frac{\omega}{\sin\omega} \left(a_k^2 + b_k^2\right)^{\frac{1}{2}} \qquad \text{(A4.6)}$$

For the 1st harmonic, $\frac{\omega}{\sin\omega} = 1.0115$

" " 2nd " , $\frac{\omega}{\sin\omega} = 1.0472$

To correct the phase, we must *add* the angle corresponding to half a recording interval to the phase angle f_k:

$$f_k = \arctan\left(\frac{b_k}{a_k}\right) + \frac{\pi k}{n} \qquad \text{(A4.7)}$$

Consider, for example, 12 values over one year. The corrections are:

For 1st harmonic 12 months $\equiv 2\pi$

$\therefore$ 1 month $\equiv \pi/6$

$\therefore$ Correction$=\pi/12$

For 2nd harmonic 12 months $\equiv 4\pi$

$\therefore$ 1 month $\equiv \pi/3$

$\therefore$ Correction$=\pi/6$

Errors in Amplitudes and Phases

Humble (1971) has shown that the error in R_k is given by

$$\sigma(R_k) = \sigma(u_\ell) \cdot \sqrt{\frac{2}{n}} \qquad \text{(A4.8)}$$

This relation holds provided the differences between the u_ℓ are small so that their (Poisson) errors $\sigma(u_\ell)$ are approximately the same. This is generally true.

The error in phase angle is

$$\sigma(f_k) = \arcsin\left[\frac{\sigma(R_i)}{R_i}\right] \qquad \text{(A4.9)}$$

We note that the amplitude error is the same for each harmonic whereas the phase error depends on R_k and therefore on the harmonic number.

APPENDIX 5

THE USE OF MUON INTENSITY VARIATIONS UNDERGROUND TO MEASURE UPPER AIR TEMPERATURE

Introduction

It has long been realized that the temperature dependence of the muon intensity provides, at least in theory, a means of estimating the atmosphere's temperature profile. To see this, consider the formula for the relative change in the muon intensity for a given telescope:

$$\frac{\delta I_\mu(h_0,\Delta E)}{I_\mu(h_0,\Delta E)} = \int_0^{h_0} W_T^{pos+neg}(h,h_0,\Delta E)\ \delta T(h)\,dh \qquad (A5.1)$$

This expression constitutes a first order, linear Fredholm integral equation, commonly expressed as

$$g(y) = \int_a^b K(z,y)\ f(z)\,dz \qquad (A5.2)$$

where the function $K(z,y)$ in the integrand is known as the kernel. The parallel between these two equations is obvious: knowing $K(z,y)$ $[W_T(h,h_0,\Delta E)]$ and $g(y)$ $[\delta I_\mu/I_\mu]$ we would like to solve for $f(z)$ $[\delta T(h)$ - the deviation of the temperature profile from the mean].

If only one value of $g(y)$ is known then an infinity of solutions for $f(z)$ exist. However, if $m > 1$ values of $g(y)$ corresponding to m different kernels are measured simultaneously, then a more constrained solution for $f(z)$ begins to appear. Following Twomey (1977) we see that there

exists in the (f,z) domain a set (probably infinite) of f(z) functions which are associated (through the integral equation) with our measured g(y)'s. The greater the number and accuracy of the g(y)'s, the more the f(z) functions tend to merge into one.

In practice, we may have several muon telescopes, with different geometries and threshold energies and therefore different W_T functions, to use for kernels. This technique has been investigated by Miyazaki and Wada (1970), Bolli (1970), Dorman (1977), Kohno et al. (1981) and others. If the number of kernels is small, the best method has been to approximate $\delta T(h)$ by a linear combination of orthogonal basis functions, $F_j(h)$. The coefficients are then solved for in the following way:

Let

$$\delta T(h) = \sum_{j=1}^{m} \xi_j F_j(h) \qquad \text{(A5.3)}$$

and

$$(\delta I/I)_i = S_i \ .$$

Thus

$$S_i = \int_0^{h_0} W_{T_i}(h) \ \delta T(h) dh$$

$$= \int_0^{h_0} W_{T_i}(h) \sum_{j=1}^{m} \xi_j F_j(h) dh$$

$$= \sum_{j=1}^{m} \xi_j \alpha_{ij} \qquad \text{(A5.4)}$$

where

$$\alpha_{ij} = \int_0^{h_0} W_{T_i}(h) \ F_j(h) dh \qquad \text{(A5.5)}$$

Equation (A5.4) is then the matrix equation

$$\underset{(m \times 1)}{\underline{S}} = \underset{(m \times m)}{A} \; \underset{(m \times 1)}{\underline{\xi}} \qquad \text{(A5.6)}$$

which has the solution

$$\underline{\xi} = A^{-1} \underline{S} \qquad \text{(A5.7)}$$

Empirically, simple power functions of the form $F_j(h) = h^n$ (n integral) have given reasonable results. The accuracy of the temperature reconstruction depends on maximizing the detectors' area and the time of observation. However, if the period of the temperature variations is small compared with the counting interval, the reconstruction will be very crude. A trade-off also exists between the fraction of the atmosphere covered by $\delta T(h)$ and the overall accuracy. Finally, if the kernels in (A5.4) are too similar to each other or are poorly determined, the matrix equation may be ill-conditioned. In other words, A may tend to singularity.

Ideally, each kernel should overlap with its neighbour but also "uncover" a new strip of the z-domain. This is illustrated in Figure A5.1.

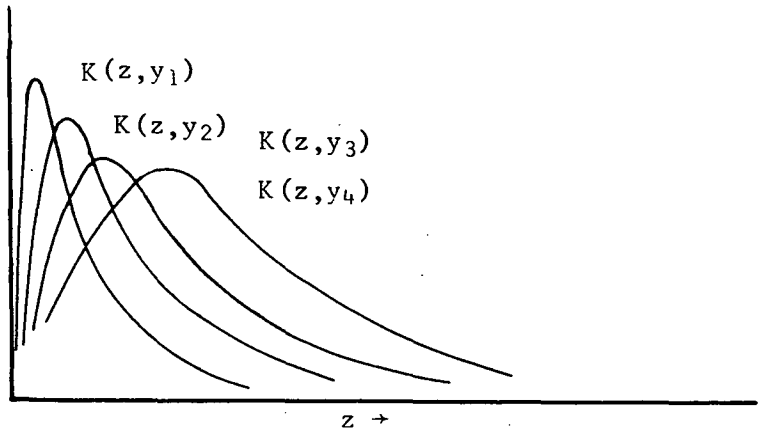

Figure A5.1. An example of a "good" set of kernels.

The Use of Underground Telescopes

From Chapter 3, the temperature coefficient weighting functions for telescopes deep underground (such as at Poatina) tend to peak sharply in the stratosphere and fall to zero at greater atmospheric depths. However, the W_T functions for the various Cambridge telescopes show a considerable portion which is constant and negative (Figures 3.5 - 3.9). This is due to the appreciable negative temperature effect caused by muon decay. Therefore, unfortunately, the Cambridge curves would make poor kernels.

For these reasons, it was decided to use simply the Poatina intensity in an attempt to reconstruct the "mean" temperature of the stratosphere. It is assumed that upper air temperature T is solely responsible for changes in intensity ΔI. Using the predicted temperature coefficient $b_{IT} = 0.25\ \% K^{-1}$ (Chapter 3), we then have for the "reciprocal temperature coefficient"

$$b_{TI} = \frac{100}{b_{IT}\,\bar{I}} \quad K\ count^{-1} \qquad (A5.8)$$

so that the reconstructed temperature will be

$$T = \bar{T} + b_{TI}\,\Delta I \qquad (A5.9)$$

where $\bar{T}$ is some long term average. (It should be noted that Equation (A5.8) assumes that b_{IT} is a law-like quantity so that the slope of the inverse relation is basically just its reciprocal. This differs from the least-squares case where correlations are never perfect and we would have $b_{TI} = r^2_{IT}/b_{IT}$).

Results from Poatina

The relative Poisson error on the daily intensity at Poatina is about 0.5%. This compares with an expected systematic change of ~0.7%, which corresponds to the long-term standard deviation in $T_{8.0}$ of 2.7 K. Thus the accuracy of the inferred diurnal temperature variations would be expected to be poor. The errors on the 2 and 4-day mean temperatures should be better.

The 1972 data were analysed according to Equation A5.9 where monthly blocks were used for the daily temperatures and bi-monthly for the 2 and 4-day temperatures. In the latter case, bi-monthly blocks were necessary so that a reasonable number of points could be obtained.

Figure A5.2 shows the results for January to April 1972.

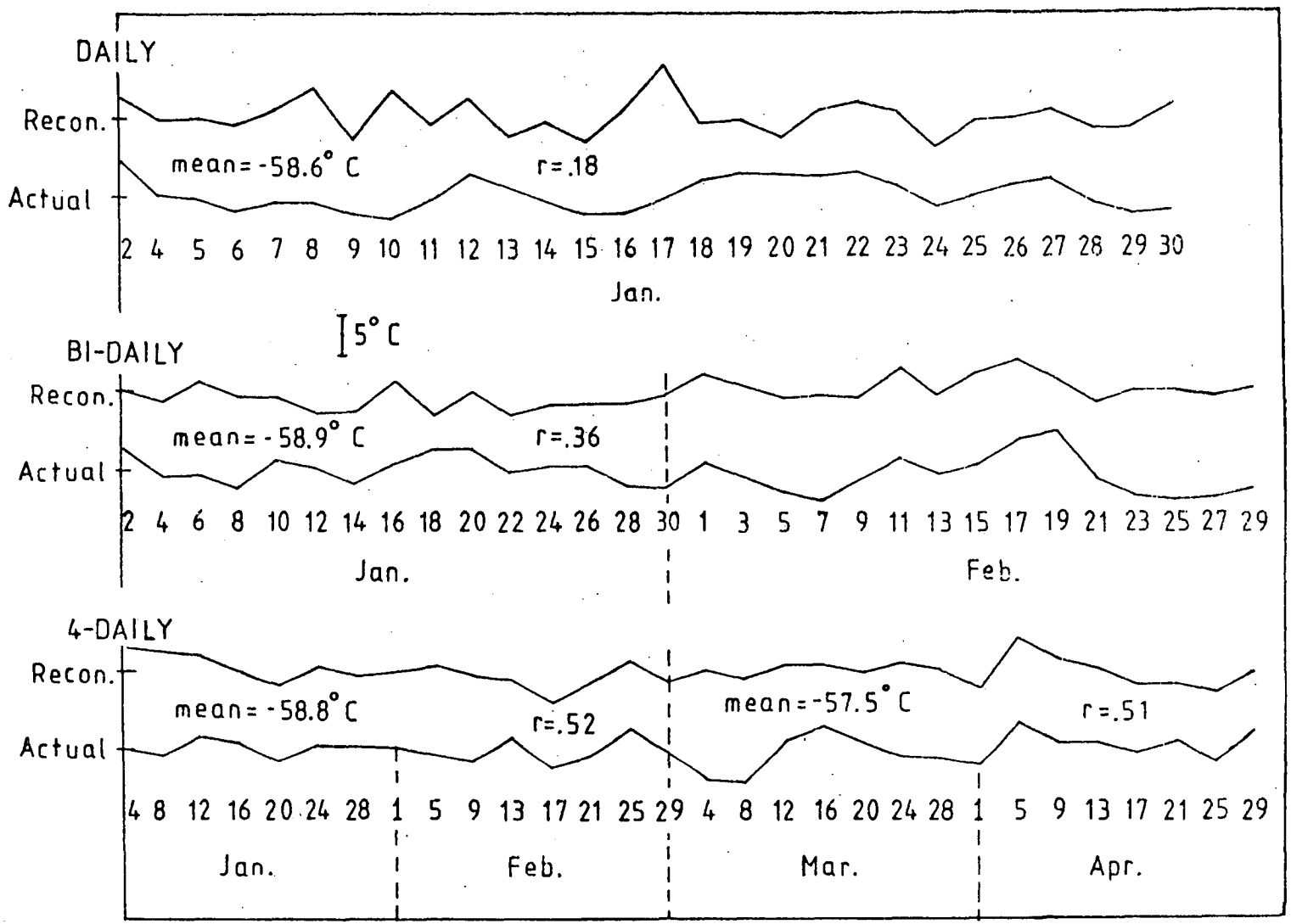

Figure A5.2. Actual and reconstructed upper air temperatures above Poatina for January to April, 1972. The dates are the closing dates of the particular 1, 2 or 4-day period. On January 1, 3 and 31, temperature data were missing, so these days have been omitted.

Plotted along with the inferred temperature is the weighted mean temperature calculated from radiosonde data according to the formula

$$T_{\text{"actual"}} = \frac{0.5T_{200} + T_{150} + T_{100} + T_{80} + 0.5T_{60}}{4} \qquad \text{(A5.10)}$$

It is seen that a correlation coefficient of ~ 0.5 is obtained between the actual and reconstructed temperatures when 4-day figures are used. This result is fairly good in view of the presence of appreciable errors on $T_{\text{"actual"}}$ (presumably $\sim$ 2K) and considering the relative Poisson error of $\sim 0.25\%$ in the muon intensity.

These results can only be regarded as a rough demonstration of using underground muon observations to sense stratospheric temperature. In addition, the 4-day mean temperature is too "slow" to be of much use. However, a ten-fold increase in detector area should provide a useful "thermometer" for the daily variation, but would still only yield the mean temperature of the upper atmosphere. To reconstruct temperature on an hourly basis using muon intensities at this depth would require ~ 1000 m^2 of detector area!

Other workers have calculated the W_T functions for telescopes at intermediate depths underground ($\sim$ 60 hg cm^{-2}). These have been shown to still be good kernels, of the form shown in Figure A5.1. Since the underground intensity varies as (depth)$^{-2.2}$, a 5 to 10-fold improvement in σ_{Pois} (compared with Poatina) is possible at such depths, using only a few square metres of detector area.

However, variations caused by changes in the primary intensity and barometric pressure must be removed first, as both these effects become significant with decreasing muon threshold energy.

Further mention should be made of the results obtained by Kohno et al. (1981) who have reconstructed atmospheric temperatures by regression methods. Using radiosonde temperature data for the 100, 500 and 900 mb levels they have determined the OLS regression coefficients β_{ij} in

$$T_i(t) = \beta_{iu}\, U(t) + \beta_{ih}\, H(t) + \beta_{is}\, S(t) \qquad \text{(A5.10)}$$

In this expression, i stands for the pressure level and t for time. U, H and S represent, respectively, muon intensities at 54 hg cm^{-2} underground (Takeyama), hard muons at sea level filtered by a 10 cm lead shield and soft muons which are stopped in 10 cm of lead. The telescope statistics are reproduced in Table A5.1.

TABLE A5.1

Muon components used in the temperature profile reconstruction of Kohno et al. (1981).

Component	Daily $\sigma_{Pois}/\bar{I}$ (%)	Intensity (h^{-1})	Energy Range
U (underground)	0.053	1.5×10^5	median ≈ 230 GeV
H (hard)	0.023	7.7×10^5	≳ 0.4 GeV
S (soft)	0.21	9.2×10^3	20 MeV band @ 0.4 GeV

Before performing the regression analysis, the three components were corrected for pressure and the H and S components for primary variations using a neutron monitor at Tokyo. The coefficients obtained from (A5.10) were averaged over a 5-month period and then used to reconstruct T(t) for March 1-27, 1981. The resulting temperatures were found to agree with the measured ones to within ~2K at the three levels.

TABLE A5.2

Regression coefficients obtained by Kohno et al. (1981). The upper figure in each pair is the average of 5 monthly coefficients, while the lower is the *continuous* 5-month coefficient. Units are K/%.

Level (mb)	β_u	β_h	β_s	No. of observations
100	3.39 ± 1.09	5.45 ± 1.11	-0.68 ± 0.62	138
	2.35 ± 0.81	7.48 ± 0.51	-1.47 ± 0.25	"
500	0.28 ± 1.05	- 9.99 ± 0.97	0.21 ± 0.54	"
	0.24 ± 0.77	-10.49 ± 0.49	1.17 ± 0.23	"
900	1.74 ± 0.71	- 7.93 ± 0.76	0.56 ± 0.44	"
	3.76 ± 0.61	- 8.90 ± 0.39	1.42 ± 0.19	"

This empirical method overcomes the problem of having to calculate the kernels analytically. However, the intensity components must still differ sufficiently from each other so that their correlation matrix does not tend towards singularity. The results in Table A5.2 show, in some cases, appreciably different coefficients according to which scheme has been used to obtain them. This suggests that bias in the coefficients

(caused by the combined effects of data collinearity and measurement errors) may be serious.

It is interesting to calculate Davies and Hutton's "c-parameter" (Section 5.8) using the results of Kohno et al. Using

$$c = \frac{n \sum_j \sigma_j |\beta_j|}{\sigma}$$

where σ in the denominator is, say 2 K, and inserting the figures from Tables A5.1 and A5.2, we find values of c in the range 30-50. Such figures are high, but should not really cause alarm; it just means that the actual coefficients do not mean much physically.

Kohno et al. found that the agreement between their actual and reconstructed temperatures was poorer when the 5-month continouus coefficients were used. This is consistent with the evidence above that, for these data, a long-term "blanket" set of coefficients is inappropriate. As in Section 5.9.2, the conclusion is that better prediction of the response variable (in this case, temperature) is obtained using the data set's *own* sample coefficients.

REFERENCES

Bachelet, F. and Conforto, A.M., Il Nuovo Cimento, *4*, 1479 (1956).

Barish, B.C., Bartlett, J.F., Buchholz, D., Humphrey, T., Merritt, F.S., Nagashima, Y., Sciulli, F.J., Shields, D., Suter, H., Krafczyk, G. and Maschke, A., Phys. Rev. Lett., *31*, 8, 565-8 (1973).

Barret, P.H., Bollinger, L.M., Cocconi, G., Eisenberg, Y. and Greisen, K., Rev. Mod. Phys., *24*, 3, 133 (1952).

Belsley, D.A., Kuh, E. and Welsch, R.E., Regression Diagnostics, Wiley, New York (1980).

Bercovitch, M., 9th International Cosmic Ray Conference, *1*, 495 (1965).

Bergeson, H.E., Cutler, D.J., Davis, J.F. and Groom, D.E., 16th International Cosmic Ray Conference (Kyoto), Paper MG7-6 (1979).

Bolli, W., Ph.D. Thesis, University of Bern, Switzerland (1971).

Burcham, W.E., Nuclear Physics - An Introduction, 2nd Edition, Longmans, London (1973).

Carmichael, H., Bercovitch, M. and Steljes, J.F., Tellus, *19*, 1 (1967).

Cini Castagnoli, G. and Dodero, M.A., Il Nuovo Cimento, *51*B, 2, 525 (1967).

Cospar International Reference Atmosphere, Cospar Working Group IV, North Holland, Amsterdam (1965).

Cutler, D.J., Ph.D. Thesis, University of Utah (1980).

Davies, R.B. and Hutton, B., Biometrika, *62*, 2, 383 (1975).

Dorman, L.I., Cosmic Ray Variations, State Publ. House for Tech. and Theoretical Literature, Moscow; translated by USAF Technical Documents Liason Office, Wright-Patterson AFB, Ohio (1957).

Dorman, L.I., 15th International Cosmic Ray Conference (Plovdiv), Paper MG-148, *4* (1977).

Draper, N.R. and Smith, H., Applied Regression Analysis, Wiley, New York (1966).

Duperier, A., Terr. Mag. Atmos. Elect., *49*, 1 (1944).

Duperier, A., Proc. Phys. Soc., *A62*, 684 (1949).

Dutt, J.C. and Thambyahpillai, T., J. Atm. Terr. Phys., *27* 349 (1965).

Dyring, E. and Lindgren, S., Tellus, *14*, 247 (1962).

Ehmert, A., Nuovo Cimento, *8*, Suppl., 318 (1958).

Elliot, H., 16th International Cosmic Ray Conference (Kyoto), *14*, 200 (1979).

Fenton, A.G. and Fenton, K.B., 14th International Cosmic Ray Conference (Munich), Paper MG10-9, *4*, 1482 (1975).

Fenton, A.G. and Fenton, K.B., 2nd International Cosmic Ray Symposium on High Energy Cosmic Ray Modulation, Univ. of Tokyo, 308 (August 1976).

Fenton, A.G., Jacklyn, R.M. and Taylor, R.B., Il Nuovo Cimento, *22*, 2, 285 (1961).

Fujii, Z., and Jacklyn, R.M., 16th International Cosmic Ray Conference (Kyoto), Paper MG-9.3 (1979).

George, E.P., Progress in Cosmic Ray Physics, J.G. Wilson (Ed.), North Holland, Amsterdam (1952).

Golub, G.H. and Reinsch, C., Numer. Math., *14*, 403 (1970).

Gombosi, T., Kota, J., Somogyi, A.J., Varga, A., Betev, B., Katsarsky, L., Kavlakov, S., and Khirov, I., Nature *255*, 687 (1975).

Gradshteyn, I.S. and Rhyzik, I.M., Tables of Integrals, Series and Products, Academic Press, New York (1965).

Hammersley, J.M. and Hanscomb, D.C., Monte Carlo Methods, Methuen, London (1964).

Hanson, R.J. and Lawson, C.L., Math. of Computation, *23*, 787 (1969).

Hodges, S.D. and Moore, P.G., Applied Statistics, *21*, 185 (1972).

Hoerl, A.E. and Kennard, R.W., Technometrics, *21*, 1, 55 (1970).

Hook, J.R. and Turver, K.E., J. Phys. A: Math, Nucl. Gen., *7*, 6 (1974).

Humble, J.E., Ph.D. Thesis, University of Tasmania (1971).

Humble, J.E., Fenton, A.G., Fenton, K.B. and Lyons, P.R.A., 16th International Cosmic Ray Conference (Kyoto), *4*, Paper MG8-5 (1979).

Johnston, J., Econometric Methods, McGraw-Hill, New York (1963).

Kendall, M.G., A course in multivariate analysis, Griffin, London (1957).

Kmenta, J., Elements of Econometrics, Macmillan, New York (1971).

Kohno, T., Imai, K., Inoue, A., Kodama, M. and Wada, M., 17th International Cosmic Ray Conference (Paris), Paper SH9.2-9 (1981).

Lindgren, S., Ark. Fys., *5*, 23 (1965).

Lindgren, S. and Lindholm, F., Tellus, *13*, 280 (1961).

Maeda, K., J. Atm. Terr. Phys., *19*, 184 (1960).

Marquardt, D.W., Technometrics, *12*, 3, 591 (1970).

Miyazaki, Y. and Wada, M., 11th International Cosmic Ray Conference (Budapest), *2*, 591 (1969).

Nagashima, K., 14th International Cosmic Ray Conference (Munich), *4*, 1503 (1975).

Parsons, N.R., Ph.D. Thesis, University of Tasmania (1959).

Pine, J., Davisson, R.J. and Greisen, K., Il Nuovo Cimento, *14*, 6, 1181 (1959).

Quang, T.T., Honours Thesis, University of Tasmania (1970).

Quang, T.T., Ph.D. Thesis, University of Tasmania (1974).

Rossi, B.B., High-energy particles, Constable, London, 1952

Sagisaka, S., Murakami, K., Inoue, K., Inoue, A. and Nagashima, K., 16th International Cosmic Ray Conference (Kyoto), *4*, Paper MG8-1, 235 (1979).

Seber, G.A.F., Linear Regression Analysis, Wiley, New York (1977).

Silvey, S.D., J. Royal Statistical Soc., B, *31*, 539 (1969).

Simpson, J.A., Fonger, W. and Treiman, S.B., Phys. Rev. *90*, 934 (1953).

Spearman, G., American J. Psych. *15*, 242 (1904).

Torsti, J.J. and Valtonen, E., Physica Scripta, *14*, 187-191 (1976).

Trefall, H. and Nordö, J., Tellus, *11*, 467 (1959).

Trefall, H., Naturvitenskapeligrekke No. 10, University of Bergen (1956).

Twomey, S., Introduction to the Mathematics of Inversion in Remote Sensing and Indirect Measurements, Elsevier, Amsterdam (1977).

Upper Air Statistics, 1957-75, Australian Bureau of Meteorology, Melbourne (April 1977).

Wolfendale, A.W., Cosmic Rays, Newnes, London (1963).

Yasue, S., Mori, S. and Sagisaka, S. 17th International Cosmic Ray Conference (Paris), Paper SH9.2-3 (1981).

ADDENDUM

Myssowsky, L. and Tuwim, L., Zeit. für Physik, *39*, 146 (1928).

N.B. At this time, the muon component of cosmic rays had not been separately identified.

Eliassen, A., Videnspapsakademiets Institut for Voerogklimaforsking, Oslo, Report Number 5 (1954).

Leviton, R., A.F. Surveys in Geophys., Number 60 (1954).

Nyberg, A., Sveriges Met. Hydr. Inst. Medd B, *9* (1952).

Raab, L., and Rodskjer, N., Arkiv für Geofys, *1*, 33 (1950).